DEVELOPMENT AND HEAT TRANSFER SIMULATION OF EPOXIDIZED JATROPHA BIOLUBRICANT FOR SPARK IGNITION ENGINES

BY

ALIYU JA'AFARU

DEPARTMENT OF MECHANICAL ENGINEERING,

FACULTY OF ENGINEERNG,

AHMADU BELLO UNIVERSITY,

ZARIA, NIGERIA

April, 2021

DEVELOPMENT AND HEAT TRANSFER SIMULATION OF EPOXIDIZED JATROPHA BIOLUBRICANT FOR SPARK IGNITION ENGINES

BY

ALIYU JA'AFARU

B.Eng. (BUK, 1995), M.Eng. (BUK, 2008)

P15EGME9009

A PHD THESIS SUBMITTED TO THE SCHOOL OF POSTGRADUATE STUDIES AHMADU BELLO UNIVERSITY IN PARTIAL FULFILLMENT OF THE REQUIREMENTS FOR THE AWARD OF DOCTOR OF PHILOSOPHY DEGREE IN MECHANICAL ENGINEERING

DEPARTMENT OF MECHANICAL ENGINEERING,

FACULTY OF ENGINEERING,

AHMADU BELLO UNIVERSITY,

ZARIA, NIGERIA

MAY, 2021

DECLARATION

I hereby declare that the work in this thesis entitled "Development and Heat Transfer Simulation of Epoxidized Jatropha Biolubricant for Spark Ignition Engines" has been carried out by me in the Department of Mechanical Engineering. The information derived from the literature has been duly acknowledged in the text and a list of references provided. No part of this work has been presented for another degree or diploma at this or any other institution.

Aliyu JA'AFARU ---------- ----------

Signature Date

CERTIFICATION

This thesis entitled "DEVELOPMENT AND HEAT TRANSFER SIMULATION OF EPOXIDIZED JATROPHA BIOLUBRICANT FOR SPARK IGNITION ENGINES" by Aliyu JA'AFARU meets the regulations governing the award of the degree of Doctor of Philosophy in Mechanical Engineering, of the Ahmadu Bello University, and is approved for its contribution to knowledge and literary presentation.

Prof. D.M. Kulla (Signature) _____

(Chairman Supervisory Committee) (Date) _____

Dr. S. Umaru (Signature) _____

(Member Supervisory Committee) (Date) _____

Dr. S.M. Waziri (Signature) _____

(Member Supervisory Committee) (Date) _____

Prof. D.M. Kulla (Signature) _____

(Head of Department) (Date) _____

Prof. S.A. Abdullahi (Signature) _____

(Dean School of Postgraduate Studies) (Date) _____

ACKNOWLEDGEMENT

I will start by acknowledging my supervisory team: Prof. D.M. Kulla, Dr. S. Umaru and Dr. S.M. Waziri for their tireless efforts in guiding, motivating and advising me throughout the period of this research. The time and resources they invested in this work are indeed priceless. May God continue to help, protect and elevate them. I immensely appreciate the persons who inspired me directly or indirectly and made this work a reality like Prof. Muhammad-Dabo, I. A. of Chemical Engineering Department ABU, Zaria who taught me Biofuels Technology and offered valuable advice for the success of this work; and Prof. F.O Anafi of Mechanical Engineering Department, ABU, Zaria who taught me Internal Combustion Engines. I have been teaching Internal Combustion Engine course for more than a decade, but when I attended the lectures of Prof. F.O. Anafi on Internal Combustion Engines, I realized that I was simply a novice in the area. I have benefitted tremendously from his lectures. His rich and straight-to-the-point lecture note has immensely helped me in my engine performance analyses.

I equally acknowledge the hot brains that greatly helped in shaping this work like Prof. D.S. Yawas and Prof. G.Y. Pam. The wealth of knowledge and wisdom these academic dons posses have really helped in making this work successful. Other intellectuals who contributed to the success of this work include Dr M.O. Afolayan, Dr. A. Alabi, Dr. H.A. Dandajeh, Dr. M.U. Kaisan, Dr. S. A. Alim, Dr. Y.S. Sanusi , Dr. L.S. Laminu, Engr. M.A. Adamu and lots of them all from mechanical engineering department, ABU, Zaria . I also highly appreciate Engr. Timothy Ahu and Engr. Nuhu Mohammed of Chemical Engineering Department, ABU, Zaria who greatly assisted me in understanding many complex chemical terminologies.

The work wouldn't have been possible without the contributions of Dr. Hassan Adamu Hamidu of College of Agriculture and Animal Science, ABU, Mando, Kaduna; Engr. Issah Momoh of Total Blending Company, Kaduna; Mal. Garba Shehu of Food Technology Laboratory Kaduna Polytechnic, Kaduna; Mal. Iliyasu Maude of Physics Lab. Kaduna Polytechnic, Kaduna, Mal. Musa Abdullahi of Research Laboratory II, Chemical Engineering Laboratory ABU, Zaria; Mal. Muazu Muhammad of Multi-User Lab. Chemistry Department, ABU, Zaria; Mal. Auwal of Heat Engine Lab. Mechanical Engineering Department, ABU Zaria; Engr. Kabir El-Hussain of KRPC and many of them.

I would also like to acknowledge all my family members for their immense support, understanding and motivation. May Allah reward you all.

DEDICATION

This work is dedicated to Almighty Allah who creates plants and made them to bear fruits and put inside the fruits seeds that contain oil from which fuels and lubricants can be made.

ABSTRACT

Vegetable oils need to be chemically modified before being used for biolubricant production for internal combustion engines applications. One of the most effective chemical modifications for vegetable oils is epoxidation of its double bonds. In this work, Crude Jatropha oil (CJO) was epoxidized using peracid generated in-situ by the reaction of formic acid and hydrogen peroxide using sulfuric acid as catalyst. FTIR and Iodine Value were used to confirm the formation of epoxides. Epoxidized Jatropha biolube (EJBL) was produced by two stage transesterification; the first is aimed at producing an intermediate product-methyl ester of the jatropha oil, while the second uses the methyl ester as a reactant to produce a polyol ester (biolubricant) using Trimethylolpropane (TMP). The EJBL was blended with B023232/B023333 additive from 1 % to 10 % by volume with 1 % increments. The physico-chemical properties of the blends were determined and the blend whose physico-chemical properties are close to that of reference oil was chosen for the engine test. A TecQuipment TD201 small engine test set located at the heat engine laboratory of Mechanical Engineering Department Ahmadu Bello University, Zaria, was used for engine performance test. The Equipment manufacturer specified that SAE30 or 10W30 engine oil should be used on the engine. The epoxidation process has improved the thermal and oxidative stabilities of the jatropha oil from 76^{o}C to 130^{o}C. The physico-chemical analyses of the EJBL and its blends show that EJBLO5 is close to SAE 30. It was observed that EJBL05 is better than SAE 30 in Viscosity Index, Flash Point, Pour Point, Evaporation Loss, Specific Heat Capacity, Coefficient of thermal Conductivity and demulsibility. The torque developed by the test engine (TecQuipment TD 201) within the test range used (0- 3450 rev min^{-1}) for EJBL05 were 0 – 9.9 Nm and for SAE 30 (reference engine oil), 0 – 9.4 Nm; Similarly the engine Brake Powers for EJBL05 were 0 – 3577 W and for SAE30, 0 – 3396 W; The Brake Mean Effective Pressures (BMEP) for EJBL05 were 0 – 6.22 bar and for SAE 30, 0 - 5.99 bar. The Brake Specific Fuel Consumptions (BSFC) for EJBL05 were 0 – 0.3492 kg kWh^{-1} and for SAE30, 0 – 0.3762 kg kWh^{-1}. The simulated results obtained for oil temperatures, engine outer surface temperatures and exhaust valve temperatures were close to the experimented results with R^2 value of 0.988, 0.969 and 0.977 respectively; signifying that the simulation was valid.

TABLE OF CONTENTS

Declaration	iv
Certification	v
Acknowledgment	vi
Dedication	vii
Abstract	viii
Table of Contents	ix
List of Figures	xvii
List of Tables	xx
List of Plates	xxi
List of Appendices	xxii
Abbreviations and Symbols	xxiii
CHAPTER ONE: INTRODUCTION	1
1.1 Background of the Study	1
1.2 Statement of Research Problems	3
1.3 The Present Research	3
1.4 Aim and Objectives of the Research	4
1.5 Justification	5
1.6 Scope	5
CHAPTER TWO: LITERATURE REVIEW	6
2.1 Lubricant Base Oil	6
2.1.1Synthetic Oils	6
2.1.2 Mineral Oils	6

2.1.3 Natural Oils 6

2.2 Lubricant Base Oil Classifications 7

2.3 Application of Lubricants 7

2.4 Automotive Engine Lubrication 8

2.4.1Essentials of a Lubricating System 8

2.5 Functions of a Lubricating System 8

2.6 Types of Lubrication 9

2.7 Biolubricants and their Feedstocks 10

2.8 Chemical Composition of Vegetable oils 10

2.9 Chemical Modification of Vegetable Oils 11

2.9.1 Epoxidation 12

2.10 Biolubricant Production 12

2.11Automotive Biolubricants 13

2.12 Automotive Lubricating Oil Base Stocks Quality Determinant 13

2.12.1 Refractive Index 13

2.12.2 Iodine Value 13

2.13 Requirements of Engine Oil 14

2.13.1Density 14

2.13.2 Viscosity 14

2.13.3 Viscosity Index 14

2.13.4 Pour Point 15

2.13.5 Flash Point/Fire Point 15

2.13.6 Thermal Stability 16

2.13.7 Shear Stability 16

2.13.8 Evaporation Loss 16

2.13.9 Foaming Tendency 16

2.13.10 Total Base Number (TBN) 17

2.13.11 Total Acid Number (TAN) / Neutralization Number (NN) 17

2.13.12 Elemental Content 17

2.13.13 Seal Compatibility 18

2.13.14 Oxidation Stability 18

2.13.15 Specific Heat Capacity 19

2.13.16 Coefficient of Thermal Conductivity 19

2.13.17 Ash Content 19

2.13.18 Demulsibility 19

2.13.19 Corrosion Stability 20

2.14 Additives 20

2.14.1 Oxidation Inhibitors 21

2.14.2 Anti-wear 21

2.14.3 Dispersants 21

2.14.4 Detergents 22

2.14.5 Viscosity Index Improvers (VII) 22

2.15 Additive Packages 22

2.16 Engine Oil Grades 23

2.17 Engine Oil Specifications 23

2.17.1 American Petroleum Institute (API) 23

2.17.2 International Lubricant Standardization and Approval Committee 24

2.17.3 Association of Constructors of European Automobile 24

2.17.4 Japanese Automotive Standard Organization 24

2.17.5 Original Equipment Manufacturers 25

2.18 National Industrial Standards 25

2.19 Minimum Requirements of Biolubricants 25

2.20 Oil Circulation in Internal Combustion Engine 25

2.21 Internal Combustion Engine Performance 27

2.21.1Specific Fuel Consumption 27

2.21.2 Air Consumption 27

2.21.3 Air/Fuel Ratio 28

2.21.4 Mean Effective pressure 28

2.21.5Brake Power 28

2.21.6 Brake Thermal Efficiency 29

2.22 Engine Oil Flow Regimes in the Spark Ignition Engine 29

2.23 Internal Combustion Engine Heat Transfer 30

2.23.1 Heat transfer in the Intake and Exhaust Manifolds 30

2.23.2 Engine Oil Heat transfer 31

2.24 Modeling and Simulation 31

2.24.1 Types of Spark Ignition Engine Numerical Models 32

2.25 Review of some Related Past Research on Biolubricant 32

2.25.1Production of Biolube and Determination of their Properties 32

2.25.2 Effects of Additives on the Performance of Biolubricants 35

2.25.3 Effect of Epoxidation on Performance of Biolubricants 35
2.26 Review of Related Works on Modeling and Simulations 37
2.27 Methods of Modelling Internal Combustion Engines Heat Transfer 40
2.27.1 Global Model 40
2.27.2 Zonal Model 43
2.27.3 One-Dimensional Models 44
2.27.4 Multidimensional Models 45
2.27.5 Radiative Heat Transfer Models 46
2.28 Research Gap 46
CHAPTER THREE: MATERIALS AND METHODS 48
3.1 Materials and Equipment 48
3.1.1 Materials 48
3.1.2 Equipment 48
3.2 General Methodology 51
3.2.1 Epoxidation of Jatropha Oil 51
3.2.2 Confirmation of Epoxides Formation 53
3.2.3Characterization of crude and Epoxidized Jatropha Oil 54
3.2.4 Production Epoxidized Jatropha Biolubricant (EJBL) 55
3.2.5 Blending 56
3.2.6 Characterization of the Epoxidized Jatropha Biolubricants 56
3.2.7 Engine Performance Test 69
3.2.8 Modelling and Engine Heat Transfer Simulation 74
3.2.9 Simulation Settings 83

CHAPTER FOUR: RESULTS AND DISCUSSION 89

4.1 Fourier Transform Infrared (FTIR) Spectrum of CJO and EJO 89

4.2 Confirmation of Epoxides Formation Using Iodine Value (IV) 91

4.3 Effect of Epoxidation on Oxidation Stability 92

4.4 Assessment of Crude Jatropha Oil and its Epoxy 93

4.4.1 Refractive Index 93

4.4.2 Moisture Content 94

4.4.3 Saponification Value (SV) 95

4.4.4 Iodine Value (IV) 96

4.5 Min Requirements of Lubricant Base Stock for SI Engine Oil Formulation 96

4.5.1 Viscosity / Viscosity Index 97

4.5.2 Flash Point 98

4.5.3 Pour Point 99

4.6 Performance Parameters of EJBL and its blends 99

4.6.1 Density 100

4.6.2 Viscosities / Viscosity Index 101

4.6.3 Pour Point 102

4.6.4 Flash Point 103

4.6.5 High Temperature High Shear (HTHS) Viscosities 104

4.6.6 Evaporation Loss 106

4.6.7 Foaming Tendency 107

4.7 Additional Requirements not Specified by NIS 107

4.7.1 Total Base Number (TBN) 108

4.7.2 Phosphorus / Sulfur Content 109

4.7.3 Seal Compatibility 110

4.7.4 Oxidation Induction Temperature 112

4.7.5 Oxidation Induction Time 112

4.7.6 Specific Heat Capacity (SHC) 113

4.7.7 Coefficient of Thermal Conductivity 114

4.7.8 Ash Contents 115

4.7.9 Demulsibility 116

4.7.10 Copper Strip Corrosion 117

4.8 Choice of Blend for Engine Test 117

4.9 Engine Performance Results 119

4.9.1 Engine Torque 119

4.9.2 Engine Brake Power 120

4.9.3 Brake Mean Effective Pressure (BMEP) 120

4.9.4 Brake Specific Fuel Consumption (BSFC) 121

4.9.5 Thermal Efficiency 122

4.9.6 Oil Temperature 123

4.9.7 Exhaust Valve Temperature 124

4.8.8 Engine Outer Surface Temperature 125

4.10 Coefficient of Friction/Wear Rate 126

4.11 Simulation Result 127

4.11.1 Oil Temperature 127

4.11.2 Exhaust Valve Temperature 128

4.11.3 Engine Outer Surface Temperature 129

CHAPTER FIVE: CONCLUSIONS AND RECOMMENDATIONS 131

5.1 Conclusion 131

5.2 Recommendations 132

5.3 Contribution to Knowledge 133

References 135

Appendices 146

LIST OF FIGURES

Figure 2.1: Engine Oil Circulation in IC Engine 26

Figure 3.1: General Methodology 51

Figure 3.2: Epoxidation Process 52

Figure 3.3: Biolubricant Production Process 55

Figure 3.4: Flow Chart for Running the Simulation on GT-Suite 75

Figure 3.5: Engine Energy Balance 76

Figure 4.1: Infrared Spectrum of CJO 89

Figure 4.2: Infrared Spectrum of EJO 90

Figure 4.3: Superimposed Infrared Spectrum of CJO and EJO 90

Figure 4.4: Iodine Values of CJO, EJO and EN 14214 Standard 91

Figure 4.5: Oxidation Induction Time for Crude Jatropha Oil (CJO) 92

Figure 4.6: Oxidation Induction Time for Epoxizided Jatropha Oil (EJO) 93

Figure 4.7: Refractive Index of CJO and ISO Standard for Refractive Index 94

Figure 4.8: Water Contents of CJO, and EJO 95

Figure 4.9: Saponification Values of CJO and EJO 96

Figure 4.10: Viscosity Index of CJO and EJO Compared to Mineral Base Oils 97

Figure 4.11: Flash Points of CJO & EJO Compared to Mineral Base Oil 98

Figure 4.12: Pour Points of CJO & EJO Compared to that of Mineral Base Oils 99

Figure 4.13: Density @15^{o}C of EJBL and its Blends 100

Figure 4.14: Viscosity @ 40^{o}C of EJBL and its Blends 101

Figure 4.15: Viscosity @ 100^{o}C of EJBL and its Blends 102

Figure 4.16: Viscosity Index of EJBL and its Blends 102

Figure 4.17: Pour Point of EJBL and its Blends 103

Figure 4.18: Flash Point of EJBL and its Blends 104

Figure 4.19: HTHS Viscosity @ 150^{o}C of EJBL and its Blends 105

Figure 4.20: Evaporation Loss of EJBL and its Blends 106

Figure 4.21: Foaming Limit 107

Figure 4.22: TBN of EJBL its Blends and Various Engine Oil Grades 108

Figure 4.23: Phosphorus Contents of EJBL and its Blends 109

Figure 4.24: Sulfur Contents of EJBL and its Blends 110

Figure 4.25: Seal Compatibility of EJBL and its Blends 111

Figure 4.26: Oxidation Induction Temperature of EJBL and its Blends 112

Figure 4.27: Oxidation Induction Time of EJBL and its Blends 113

Figure 4.28: Specific Heat Capacity of EJBL and its Blends 114

Figure 4.29: Coefficient of Thermal Conductivity of EJBL and its Blends 115

Figure 4.30: Sulfated Ash of EJBL and its Blends 116

Figure 4.31: Demulsibility of EJBL and its Blends in Water 116

Figure 4.32: Engine Speed and Engine Torque 119

Figure 4.33: Engine Speed and Engine Power 120

Figure 4.34: Engine Speed and Brake Mean Effective Pressure 121

Figure 4.35: Engine Speed and Brake Specific Fuel Consumption 122

Figure 4.36: Engine Speed and Thermal Efficiency 123

Figure 4.37: Engine Speed and Engine Oil Temperature 124

Figure 4.38: Engine Speed and Exhaust Valve Temperature 125

Figure 4.39: Engine Speed and Engine Outer Surface Temperature 126

Figure 4.40: Oil Temperature Experimented Against Simulated 127

Figure 4.41: Exhaust valve Temperature Experimented against Simulated 129

Figure 4.42: Engine Outer Surface Temperatures Experimented Against Simulated 130

LIST OF TABLES

Table 2.1 Chemical Formula of Common Fatty Acids 11

Table 3.1: Test Engine Technical Details 70

Table 4.1: Choice of Biolubricant Blend for TecQuipment TD201 109

Table A.1a: Physico-chemical Properties of CJO and EJO with Standard 146

Table A.1b: Physico-chemical Properties of CJO, EJO and Mineral Base oil 147

Table B.1: Physico-chemical Properties of EJBL, EJBL Blends and NIS Standard 147

Table B.2a: Physico-chemical Properties of EJBL, EJBL Blends and Engine oil Grades 149

Table B.2b: Physico-chemical Properties of EJBL, EJBL Blends and Engine oil Grades 150

Table B.3: ILSAC Passenger Car Engine Oil Lab Tests Standards for GF-1 Class 151

Table B.4: API/ILSAC Passenger Car Engine Oil Lab Tests Standards for SJ/GF-2 Class 152

Table B.5: ILSAC Passenger Car Engine Oil Lab Tests Standards for SL/GF-3 Class 153

Table B.6: ILSAC Passenger Car Engine Oil Lab Tests Standards for SM/GF-4 Class 154

Table B.7: ILSAC Passenger Car Engine Oil Lab Tests Standards for SN/GF-5 Class 155

Table C.1: Engine Torque and Power 156

Table C.2: Engine Brake Specific Fuel Consumption 157

Table C.3: Engine Mean Effective Pressure and Thermal Efficiency 158

Table C.4: Engine Temperature Profile 159

Table D.1: Heat Transfer Parameters 160

Table D.2: Air Properties at Mean Bulk Temperature 161

Table D.3: Simulation Results I 162

Table D.4: Simulation Results II 162

Table D.5: Simulation Results III 163

LIST OF PLATES

Plate 3.1: Cary 630 Fourier Transform Infra red Spectrometer 54

Plate 3.2: Abbe's Refractometer 57

Plate 3.3: Cleveland Open Cup Tester 59

Plate 3.4: Foaming Tendency Apparatus 61

Plate 3.5: XRF Spectrometer 63

Plate 3.6: Differential Scanning Calorimeter 64

Plate 3.7: Joule's Apparatus 65

Plate 3.8: Lee's Apparatus 65

Plate 3.9: Demulsibility Tester 68

Plate 3.10: Tribometer 69

Plate 3.11: Engine Instrument Frame 71

Plate 3.12: Engine Showing Locations of Thermocouples 72

Plate 3.13: Engine Showing Location of Thermocouple for Exhaust Valve 73

Plate 3.14: Modelled 1Cyl, 4-Stroke Engine on GT-Suite 74

Plate 3.15: The Engine Crankcase 77

Plate 3.16: GT Window Showing Case Setup 84

Plate 3.17: GT Window Showing Crankcase Setup for SAE30 85

Plate 3.18: GT Window Showing Crankcase Setup for EJBL05 86

Plate 3.19: GT Window Showing Oil Flow Setup 87

Plate 3.20: GT Settings for the Experiment 88

LIST OF APPENDICES

A: Results for Properties of CJO and EJO with Standards 132

B: Results for Properties of EJBL, EJBL Blends and NIS Standards 134

C: Results for Engine Performance 138

D: Results for Simulations 139

ABBREVIATIONS AND SYMBOLS

Symbol	Meaning
A	Area (m^2)
C_P	Specific heat capacity at Constant Pressure (kJ/kgk)
C_f	Coefficient of Skin Friction
d	Inner Diameter (m)
D	Outer Diameter (m)
f	Friction Factor
Gr	Grasshof Number
h	Heat Transfer Coefficient (W/m^2k)
H	Specific Enthalpy (kJ/kgk)
HHV	Higher heating value (kJ/kg)
L	Length (m)
LHV	Lower heating value (kJ/kg)
$\dot{m}$	Flow rate (kg/s)
Nu	Nusselt Number
P	Pressure (N/m^2)
Pr	Prandtl Number
$\dot{q}$	Heat Flux (W/m^2)
Q	Heat Transferred (kJ)
$\dot{Q}$	Heat Transfer Rate (W)
Re	Reynolds Number
U	Mean Speed (m/s)

U	Specific Internal Energy (kJ/kgk)
V	Volume (m^3)
w	Width (m)
W	Work (kJ)
x	Thickness (m)
t	Temperature (k)

Greek symbols	**Meaning**
δ	Change
θ	Crank Angle (rad)
Δ	Temperature Difference (K)
ω	Angular Speed (rad/s)
ε	Emissivity
ρ	Density (kg/m^3)
η	Efficiency
μ	Dynamic Viscosity (kg/ms)
υ	Kinematic Viscosity (m^2/s)

Subscripts

a	Ambient
b	Brake
c	Cylinder
ch	Chemical

f	Fluid
g	Gas
L	Loss
m	Mean
s	System
i	Inside
in	Inside
o	Outside
out	Outside
w	Wall Side

CHAPTER ONE

INTRODUCTION

1.1 Background of the Study

Emphases on the development of renewable, biodegradable and environmentally friendly industrial fluids such as biolubricant and biodiesel have resulted in widespread use of vegetable oils for non-edible purposes. The desirability of developing alternative fuels and biolubricants and decreasing the dependency on petroleum based fuels has been discussed by many over the last decades (Tiwari and Santosh, 2015). The use of vegetable oil as lubricants preceded mineral oil discovery, however it was abandoned for mineral oil because the later was cheaper and more efficient. Now, many researchers focus on vegetable oil for lubricant formulation because of environmental concerns and sustainability. Vegetable oils are perceived to have the potentials to replace petroleum oils for lubricant formulations because of certain inherent technical properties and their ability towards biodegradability.

The reliable and safe operation of an automobile at desired operating conditions requires effective lubrication of moving parts to allow them slide smoothly over each other. Reducing wear and friction is a key element to decreasing energy loses, particularly in engines and drive trains (Mobarak *et al.*, 2014). Engine operating temperature must not exceed a specified limit, for proper functioning of the engine. Lubricating oil assists tremendously in maintaining the engine temperature, because the constant flow of oil carries heat away from localized “hot spots” (Singh, 2004). The principal parts from which oil absorbs heat are the bearings, the journal surfaces, and the pistons. The thermal properties of lubricating oil play a major role in that regards. Engine oil plays an important role as lubricant for moving parts such as piston rings and

cylinder liners, and it also cleans, inhibits corrosion, improves sealing, and acts as a coolant by carrying heat away (Gill, 2013).

Synthetic, semi-synthetic and mineral engine oils are not directly involved in the ecological cycle of air and soil. However, leakage, human error, or blown pipes may occur and the disposal of engine oil, with its toxicity, may affect and damage the ecosystem. Knowledge and concern over the use of petroleum-based products have created the opportunity to produce environmentally friendly lubricants from biodegradable feedstock (Zulkifli *et al*., 2014).

Under the current industry and market environment, there is increasing demand for bio-based lubricants in all automotive and industrial applications. Vegetable oils continue to be a valuable raw material but in most cases, some chemical manipulation is required in order to meet international and local standard performance requirements (Bergstra, 2016).

Chemical modification is necessary in order to mitigate the vegetable oil's poor oxidative and thermal stabilities, which are due to high level of multiple double bonds present in the fatty acids chains. Chemical modification can overcome these shortcomings by reducing or eliminating unsaturations in the vegetable oils (Sammaiah *et al*., 2014). It is anticipated that new modified vegetable oils will provide a blending option for formulators looking to increase the bio-based content in lubricants, potentially at a lower cost than synthetic oils and at a higher performance than conventional petroleum or vegetable oils (Bergstra, 2016).

Simulation is the act of imitation of real world process over time, using computer codes. It is carried out on models that correctly describe the real system (Meyer, 2004). During simulation, one or more variables affecting the system are altered and the resulting effect on the system is observed. Heat transfer simulation of epoxidized biolubricant in spark ignition engine will help

in establishing the efficacy of the biolubricant in heat removal process in SI engine. The results of the simulation can be validated using experimental results.

Consequently, a lot of research is being carried out to develop cheap, effective and eco-friendly lubricants that can outperform the mineral based lubricant for both automotive and industrial applications. It is in view of that, this research wants to contribute towards biolubricants developments and applications.

1.2 Statement of Research Problem

Internal combustion engine lubricants supposed to be eco-friendly. Their production and use should not have any threat to the environment and the users. However, production, use and unsafe disposal of lubricants such as engine oils for internal combustion engines have raised concern over environmental pollutions (Mobarak *et al.,* 2014 and Aji *et al.,* 2015). This has brought in attention towards the use of non-edible vegetable oils as an alternative to petroleum oil based lubricants (Bergstra, 2016). Non edible vegetable oil plants contain high amount of oils in their seeds which can be converted into biolubricant. Lubricants produced from vegetable oils are mostly used for low temperature applications and cannot be reliably used in Internal Combustion Engines due to their poor oxidative and thermal stabilities, gumming and low pour points due to the inherent weaknesses in their molecular structures (Srivastava and Sahai 2013). Development of chemically modified biolubricants which can be safely and reliably used at high and low temperatures is an option of prime importance which can overcome such problems.

1.3 The Present Research

This research focuses on the production of automotive biolube from the seeds of jatropha *curcas* and performance evaluation of the biolube on spark ignition engine. The crude jatropha oil was

epoxidized and then turned to biolubricant. The formulated biolubricant was blended with 1 % to 10 % automotive additive package by volume using 1 % increment.

Physico-chemical characteristics of the biolubricant blended with additives were determined and compared with that of the mineral base lubricant SAE30 which is the lubricant recommended by the manufacturers of the engine (TD 201) used for the test. The biolubricant blend that can be safely applied to spark ignition engine was selected and tested on a stationary single cylinder four-stroke spark ignition engine. The results of the tests were used to carry out heat transfer simulation of the engine.

1.4 Aim and Objectives of the Research

The aim of this research is to develop epoxidized jatropha biolubricant and investigate its performance in spark ignition engine and carry out heat transfer modelling of the engine.

The specific objectives of this research are to:

(i) Carry out epoxidation of a crude jatropha oil and confirm the formation of epoxides in the sample;

(ii) Characterize the epoxidized jatropha oil and compare with the physico-chemical properties of mineral base oils (NS 100, NS 150, NS 500 and BS 150);

(iii) Formulate biolubricant from the epoxidized jatropha oil; blend the biolubricant with automotive additive package BO23232/B23333;

(iv) Determine the physico-chemical properties of the blended biolubricant and compare them with that of spark ignition engine lubricating oils (SAE 30, SAE 40, SAE 50 and 15W-40) and select the blend that can be used in TecQuipment TD 201 test engine;

(v) Test the performance of the selected blend on TecQuipment TD 201 engine test set;

(vi) Model the engine and carry out heat transfer simulation of the engine when lubricated with the biolube.

1.5 Justification

The importance of this study may not be over emphasized due to the fact that there is need to find reliable and sustainable substitutes to mineral based lubricants for automotive and industrial uses; also there is need to preserve our ecosystem by developing environmentally friendly biolubricants that are nontoxic and can biodegrade easily for the safety of our ecosystem.

Falling back to agriculture (for alternative resources), using non-edible raw materials such as seed oils of *jatropha caucus, ricinus communis, lanneami crocarpa, vitex doniana,* etc, would not only be a sustainable energy source but will help check desertification and reverse the greenhouse effect. Plantation of jatropha in the Northern fringes of Nigeria, for example, will surely reduce the encroachment of desert and ensure sustainability (Bugaje and Muhammad, 2008).

The results of this work can help in making decisions regarding choosing biolubricants for automotive applications. Similarly, the simulation results assisted in verifying the effectiveness of the biolubricants in engine heat removal process.

1.6 Scope

This research is focused on investigating the suitability of jatropha oil and its epoxy for biolubricant production; formulation of epoxidized jatropha biolubricant; blending the biolubricant with additive; determination of its physico-chemical properties; application of the biolubricant to spark ignition engine and heat transfer simulations of the SI engine lubricated with the biolube using GT-Suite.

CHAPTER TWO

LITERATURE REVIEW

2.1 Lubricant Base Oil

Lubricant base oils are oils that posses the required lubrication properties for a given application. They are normally blended with additives for better performance. They are categorized as follows:

2.1.1 Synthetic Oils

These are oils artificially produced that are tailored for optimum lubrication requirements; examples are synthetic esters, polyglycols, phosphate esters, silicones, and polyalphaolefines. They have excellent lubricant properties such as vey high viscosity index, low volatility, high thermal and chemical stabilities, low pour point, high flash point, increased fuel economy, etc. The downside of these oils is they are relatively more expensive than mineral base oils (Gill, 2013).

2.1.2 Mineral Oils

Oils derived from crude or petroleum reserves, such as paraffinic, naphthenic and aromatic oils are called mineral oils. They are most widely used lubricant base oil for automobile applications. The merits of these oils over the others include greater chemical stability at elevated temperature; they are readily available at affordable price (Singh, 2004).

2.1.3 Natural Oils

These are oils produced from plants and animals. Natural oils have good lubrication properties such as high viscosity index and flash point, good lubricity, less toxic and are highly biodegradable. They however have poor low-temperature performance and lack thermal and

oxidative stabilities. When in use, they easily polymerize and become gummy at high temperatures (Singh, 2004).

2.2 Lubricant Base Oil Classifications

The American Petroleum Institute (API) classified lubricant base oils into the following classes, based on the source and characteristics of the oil (Totten, 2006).

Group I Conventional Base Oils

These are mineral oil selected from fractions of crude oil distillation. They have < 90% saturates, with viscosity index (VI) 80-119 and, or >300 ppm sulfur content.

Group II Modern Conventional Base Oils

These are Mineral oil produced through hydro-cracking, hydro-isomerization, etc. They have ≥ 90% saturates, therefore more stable than group I oils; with VI, 80-119 and ≤ 300 ppm sulfur contents.

Group III Unconventional Base Oils

They have > 90% saturates; with VI < 120 and < 300 ppm sulfur contents. They are characterized with high viscosity index.

Group IV Traditional Synthetic Base Oils

These are Polyalphaolefin (PAO) base oils. They have excellent lubrication properties more than Mineral oils. However, they are expensive.

Group IV Specialized Synthetic Base Oils

These are engineered base oil with high boiling points and excellent thermal stability. These include: polyglyco esters, silicones, etc.

2.3 Applications of Lubricants

Automotive Oils: Lubricants used for automotive applications include engine oil, transmission fluids and hydraulics used in automobiles.

Industrial Oils: These are lubricants used as cutting fluids, quenching medium, machine lubricants, etc in the industry.

Special Oils: Oils used for special and specific operations on equipments and laboratories (Mubarak, 2014).

2.4 Automotive Engine Lubrication

The lubricating system is one of the crucial elements of an automotive engine. The lifespan and proper functioning of an engine depends largely on the effectiveness of its lubricating system. An internal combustion engine has a large number of components that either slide, reciprocate or spin relative to each other with high rubbing velocities and bearing loads. The performance of such components will only be enhanced if the friction that exists between them is reduced through lubrication (Gill, 2013).

2.4.1 Essentials of a Lubricating System

A lubricating system, according to Gill (2013), has to have the following features:

(i) Reliability

(ii) Proper lubrication of all working parts

(iii) Minimum oil consumption

(iv) Accessible replenishing filler, strainer or filter

(v) Good oil pressure indicator

(vi) Suitable lubricant

(vii) Efficient filtration of lubricant

2.5 Functions of a Lubricating System

The main functions of an automotive lubricating system are (Singh, 2004):

(a) Reduction of friction and wear between sliding parts

(b) Minimizing noise and vibration by absorbing shocks between relatively moving engine parts

(c) Cleaning engine by removing dirt, sludge and suspended particles

(d) Cooling engine by carrying away heat from the engine and reducing the risk of overheating

(e) Improving engine performance and reducing fuel consumption.

2.6 Types of Lubrication

Automotive engine lubrication may exist in four forms depending on the location and period of the lubrication (Shigley and Mischke, 2001):

(i) Hydrodynamic lubrication: in this a converging or wedge- shaped film of lubricant is developed between the bearing and its rotating journal such that the journal floats on the lubricating oil film. A crank shaft main bearing is a typical case that describes hydrodynamic bearing lubrication. The thickness of the oil film depends on the oil viscosity, relative speed of the bearing surfaces, and the adhesion of the oil molecules on the bearing surfaces (Gill, 2013).

(ii) Elasto-hyrodynamic lubrication; at extreme contact pressure, which occurs between surfaces in rolling contact, e.g. cams and followers, gear teeth and rolling bearings, the viscosity of the oil film increases considerably thereby generating an elasto-hydrodynamic oil film between the surfaces (Shigley and Mischke, 2001).

(iii) Boundary lubrication, when the lubricating film becomes so thin, the asperities of the rubbing surfaces continue to strike each other and occasionally establish contact. This happens when the relative speed of the moving parts is too low, the load acting on the bearing is too high,

or when there is sufficient supply of oil. Under this condition coefficient of friction is very high (Singh, 2004).

(iv) Hydrostatic lubrication: this is also termed squeeze oil film lubrication, can exist in a bearing if the load reverses in direction and the speed of the moving surface is low (Gill, 2013).

2.7 Biolubricants and their Feedstocks

Biolubricants are produced from vegetables such as rapeseed, palm, castor, karanja, soy bean and sun flower. The main advantage of biolubricants is they have high biodegradability and are less toxic to human and the environment (Kumar and Sharma, 2011).

Feedstocks used for biolubricant production may differ from country to country and depend on geographical locations. Mobarak *et al.* (2014) reported that more than 350 oil-bearing plants are known, among which, only palm, soybean, rapeseed, coconut, safflower, cotton-seed, sunflower, and peanut oils are considered as potential alternative biolubricants. Moreover, other non-edible oils such as Jatropha, castor, neem, have received worldwide interest (Mofijur *et al.*, 2012).

2.8 Chemical Composition of Vegetable Oils

Vegetable oils are composed predominantly of triglyceride with varying blend of fatty acids as shown in table 2.1. A triglyceride is a 3 carbon glycerol backbone with a long chain of fatty acids attached to each carbon. Each vegetable oil has a distribution of common fatty acids. The fatty acids are either saturated or unsaturated. The properties of vegetable oils are determined by their fatty acid composition. A high content of unsaturated fatty acid decreases oxidative stability. Whereas, a higher proportion of long chain saturated fatty acid leads to inferior cold flow behavior (Salimon *et al.*, 2012).

Table 2.1 Chemical Formula of Common Fatty Acids (Saurabh *et al.* 2011)

Fatty Acid	**Systematic Name**	**Structure**	**Formula**
Lauric	Dodecanoic	12:0	$C_{12}H_{26}O_2$
Myristic	Tetradecanoic	14:0	$C_{14}H_{28}O_2$
Palmitic	Hexadecanoic	16:0	$C_{16}H_{32}O_2$
Stearic	Octadecanoic	18:0	$C_{18}H_{36}O_2$
Arachidic	Eicosanoic	20:0	$C_{20}H_{38}O_2$
Behenic	Docosanoic	22:0	$C_{22}H_{44}O_2$
Lignoceric	Teracosanoic	24:0	$C_{24}H_{48}O_2$
Oleic	Cis-9-octadecanoic	18:1	$C_{18}H_{36}O_2$
Linoleic	Cis-9, cis-12-octadecanoic	18:2	$C_{18}H_{28}O_2$
Linolenic	Cis-9, cis-12, cis-15-Octadecatrienoic	18:3	$C_{18}H_{33}O_2$
Erucic	Cis-13-Docosenoic	22:1	$C_{22}H_{42}O_2$

2.9 Chemical Modification of Vegetable Oils

Unmodified vegetable oil when used for biolubricant formulation cannot perform satisfactorily due to low oxidative stability, poor low temperature performance, low volatility and deposit formation. All these are due to some inherent weaknesses in their molecular structures. Therefore vegetable oils need to be chemically modified before being used for biolubricant production. One of the most effective chemical modifications for vegetable oils is epoxidation

of its double bonds. Epoxidation is a chemical reaction at the olefinic functionality of the fatty acid chain of a vegetable oil so as to increase its stability (Sharma *et al.*, 2017).

2.9.1 Epoxidation

Epoxidation of fatty acids or vegetable oil can be carried out using peracid generated in-situ or ex-situ by the reaction of carboxylic acid (acetic or formic acid) and hydrogen peroxide in the presence of a suitable catalyst. Optimum epoxide formation can be achieved by varying the reaction parameters such as temperature, reactant molar ratio, type of peracid used, agitation speed, etc.

Dinda *et al*. (2008) reported that acetic acid was more effective than formic acid as oxygen carrier in epoxidation reaction. Similarly Goud *et al.* (2006) and Dinda *et al.* (2008) stated that inorganic sulfuric acid was the most efficient catalyst for epoxidation; also the optimum temperature for highest conversion of double bonds to oxirane group was 55^{o}C to 65^{o}C.

Saurabh *et al*. (2011) listed some drawbacks for in-situ epoxidation which included difficulty of separating acidic byproducts, whose presence may be detrimental for further application; the danger of handling highly concentrated hydrogen peroxides and strong acids for the reaction.

2.10 Biolubricant Production

The production of biolubricant is normally done via two stage transesterification reactions. The first is done to produce methyl ester of the vegetable oil. The methyl ester produced is reacted, in the second stage, with trimethylolpropane (TMP) in the presence of a suitable catalyst.

In the first stage, the triglyceride of the vegetable oil reacts with an alcohol usually methanol or ethanol in the presence of a catalyst (usually NaOH/KOH) resulting into the formation of 1 glycerol and 3 methyl esters. The second stage involves reaction between the methyl ester and trimethylolpropane in the presence of sodium methoxide to produce polyol ester (biolubricant).

It was established that, for jatropha biolubricant synthesis, the following were sufficient for optimum yield; reaction time: 3 hr; temperature: 150^{o}C; sulfuric acid concentration: 2% w/w, molar ratio: TMP: Fatty acid, 1:4 (Sammaiah *et al*., 2014).

2.11 Automotive Biolubricants

Automotive biolubricants are those lubricants produced from vegetable oils that have the required property to be used for automotive uses, such as engine oil, gearbox fluid, transmission oil, brake and hydraulic oil and grease. The benefits of using biolubricants for automotive applications include decreased exhaust emissions due to lower volatility and higher boiling points of biolubricants; reduced environmental pollution due to their rapid biodegradability; increased safety due to higher flash points and improved engine performance due to better lubricity (Mobarak *et al*., 2014).

2.12 Automotive Lubricating Oil Base Stocks Quality Determinants

Before a base stock is chosen for automotive lubricant formulation its quality has to be determined. The properties used to investigate the quality of lubricant base stock include:

2.12.1 Refractive Index

Refractive Index is a dimensionless number normally in the range 1.3000 and 1.7000 for most compounds (Aji, 2015). It depends on purity and molecular structure of a substance. Refractive Index test is carried out to investigate adulteration. Lubricant base stock candidate has to undergo refractive index test to ensure its quality before lubricant formulation.

2.12.2 Iodine Value

Iodine value indicates the level of unsaturates in the oil sample. The higher the iodine value the less stable the oil is. Oil with high Iodine value will be susceptible to oxidation, polymerization

and gumming, therefore not suitable for automotive engine lubrication. EN 14214 stipulated 120 mg I_2/g as the maximum Iodine Value for biodiesel and biolubricant production.

2.13 Requirements of Engine Oil

2.13.1 Density

The density of oil is a measure of its mass per unit volume. Density is a very important parameter in lubricant selection because as density increases so does the erosive potential of the lubricant to its flow paths. Lubricant with higher density above the specified value adds more loads to the lubrication system and consequently reduces the overall engine output (Totten, 2006). Specifications for engine oil densities are available in National Industrial Standards (NIS, 2017).

2.13.2 Viscosity

This is the most important properties of lubricating oil. It is a measure of fluid's resistance to flow due to its internal friction. Meeting viscosity requirements is absolutely very critical for automotive lubricants. The dynamic viscosity, μ of fluid, measured in Pascal-second, is defined as the ratio of shear stress, τ, to the shear rate, γ. Dynamic viscosity per unit density of a substance is referred to as Kinematic Viscosity, V. The reciprocal of dynamic viscosity of a substance is commonly referred to as its fluidity. For automotive engine oils, viscosity requirements are described by SAE standards J300 and J1536. The SAE standard J300 describes viscosity requirements for CI and SI four-stroke engines and CI two-stroke engines. While J1536 describes viscosity requirements for only SI two-stroke engines (Totten, 2006).

2.13.3 Viscosity Index

Viscosity Index (VI) is a physical property used to indicate oil's viscosity change with temperature. The viscosity of oil with low viscosity index changes more with temperature than

the one with higher viscosity index. The higher the VI, the more resistant to viscosity change the oil is. High VI ensures better protection of engine parts at higher temperatures by maintaining the thickness of the oil film within acceptable limit. Lubricants with VI within the range of 80-200 are mostly used in automotive engines (Totten, 2006).

2.13.4 Pour Point

It is the lowest temperature at which a fluid can flow. Knowledge of pour point is a very critical especially for lubricants that may be used at low temperatures. Lubricant should have good fluidity at very low temperatures so that it can effectively protect engine parts during cold cranking. Unmodified vegetable oils generally have poor pour points (Mohammed, 2015). The Pour Point is considered as the lowest operating temperature of the oil. A rule of thumb commonly used in lubricant selection is to ensure that the lubricant has a pour point at least 10^{o}C below the lowest anticipated temperature of the use location (Mohammed, 2015).

2.13.5 Flash Point/Fire Point

Flash point is the lowest temperature at which enough vapors are given off from a substance to cause ignition. It indicates the evaporation loses that can be expected under high temperature applications and fire and explosion hazards of particular oil. The flash point of lubricating oil is important for safety point of view. The Fire Point is the next point beyond Flash Point and is defined as the lowest temperature at which vapors are given off in sufficient quantity to sustain combustion (Gill, 2013). The minimum flash point for internal combustion engine lubricants varies from 174^{o}C to 260^{o}C (Gill, 2013). Flash point specifications for various engine categories are available at American Petroleum Institute (API)/International Lubricant Standardization and Approval Committee (ILSAC) Catalogue.

2.13.6 Thermal Stability

This is the resistance of lubricant to physical change due to thermal stresses. Lubricant needs to retain its lubricity even at elevated temperatures. Lubricant with low thermal stability breaks down when it comes in contact with hot spots, which leads to increased friction, seizing of engine parts and total failure (Gill, 2013). Nigeria Industrial Standard uses High-Temperature High-Shear viscosity @ 150^{o}C to specify thermal and shear stabilities for various engine oil grades. HTHS Viscosity of 2.9-3.7 (cSt) is the acceptable limit for most engine oils (NIS, 2017).

2.13.7 Shear Stability

Shear stability is the ability of lubricant to withstand mechanical shear loads during service. Engine oil is subjected to extreme shear loads during operation as parts slide past each other. Lubricants with low shear stability will break down and lose viscosity at extreme shear loads (Singh, 2004).

2.13.8 Evaporation Loss

This is a measure of quantity of oil that can be lost during service due to evaporation. Evaporation loss indicates the percentage of the lighter-weight fractions of the oil that volatilizes to the atmosphere (Singh, 2004). Oil that volatilizes easily loses its lubricity and becomes thick and therefore cannot reach the remote parts of the engine well. In extreme cases, the oil forms sludge and catastrophic engine damage occurs (Totten, 2006). National Industrial Standard sets 22 % as the maximum allowable evaporation loss for engine oils (NIS, 2017).

2.13.9 Foaming Tendency

Excessive foaming of engine oil can cause collapse of valve lifters, loss of pump pressure, poor sealing and ineffective lubrication. Therefore the tendency of lubricant to foam and its foaming stability have to be ascertained before it is used in the engine. American Petroleum Institute

(API) sets max foaming/settling volume for sequence I and III at 10/0 and for sequence II at 50/0.

2.13.10 Total Base Number (TBN)

Oils and lubricants have reserve alkalinity which is responsible for fighting their acidification. Total Base Number (TBN) or simply Base Number (BN) of a lubricant is a measure of alkaline concentration present in it which hinders acid build-up due to oxidation and combustion by-products. Lubricants are formulated with TBN boosters to help increase the ability of the lubricants to fight acids build-up. TBN level in a lubricant depends on its targeted application. For spark ignition engines TBN (5-10 mgKOH/g), for compression ignition engines, TBN (15-30 mgKOH/g) and for more harsh environments such as that of marine TBN value greater than 30 mgKOH/g is used (Totten, 2006).

2.13.11 Total Acid Number (TAN) / Neutralization Number (NN)

Total acid number is the measure of acid concentration present in a lubricant. When an engine is put to use, its TAN continues to increase due to accumulation of acidic contamination and oxidation by-products. This consequently reduces its TBN. A point is reached when TAN = TBN. At this point, called neutralization number, the lubricant is no longer able to perform its function and the engine is at risk of sludge formation, wear and corrosion (Totten, 2006).

2.13.12 Elemental Content

Various types of elements are found in lubricating oil depending on the origin of the oil, method of production and types of additives used. Traces of elements are found in used lubricating oils from mechanical wear of engine parts, or as contaminants from fuel, air or coolant. The presence of some elements in used lubricant can be ascribed to mechanical wear of certain engine parts. For example, presence of Al in a used engine oil may indicate wear of piston, push rod, bearings,

gear casings or air cooler. Phosphorus and sulfur are the most critical elements in elemental analysis of fresh engine oil due to their role in deterioration of after treatment devices. The maximum permissible limit of each element present in fresh or used lubricating oil has been specified by oil standardization organizations such as International Lubricants Standardization and Approval Committee (ILSAC). For Phosphorus, 0.06-0.08 % are considered acceptable limit. While 0.5 % is the maximum acceptable limit for sulfur in engine oils (API/ILSAC, 2015).

2.13.13 Seal Compatibility

Lubricant has to be chemically compatible with the materials of oil seals used in the engine. Failure to use lubricating oil which is chemically compatible with elastomers results in swelling or shrinkage, excessive hardening, loss of elasticity, decomposition, and failure of the elastomers. This results in oil leaks, loss of pressure, shortage of lubricant and engine damage. So it is very important to carry out seal compatibility test of lubricating oil before use in the engine.

2.13.14 Oxidation Stability

Oxidation is a chemical reaction that changes the structure of molecules due to presence of oxygen and heat. Oxidation leads to change in the desirable properties of the lubricant and renders it less effective at preventing even parts (Singh, 2004). It also decomposes lubricants to polar compounds like aldehydes, ketones, carboxylic acids and oxygenated polymers. These compounds are either acidic or can lead to formation of resins, deposits and sludge which are harmful to engine parts (Fan, 2010).

2.13.15 Specific Heat Capacity

The Specific heat capacity of lubricating oil plays a special role in cooling the engine. The thermal energy absorption capacity of lubricating oil depends on its specific heat capacity.

Therefore the higher the specific heat capacity of a lubricant the better its ability to absorb heat at hot spots and reject it to the surroundings.

2.13.16 Coefficient of Thermal Conductivity

Engine lubricating oil aids in both conductive and convective heat transfers of the engine. Conductive heat transfer occurs through the boundary layers formed by the lubricant between the engine components. Whereas, convective heat transfer occurs between the lubricating oil and all the engine parts that come in contact with it. Lubricant with high coefficient of thermal conductivity will be more effective in dissipating heat to the surroundings.

2.13.17 Ash Content

The sulfated ash of lubricating oil is a measure of the noncombustible constituents (usually metallic materials) contained in a sample. It is determined by burning the oil sample in a container, treating the residue with sulfuric acid and burning it again to a very high temperature. The remaining residue is then used to compute the ash content. New, straight mineral lubricating oils contain essentially no ash-forming materials. Most additives used in engine oils, contribute to the total ash content of the lubricant (Fan, 2010). API did not specify ash contents for SI engines. It however specified 1.0 % max for CI engines and 35 mg as the max total engine deposits for SM and SL service classes (API/ILSAC, 2015)

2.13.18 Demulsibility

This refers to the ability of lubricating oil to separate from water after mixing. Emulsification of engine oil with water often occurs due to condensation of water vapor in the crankcase, or leakage of engine coolant. Lubricating oil should have quick separability from water in the event of water contamination so as to have effective lubrication to avoid engine damage. Chemicals known as demulsifiers are often used to enhance demulsibility of lubricating oils by altering the

surface tension at oil/water interface to accelerate separation. Examples of demulsifiers are polyoxyalkylate resins, alkylphenol ethers and light synthetic sulfanotes (Totten, 2006).

2.13.19 Corrosion Stability

Corrosion is the disfiguring of metal by chemical or electrochemical action of its environment. Lubricants shield metallic surfaces from corrosion by coating them. This prevents their exposure from oxidizing agents such as oxygen and moisture. Engine oil should not corrode pipe lines or any engine part during service (Singh, 2004). Methods used for evaluation of corrosion resistance of lubricating oil include the ASTM D 5844 for SI Engine oils (Sequence IID). ASTM D 6557 is a bench test designed to replace the ASTM D 5844 method. ASTM D 6557 uses a Ball Rust Test (BRT) method that subjects metal test specimen to an acidic solution in test tubes. The test shows the ability of an oil to prevent or resist rust under short trip conditions (Totten, 2006). Heavy Duty Diesel Engine Oil Test uses the ASTM D 5968 Standard. The method evaluates the tendency of diesel engine lubricant to corrode alloys of lead and copper commonly used in cam followers and bearings (Totten, 2006).

2.14 Additives

Lubricant base oils do not have the necessary properties to perform satisfactorily in all environments and at all operating conditions without support (Fan, 2010). Lubricant additives are chemical compounds that enhance the performance of lubricating base oil or add new desirable property to the lubricant. Such properties include suitable viscosities at all operating conditions, high flash point, thermal, oxidative and shear stabilities, good cleaning and dispersing ability, fluidity at low temperature, etc. Examples of automotive lubricant additives are:

2.14.1 Oxidation Inhibitors

All lubricants by virtue of their hydrocarbon origin are susceptible to oxidation. Oxidation makes oil thick and forms harmful deposits that can corrode and hinder free movement of engine parts. Excessive oil oxidation is normally due to overworking and overheating. Biolubricants are least stable to oxidation compared to Mineral base and Synthetic lubricants (Kumar and Sharma, 2011 and Mobarak *et al.,* 2014). Oxidation inhibitors are used to hinder oxidation reaction in lubricants. They are classified as hydro-peroxides decomposers, radical scavengers or metal deactivators, depending upon the mode of their controlling action. The most commonly used oxidation inhibitor is zinc dialkyl dithiophosphate (ZDDP) additive (Totten, 2006).

2.14.2 Anti-wear

Anti-wear additives form protective film on the metallic surface to protect them from tear and wear. Polar organic compounds such as alcohols, fatty amines, fatty esters and organic compound of phosphorous, sulphur, zinc, lead and molybdenum are good examples of anti-wear agents. Zinc dialkyldithioposphate ZDDP additive can be used as both anti-oxidant and anti-wear additive (Audibert, 2006).

2.14.3 Dispersants

These are additives that suspend oil-insoluble resinous oxidation products and particulate contaminants in the bulk of the lubricant, thereby minimizing sludge formation, viscosity increase and deposit formation. Dispersants suppress the interaction between resin and soot particles, by preferentially associating with them, and at the same time, keeping them suspended in the bulk of the oil. Dispersant agent commonly in use include polybutenyl succinimide. (Totten, 2006).

2.14.4 Detergents

These perform like dispersants, and in addition, have the ability of controlling rust, corrosion, and resinous build-up by neutralizing oxidation products and acidic combustion. Detergents are normally described chemically in terms of their metal ratio, soap content, sulfated ash, degree of over-basing or conversion, and Total Base Number TBN. Common examples of additives used as detergents are: calcium sulfonates, and alkyl phenyl sulfides (Totten, 2006).

2.14.5 Viscosity Index Improvers (VII)

The Viscosity index of lubricating oil is the grade indicator of the lubricant. The higher the viscosity index the better the lubricant. Viscosity Index Improvers are additives used to help the lubricant retain its viscosity when there is temperature change. The materials commonly used as viscosity index improvers are the long-chain polymers which are capable of changing their molecular structure with temperature. The Polymers stretch out at high temperatures to interact with each other to maintain viscosity. The polymers which can perform such effects include hydrogenated styrene butadiene polymers and olefin polymers (Audibert, 2006).

2.15 Additive Packages

Additive manufacturers produce automotive additive packages for various applications. These include additives for passenger car motor oil (PCMO) for both gasoline and diesel engines, additives for small engines such as 2-stroke and 4-strokes motorcycles, additives for marine engine, etc. The additives come either as single, like TBN boosters, viscosity index improvers (VII), anti-oxidants, etc. or universal which combines various additives in one package. Various trade names are used for the additive packages depending on the manufacturer's choice. Examples are OLOA (e.g. OLOA 219, OLOA 11000, OLOA 55402, etc.). The additives are produced for various API/ILSAC performance classes. Such as SF, SG, SM, SN, CF-4, CF-2, CF, etc.

2.16 Engine Oil Grades.

The Society for Automotive Engineers (SAE) has classified engine oils based on their viscosities in its SAE J300 Series. This classification has received universal acceptance though other similar classifications exist like those of the International Organization for Standardization (ISO). In the SAE Classification, two series of viscosity grades are defined; Multigrades and Monogrades. Most oils used in modern vehicles are Multigrade oils. This is indicated by the familiar nomenclature like 10W30 or 15W40. The first number is the winter weight of the oil. It indicates how the oil behaves when cold. '10W' indicates that the oil behaves as a straight SAE 10 weight oil when cold .The second number (30, 40, 50, etc) is the nominal viscosity of the oil at $100^{O}C$. Thus, a 10W30 behaves the same as straight 30 weight oil when it is hot (Fan, 2010). Many new engines now use lighter oils, like 5W20, to achieve higher fuel efficiency (Humphrey, 2016).

2.17 Engine Oil Specifications

The quality of engine oil is assessed based on universally accepted specifications for engine lubricants. These specifications are commonly referred to as service ratings. The followings are most accepted standards for engine lubricants specifications (Totten, 2006):

2.17.1 American Petroleum Institute (API)

The API sets minimum performance standard for lubricants. The service classes are divided into S for service/ spark ignition engine for passenger cars and light trucks using petrol and C for commercial/ compression ignition engine. The standard carries designations which show the quality level of the oil. The API uses standard bench tests to evaluate chemical and physical properties of oil. These properties include high temperature behavior, oxidation stability, fuel economy and components wear. Petrol engines designations are SA, SB, SC, SD, SE, SF, SG,

SH, SJ, SL, SM and SN. The first seven are considered obsolete with SN being the most recent (API/ILSAC, 2015).

2.17.2 International Lubricant Standardization and Approval Committee (ILSAC)

This governs international oil specifications and represents the interest of American and Japanese manufacturers association to API. ILSAC and API jointly develop newest specifications. However, ILSAC puts more emphasis on exhaust system efficiency and fuel economy. The designations of ILSAC include: GF-2, GF-3, GF-4 and lately, GF-5 (API/ILSAC, 2015).

2.17.3 Association of Constructors of European Automobile (ACEA)

The ACEA is the European equivalent of API. The ACEA creates its Specifications by subjecting oils to sequence tests which are regularly updated. The designations used by ACEA are (ACEA, 2016):

A= Petrol engine with A_1, A_2, A_3, A_4 and A_5 specifications;

B= Diesel engine with B_1, B_2, B_3, B_4 and B_5 specifications;

C= Catalyst compatible (low sulfated ash, phosphorus and sulfur, SAPS) = C_1-04, C_2-04, C_3-04 specifications.

2.17.4 Japanese Automotive Standard Organization (JASO)

The JASO T904 Standard is used for four-stroke petrol engine. JASO T904-MA are meant for wet clutch engines, whereas JASO T904-MB for non-wet clutch engines.

2.17.5 Original Equipment Manufacturers (OEM)

The OEM publishes list of all lubricants it approves based on their engine requirements. Before approving a lubricant, the OEM subjects the oil to series of physical and chemical analyses deemed critical by OEM for their engines applications.

2.18 National Industrial Standards (NIS)

The Standard Organization of Nigeria (SON) publishes standards known as National Industrial Standard (NIS). The standard specifies the minimum performance requirement of engine lubricating oils among other things for use in reciprocating internal combustion engine of spark ignition and compression ignition (NIS, 2017). This standard is therefore also used here to evaluate the quality of the engine oil produced.

2.19 Minimum Requirements of Biolubricants

The Organization for Economic Cooperation and Development (OECD) and the European Standards Organization EN ISO have established standards for minimum requirements for biolubricants. These standards include bio-based carbon content, biodegradability, ecotoxicity and performance. Biolubricants are therefore evaluated for such properties against the OECD and EN ISO Standard. In the standard, engine oils are of family E with international standard code: ISO 2454 and ISO 13738.

2.20 Oil Circulation in Internal Combustion Engine

The oil sump of internal combustion engine is a rigid container made of pressed steel sheet or in some cases aluminium alloy. It has a shallow downward slope at one end, forming a deep shallow reservoir at the other end. It serves as a store to the engine oil. It collects oil draining from the crankshaft bearing, piston assembly, cylinder wall and the top cylinder. Figure 2.1 shows a typical oil circulation circuit of four stroke internal combustion engine. Sludge and contaminants such as metal particles settle at the bottom of the sump before they are drained during service. The oil pan performs a crucial task of dissipating heat from the engine oil to the atmosphere. Oil strainer in the oil sump filters oil from the sump. Oil pump sucks oil from the sump through the strainer and supplies it to secondary oil filter which is regulated by an oil

pressure regulator. Clean oil leaves the oil filter to the oil lines and galleries meant to lubricate the moving engine parts.

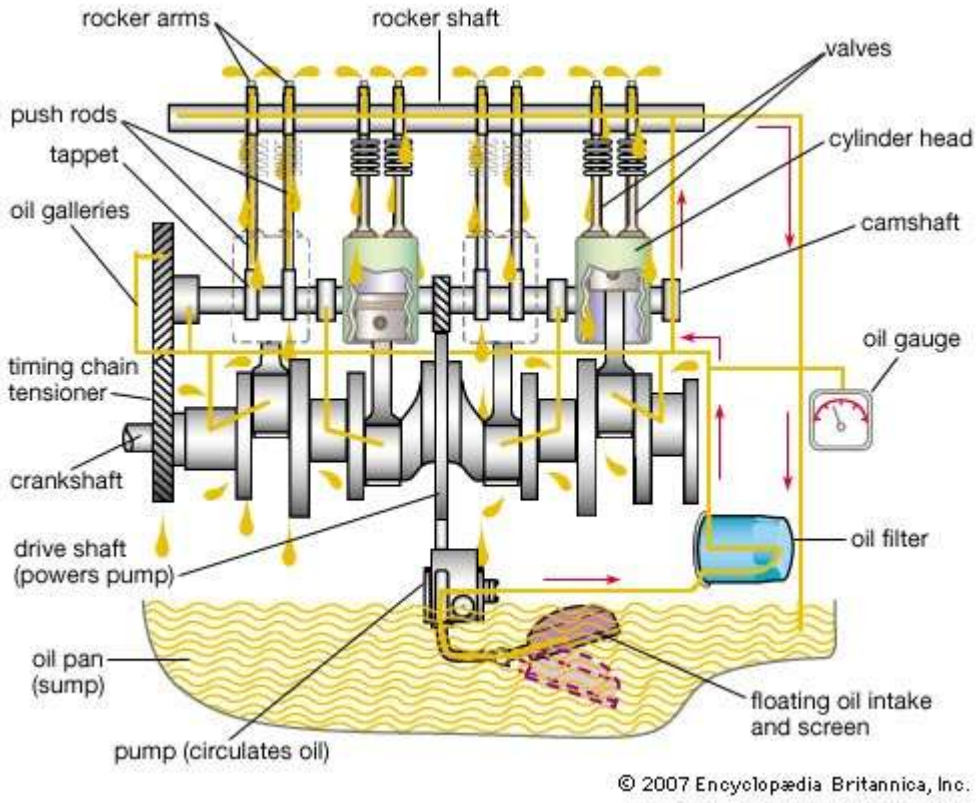


Figure 2.1: Engine Oil Circulation in IC Engine (2007 Encyclopedia Britannica,Inc.)

Oil from the main gallery flows through the crank shaft and main bearing holes to lubricate them. Oil sprout sprays the oil upward to lubricate the piston assembly from its inside. The oil flows through the oil rings to lubricate and form a thin film around the cylinder walls. The second gallery and the sprouts connected to it help in lubricating the camshaft, valves and valve springs after lubricating the engine parts, oil begins to flow downwards through a separate passage back to oil sump. In an engine that uses splash lubrication system, oil is splashed to the engine components by means of a scoop attached to the crankshaft (Gill, 2013).

2.21 Internal Combustion Engine Performance

The internal combustion engine performance is a measure of how effectively the chemical energy content of its fuel is converted to useful power output. To study engine performance, both the power and the torque characteristics are considered. The following are imperative for internal combustion engine performance analysis (Gill, 2013):

2.21.1 Specific Fuel Consumption

This is a measure of the amount of fuel consumed per unit mechanical power developed by the engine. It is expressed as (Singh, 2004):

$$\text{Specific Fuel Consumption} = \frac{\text{Mass of Fuel Consumed X 3600}}{\text{Mechanical Power}} \qquad (2.1)$$

where:

Specific Fuel Consumption $\{kg.(kW.h)^{-1}\}$

Mass of fuel consumed ($kg.s^{-1}$)

Mechanical Power (kW).

2.21.2 Air Consumption

The mass flow rate of air through the combustion chamber is determined by computing the quantity of air that passes through an orifice fitted into the test set up. It is expressed as:

$$\dot{m} = \frac{\pi d^2 C_d}{4}\sqrt{\frac{2 p_A \Delta p}{R T_A}} \qquad (2.2)$$

where:

d Orifice diameter (m)

C_d Discharge coefficient

p_A Ambient air pressure (bar)

Δp Difference between ambient air pressure and pressure just after the orifice (bar)

T_A Ambient air temperature (K)

R Molar gas constant (J kg^{-1} K^{-1})

2.21.3 Air/Fuel Ratio

This is the ratio of air mass flow rate ($\dot{m}_a$) to fuel mass flow rate ($\dot{m}_f$). It is given by:

$$\text{Air/Fuel Ratio} = \frac{\dot{m}_a}{\dot{m}_f} \tag{2.3}$$

2.21.4 Mean Effective pressure

This is the average mean effective pressure in the cylinder that would produce the measured brake output. BMEP is considered as the uniform pressure in the cylinder as the piston travels from TDC to BDC during each power stroke. It is determined from (Gill, 2013):

$$BMEP = \frac{60 \text{ X Power X } (\frac{\text{Strokes}}{2})}{0.1 \text{ x Speed x Engine Capacity}} \tag{2.4}$$

where:

BMEP (bar)

Power (W)

Speed ($rev.min^{-1}$)

Engine Capacity (cm^3)

2.21.5 Brake Power

This is the power available at the engine output shaft as measured by the dynamometer. It is expressed as (Singh, 2004):

$$\text{BP} = \frac{2\pi NT}{60} \tag{2.5}$$

where:

BP = Brake Power (W)

N = Engine Speed (rev. min^{-1})

T = Engine Torque (Nm) measured by the dynamometer

2.21.6 Brake Thermal Efficiency

This indicates the percentage of energy present in the fuel which is converted to useful work. It is expressed as (Singh, 2004):

$$\text{Brake thermal efficiency} = \frac{BP}{\dot{m}_f . Q_{LHV}} \qquad (2.6)$$

where:

BP = Brake Power (W)

$\dot{m}_f$ = fuel flow rate (kg/s)

Q_{LHV} = fuel lower heating value (kJ/kg)

2.22 Engine Oil Flow Regimes in the Spark Ignition Engine

Flow of engine oil in the spark Ignition engine is predominantly turbulent. The engine used for this work uses splash lubrication system. Oil stored in the oil pan at the bottom of the engine is thrown upward to the upper part of the engine by a dipper attached to the crank shaft. The oil splashed lubricates all the engine bearings, cylinder wall, piston and piston rings, intake and exhaust valves and cam assembly. The oil passes through all the oil holes and then is drained down and collected again in the pan (Gill, 2013).

2.23 Internal Combustion Engine Heat Transfer

Heat transfer analysis in internal combustion engine is indispensable due to the special role it plays in the performance, emission and lifespan of internal combustion engines. Agrira (2012) reported that about 25-35 % of the energy content of fuel is dissipated in the engine through heat transfer The temperature in the combustion chamber is about 2800 K, and the materials of the

engine components cannot withstand it (Lounici *at al.,* 2010). The components with the highest temperature are the spark plug, the piston face and exhaust valve and port. The heat transfer process in the internal combustion engines involves all the three modes of heat transfer, namely, conduction, convection and radiation.

The heat transfer from the gases to the solid walls of the engine is mainly by forced convection with some contribution by radiation. Heat is transferred through the solid walls purely by conduction and then convected to the cooling medium. According to Stone (1999) and Borman and Nishiwaki (1987), the radiation heat transfer is negligible in spark ignition engine.

2.23.1 Heat Transfer in the Intake and Exhaust Manifolds

The inlet manifold carries the air-fuel mixture to the combustion chamber through the inlet valve. Due to the proximity of the manifold to the combustion chamber, its surface temperature is much higher than that of the charge. Thus, the charge is heated and starts vaporizing before it enters the combustion chamber. On some designs, both the inlet and the exhaust manifolds are mounted on the same side of the engine, thereby enhancing heat transfer between the hot exhaust gases and the air-fuel mixture and facilitate vaporization of the charge. By making the fuel vaporize at an earlier time, this gives enough time for the air and the fuel to mix, therefore providing a homogenous charge that is ready for combustion in the combustion chamber. The heat flux between the manifold and the charge is given by:

$$\dot{q} = h\left(t_w - t_f\right) \qquad (2.7)$$

where t_w and t_f are the inner surface temperature of the manifold and the temperature of the charge respectively; h is the heat transfer coefficients and depends on some parameters such as the charge's physical and thermal properties, velocity, etc.

2.23.2 Engine Oil Heat Transfer

As the engine oil circulates from the oil sump through oil galleries, holes and over surfaces to the cylinder head and back to the oil sump it acts as a heat transfer medium carrying away heat from hot surfaces and dissipating it to the surroundings. A thin film of oil is formed on surfaces and in between sliding and rubbing surfaces. The type and thickness of film formed depend on the part geometry, location and the relative speed of the part and the lubricating oil at the point.

Heywood (1988) reported that heat is transferred from the gases to the engine coolant by the engine oil. This transfer may be by conduction or convection depending on the location.

2.24 Modeling and Simulation

According to Meyer (2004), model is an object or concept that is used to represent something else. It is reality scaled down and converted to a form we can comprehend. A model can be mathematical or nonmathematical. A mathematical model consists of variables, constants, functions, equations, etc. whereas a nonmathematical model is a physical (concrete) model that can be used for experimentation. For example a model car made of plastic or wood. Utilizing mathematical models to analyze and improve the performance of a device or situation is quite cheaper, faster and simpler than experimentation on a physical model.

Simulation is a computer technique used to analyze the behavior of a real or imaginary system. One or more variables affecting the system behavior is changed and the resulting effect on the system is studied. Simulation helps designers to analyze the behavior of a system under different operating conditions easily and conveniently.

2.24.1 Types of Spark Ignition Engine Numerical Models

Basically two types of model exist for heat transfer modeling of SI engine. These are fluid dynamic models and thermodynamic models (Spitsov, 2013).

2.24.1.1 Fluid Dynamics Models

Fluid dynamic models also called multi-dimensional models are used for Computational Fluid Dynamic (CFD) simulations. They are utilized in SI engine analyses to predict intake and exhaust flow characteristics; combustion processes and flow patterns of combustion gases; engine oil circulations and heat transfer (Spitsov, 2013). All these are performed by numerically solving continuity, momentum and energy conservation equations. Examples of computer codes that perform fluid dynamic modeling are DNS (Direct Numerical Simulation), LES (Large Eddy Simulations), URANS (Unsteady Reynolds Average Navier-Stokes), etc.

2.24.1.2 Thermodynamic Models

Thermodynamic models are also referred to as zero models. In these models, flow geometries are not required. Combustion processes, in-cylinder pressure and temperature changes with crank angle, engine performance indicators, temperature profiles, etc are predicted by inputting the engine parameters and the fluids properties. Examples of computer codes that perform this modeling are Fluent, GT- Suite, Z88, Opensees, FreeFem ++, etc.

2.25 Review of Some Related Past Research on Biolubricant

2.25.1 Production of Biolubricants and Determination of their Physico-chemical Properties

Hassan *et al*. (2006) explored the Possibility of producing biolubricant using palm oil. Physical and chemical properties of the palm oil were analyzed. Their findings showed that the crude palm oil possessed the required properties for biolubricant formulation.

Saliman *et al*. (2008) extracted and characterized jatropha oil from Malaysian jatropha seeds and

Nigerian jatropha seeds using sohxlet apparatus. Physico-chemical properties of the two oil samples showed that Malaysian jatropha oil had lower iodine value and free fatty acid of 91.70 mg/g and 1.03 % than Nigerian jatropha oil, which had 105.20

mg/g and 1.76 % respectively. Nigerian jatropha oil recorded better saponification value of 198.85 mg/g than Malaysian, which gave 208.5 mg/g.

Cheenkachorn and Fungtammasan (2010) investigated the use of palm oil as base oil for biolubricant formulation for small four-stroke motorcycle engines. Compared to mineral-based oil, the palm oil-based lubricant exhibited superior tribological properties but offers no significant advantage on engine and emission performance.

Bekal and Bhat (2012) reported the use of pongamia and mineral oils blended in the ratio (1:1 V/V) on CI engine. Various combinations of fuel and lubricant were tested. Co_2, hydrocarbons, exhaust gas temperature, particulates and nitrogen oxides and smoke were compared. Best results were obtained for the fuel-lubricant combination.

Navindgi *et al.* (2012) used straight vegetable oils of neem, mahua, linseed, and castor oils on CI engine. The performance parameters evaluated included thermal efficiency, specific fuel consumption, and exhaust gas temperature and emissions. Significant improvements have been reported in the performance parameters of the engine as well as exhaust emissions with use of neem, mahua, and castor oil as compared to baseline data of diesel.

Shahabuddin *et al.* (2013) investigated the tribological characteristics of biolubricant formulated from Jatropha oil using Cygnus friction and wear testing machine connected to a computer. The results revealed that blend of 10 % jatropha

oil with SAE 40 mineral base lubricant can be used as lubricating oil without any shortcoming.

Manji *et al*. (2013) extracted and studied the physico-chemical properties of balanites *egyptiaca* seeds oil using mechanical extraction method. The results showed that the oil yield was 49.9 %, Refractive Index, 1.4784, Sap Value, 168.6 mgKOH/g, Iodine Value, 78.7 g I_2/100 g, Peroxide Value, 6.0 mEq/kg, FFA, 0.18 %, Specific Gravity, 0.9207 and Water Content, 0.27 %. Liquid soap and shampoo were produced from the oil and the products compared favorably with similar products in the market.

Vijayakumar *et al.* (2014) investigated the usability of palm oil as a lubricant to substitute mineral oil in CI engine. They used 25 and 50 % blends with mineral oil SAE 20W40. Their findings revealed that the formulated blends of palm oil showed similar performance to commercial SAE 20W40 oil in terms of efficiency and brake specific fuel consumption.

Bongfa *et al.* (2015) investigated and compared the lubrication properties of castor oil with 20W50 engine oil using four-ball tester. The results showed that castor oil has better load bearing capability and friction and wear reduction performances than mineral base 20W50.

Ghobadian *et al.* (2015) used biolubricants (TMP-triesters) formulated from castor oil, palm oil, and waste cooking oil in a 200 cc two-stroke gasoline engine to investigate their effects on the engine performance and exhaust emissions. TOPSIS

algorithm showed that palm oil-based lubricant took up the greatest distance from the Negative Ideal Solution (NIS) and was selected as the most optimal lubricant for these types of engines.

Mohammed (2016) produced and tested biodegradable grease from balanites *aegyptiaca* seeds oil. The oil was extracted using solvent extraction method. Consistency, drop point and gear wear tests were carried out to assess the performance of the biogrease. The consistency was found to be of NLGI 'O' Class. Dropping point, 65^{o}C to 161^{o}C. Good anti wear characteristics comparable to mineral base grease was obtained for the biogrease.

2.25.2 Effects of Additives on the Performance of Biolubricants

Durak (2004) studied the effect of rapeseed oil as additive to mineral oil on specially designed experimental system and compared the lubricating oil in journal bearings. It was reported that, addition of rapeseed oil to mineral-based lubricant reduced the friction coefficient in journal even at high temperature.

Erhan *et al*. (2006) studied oxidation stabilities (using differential scanning calorimetry, rotary bomb oxidation and long-term oven oxidation methods) and low temperature behaviors (pour point) of refined soybean oil, high-linoleic soybean oil, mild-oleic soybean oil, high-oliec soybean oil, high-oleic safflower oil and high-oleic sunflower oil. Polyalphaolefin and commercially available hydraulic oils were used for comparison. Zinc diamyl dithiocarbonate and antimony dialkyldithiocarbonate

additives were used. Best results were obtained when additives were added to the samples.

2.25.3 Effect of Epoxidation of Performance of Biolubricants

Salimon and Fong (2012) epoxidized Palm Kernel Oil Fatty Acids (FAPKO) using peroxyformic acid generated in-situ. About 80 % yield was achieved, with 1.15 % oxirane ring and 99 % oxirane conversion.

Saremi *et al*. (2012) epoxidized soybean containing 26 % oleic acid, 7 % linoleinic, 4 % stearic, 11 % palmitic and 52 % linoleic using performic acid. The maximum epoxy content achieved for epoxidized Soybean oil was 6.1 % (wt).

Sammaiah *et al.* (2014) produced epoxidized jatropha oil (EJO) by peroxyformic acid generated in-situ at 60^{o}C. The sample was examined periodically for oxirane value. The maximum oxirane obtained was 5.0 % after 2 h. The EJO has PP 0^{o}C, FP 288^{o}C, IV 2 mg I_2/g, and VI 139.

Rajaendran *et al*. (2016) carried out epoxidation of neopenthyl glycol diolete (NPGDO) using formic acid and hydrogen peroxide to produce epoxidized NPG diolete (ENPGDO). The presence of epoxy in the product was confirmed using FTIR. The product was found to have VI 218, FP 205^{o}C, PP -18^{o}C, OS 197^{o}C.

Chieng *et al.* (2017) used EJO as a green plasticizer and added to poly (lactic acid) PLA. The EJO was compounded into PLA at different contents. The EJO was synthesized by in-situ epoxidation. OOC of EJO was 4.3 %, Acid Value 4.63

mgKOH/g, Iodine Value 0.68 g I_2/100g. Addition of 3 wt % of EJO to PLA demonstrates significant improvement in flexibility.

Wong *et al.* (2017) used jatropha oil to produce epoxy and epoxy acrylated as a raw material. The EJO was synthesized by in-situ epoxidation using formic acid and hydrogen peroxide. The measured oxirane-oxygen content (OOC) of EJO was 4.99%. The acid value of AEJO was 4.4 mgKOH/g.

Alejandro *et al.* (2018) used grape seed, avocado and olive oils naturally containing high percents of mono and poly unsaturates as raw materials for production of unsaturated methyl esters. It was confirmed that using 1H NMR, 13C NMR and GC-MS that addition of lauric acid to the enzymatic reaction was unnecessary to transform the alkene into epoxides.

Chen *et al.* (2019) presented a catalytic protocol for the efficient epoxidation of vegetable oils using H_2O_2 as an oxidant, acetic acid as an additive and manganese as catalyst. A homogeneous catalyst based on the non-noble metal manganese in combination with a racemic mixture of the ***N***,***N′***-bis (2-picolyl)-2,2′-bispyrrolidine ligand (***rac***-BPBP) was used. The optimized reaction conditions entailed only 0.03 mol % of the manganese catalyst with respect to the number of double bonds (***ca.*** 0.1 wt % with respect to the oil) and ambient temperature. The results showed that most of the vegetable oils studied, including cheap waste cooking oil, were fully epoxidized to EVOs with more than 90% yield within 2 h of reaction time.

2.26 Review of Related Works on Modeling and Simulations of Internal Combustion Engines

Shaari *et al.* (2010) carried out the design of connecting rod of internal combustion engine and optimization. The connecting rod was modeled using Solidworks. Finite element analysis (FEA)

and topology optimization were carried out using MSC/PATRAN and MSC/NASTRAN Softwares. Mesh convergence analysis was done to get the best mesh for the analysis. TET4 and TET10 were used in the FEA. The TET10 produced better result than TET4. The optimized connecting rod was 11.7 % lighter with low maximum stress compared to the initial design.

Vdovin (2010) modelled and simulated the cooling system of a Volvo FH truck on a module of GT-Suite. The results were evaluated against experimental results. Detailed modelling of the under-hood flow in 3D environment called Cool3D was done to construct a model of the cooling package and its surroundings. This model was added to the initial model and the results of the simulation were compared to the first simulation and experiment. The first model was constructed using a mapped engine for obtaining heat release values of different components at various engine loads and speeds.

Krishna *et al*. (2013) developed a 3-D Solidworks of diesel fuel injection nozzle of Land Rover V4 engine. Solidworks package FlowXpress was used for 3-D flow analysis. The fuel flow profile obtained from the FlowXpress at steady state conditions in the nozzle was validated with the results of the analytical calculations. From the contours generated, optimum injection angle which gave best fuel swirl was chosen.

Haqui and Raddy (2015) developed a paradigm of 4 cylinder engine assembly victimization CAD tool using Solidworks. Thermal analyses were carried out of the engine piston, crankshaft, camshaft and valve at 800 K thermal loading. Temperature distributions were presented. The best material for effective operation of the engine was chosen.

Nitnaware and Giri (2015) modeled a four stroke, single cylinder, air-cooled Bajaj Pulsan 150cc engine. Optimization of the fin profile and fin array parameters for a given heat flux were carried out using Gambit and Fluent/Ansys. Heat transfer per unit weight was found to be larger for

conical fins than rectangular fins. Also aluminium was found to be a better material for fins design for air-cooled IC engines due to their low weight, high rate of heat transfer and lower cost.

Datta and Singh (2017) carried out modeling and simulation of an air cooled, 4-stroke single cylinder SI engine for Hero bike using Solidworks. Operating gas temperature and material properties were used as the simulation parameters. The max gas temperature was 100^{o}C. The materials used for the piston were cast iron, cast alloy steel and carbon graphite. The thermal analyses performed led to the conclusion that carbon graphite was the best material for the engine under study due to its light weight, excellent thermal conductivity and excellent resistance to thermal shock.

Dominic and Gao (2017) investigated the effect of velocity stacks of C20XE Vauxhall engine for motorsports applications. Solidworks was used to model the engine. Fluent and ICEMCFD softwares were used to analyse the engine in 2D domain. All values were validated for a flow at various valve positions. Velocity and pressure contours for various valve lifts were presented. The results showed that shorter stack length was more suited for high speed applications.

Garg and Garg (2017) investigated the effect of different piston head configurations on volumetric efficiency, turbulence, swirl and tumble ratio of a single cylinder diesel engine. Solidworks was used to model various piston configurations. Analyses were done using Ansys. The effects of various configurations on the airflow velocity vectors at various points were analysed. Best piston configuration was finally chosen.

Reddy and Vaithe (2017) carried out study of two-stroke internal combustion engine connecting rod. The rod was modeled using Solidworks 2016 design software. Ansys 14.5 was used to carry out static structural analysis. The analysis was performed at 16 MPa using aluminium alloy,

titanium alloy and $42Crm0_4$ and aluminium metal matrix (KS1275) using boundary conditions. Stress, deformation, strain and maximum shear stress were determined. The results showed that titanium alloy $42Crmo_4$ had lowest deformation value, followed by aluminium metal matrix.

Menacer *et al.* (2017) used commercial GT-Power software to study the effect of various engine parameters on the convective heat transfer flux of a 6-cylinder in-line turbocharged direct injection engine. The parameters studied were compression ratio, engine speed, stroke-bore ratio, cylinder wall temperature, quantity of fuel injected and injection timing. It was concluded that stroke-bore ratio and compression ratio have less effects on the convective heat transfer. The remaining parameters have great influence on the convective heat transfer flux.

Pranita *et al.* (2018) analyzed the cooling system for 6 cylinder diesel engine using 1D method by using GT-Suite to perform a comprehensive study of mass-flow and thermal distribution over the inlet of the cooling package of a selected engine in several steady state operating points. The results showed that the predictive method successfully captured the thermal effect of recirculation while reducing the necessity for calibration done by prototype testing.

Graziano, *et al.* (2019) tested an innovative approach based on 1D simulation in the commercial 1D multi-physics code GT-Suite. A fully physical Diesel engine performance model - featuring a predictive combustion model - was integrated with a detailed finite element wall temperature solver based on the 3D meshing feature available in GT-Suite. Coolant and oil hydraulic circuits were implemented in the model and used to predict flow rate through the water jacket and oil gallery. In addition, a predictive detailed friction model of the crank train was built to better capture the interactions between metal and oil from the thermal standpoint. The integrated model was eventually validated against experimental measurements.

Hua *et al.* (2019) modelled some coupled thermal management systems with different structures which included air conditioning subsystem, waste heat recovery subsystem, engine and coolant subsystem using GT-Suite. CO_2 was chosen as the working fluid for both the air conditioning subsystem and the waste heat recovery subsystem. The system was simulated at different environmental temperatures and engine working conditions to choose the best structure. The optimal pump speed increased with the increase of environmental temperature and the decrease of engine load. The optimal coolant utilization rate decreased with the increase of engine load and environmental temperature, and the value were between 38 % and 52 %.

2.27 Methods of Modelling Internal Combustion Engines Heat Transfer

Modeling of internal combustion engine heat transfer may be grouped into five groups (Torregrosa *et al.*, 2008):

1. Global (one zone) thermodynamic models;
2. Zonal (more than one zone) thermodynamic models;
3. One dimensional analytical and numerical fluid dynamic models;
4. Multidimensional numerical Fluid-Dynamic (NFD) models and;
5. Radiative heat transfer models.

2.27.1 Global Models

In Global models the instantaneous heat flux is assumed to be dominated by convective heat transfer. Heat flow is likened to fluid flows over flat plate or in cylindrical pipes (Spitsov, 2013). Nusselt (1923) was the first to develop heat transfer correlation, based on Global model approach, for internal combustion engines. His model can be used to predict instantaneous heat flux of IC engines. The model consists of convective and radiative heat transfer coefficients added together. He used natural convection assumptions to develop the model. Thus,

$$h = 5.41.10^{-3}\left(1+1.24V_P\right)P^{\frac{2}{3}}T_g{}^{\frac{1}{3}} + \frac{4.21.10^{-12}\left(T_g{}^4 - T_w{}^4\right)}{\left(\frac{1}{\varepsilon_g}+\frac{1}{\varepsilon_w}-1\right)\left(T_g - T_w\right)} \quad (2.8)$$

where:

V_P is the average speed of the piston

T_g, P and ε_g are the respective temperature, pressure and emissivity of the working medium.

T_w and ε_w are the temperature and emissivity of the wall respectively.

Brilling (1935) modified Nusselt work by changing the mean piston speed term from (1+1.24 V_p) to (3.5+0.185 V_p). Thus Brilling Correlation writes:

$$h = 5.41.10^{-3}\left(3.5+0.185V_P\right)P^{\frac{2}{3}}T_g{}^{\frac{1}{3}} + \frac{4.21.10^{-12}\left(T_g{}^4 - T_w{}^4\right)}{\left(\frac{1}{\varepsilon_g}+\frac{1}{\varepsilon_w}-1\right)\left(T_g - T_w\right)} \quad (2.9)$$

Eichelberg (1939) proposed a heat transfer coefficient based on natural convection assumptions only. He used two stroke and four stroke large Diesel engines to measure instantaneous heat flux. Eichelberg's equation can be expressed as:

$$h = 7.67.10^{-3}V_P{}^{\frac{1}{3}}.P^{\frac{1}{2}}T_g{}^{\frac{1}{2}} \quad (2.10)$$

Eichelberg was the first to refute the additive approach of Nusselt model.

Annand (1963) reviewed the existing correlations for instantaneous heat transfer rate and experimented using two-stroke and four stroke CI engines. He used forced convection assumptions, instead of natural convection, to develop his correlations. The instantaneous heat flux is determined from:

$$h = \alpha\frac{k}{B}\mathrm{Re}^{0.7} + \beta\left(T_g{}^4 - T_w{}^4\right)/\left(T_g - T_w\right) \quad (2.11)$$

α is a constant ranging from 0.25 to 0.8 and β is a constant equal to 4.3 E^{-12} for SI engines, and 3.3E^{-11} for CI engines. The constant α represents a level of convection heat transfer; it varies from smaller value 0.25 for four stroke engine to higher value 0.8 for two-stroke engine. B is characteristic length.

Woschni (1967) also used forced convection assumptions to develop his correlations. Like Nusselt, he considered the heat transfer process to be quasi-steady and proposed:

$$h = 0.820 B^{-0.2} \left[Pw\right]^{0.8} T^{-0.53} \tag{2.12}$$

Woschni claimed that the characteristic speed w depends on the mean piston speed V_p during induction, compression and exhaust strokes and depends on swirl during combustion and expansion. Swirl is considered to be a function of the pressure rise due to combustion.

$$w = C_1 V_P + C_2 \frac{V_d T_1}{P_1 V_1} \left(P - P_m\right) \tag{2.13}$$

T_1, P_1 and V_1 are for reference state, like the beginning of combustion. Woschni suggested that for;

Induction C_1= 6.18, C_2 = 0

Compression C_1 = 2.28, C_2 = 0

Combustion and expansion C_1 = 2.28, C_2 = 3.24.10^{-3}

Hohenberg (1979) examined the Woschni model and argued that the correlation overestimates the heat transfer coefficient during compression and underestimates it during combustion, which results in overall overestimation of the heat transfer.

The modification made by Hohenberg included the use of instantaneous cylinder volume instead of cylinder bore and the characteristic speed was changed to V_p +1.4.

Also the temperature exponent was changed to -0.4. Thus, Hohenberg correlation writes:

$$h = C_1 . P^{0.8} . T_g^{-0.4} V_c^{-0.06} \left(1.4 + V_P\right) \quad (2.14)$$

where:

C_1 =130

V_P = 2 X engine speed X stroke

Some known global models include those of Tropy (1981), Borman and Nishiwaki (1987), Guibert (2005) and Ollivier (2006).

General Global models do not describe the details of local and unsteady heat transfer effects. They employ quasi-steady state assumptions to describe the overall conditions of the cylinder gas. The heat transfer coefficients provided by these models represent a spatially-averaged value for the cylinders. However, these models are still being used for heat transfer simulations in engines due to their simplicity (Spitsov, 2013).

2.27.2 Zonal Model

In this model, several separate zones are distinguished, for example, zonal model enables temperature modelling of fresh air zone and the burned zone. Also radiation effect can be separated from convection effect since they are driven by different temperature difference. The model helps in determining heat flux at a specific location (Spitsov, 2013).

LeFeuvre *et al*. (1969) used Zonal Model approach to develop a correlation for determining instantaneous heat flux on the cylinder head or piston of CI engine. They got:

$$q = \alpha \frac{k_g}{r} \mathrm{Re}^m \, \mathrm{Pr}^n \left(T_g - T_w\right) \quad (2.15)$$

where, $\alpha = 0.047$, $m = 0.8$ and $n = 0.33$.

Poulus and Heywood (1983) similarly, incorporated turbulence effect into cycle simulation of SI engines. They calculated effective gas velocity using:

$$U_{EFF} = \left[2(K + k) + \frac{V_P{}^2}{4} \right]^{\frac{1}{2}} \tag{2.16}$$

K stands for kinetic energy of the mean flow while, k stands for kinetic energy for turbulent flow.

Morel and Keriber (1985) developed their heat transfer correlation as follows:

$$h = 0.5 C_f \rho U_{EFF} C_P \, \mathrm{Pr}^{-0.67} \tag{2.17}$$

where U_{EFF} is the effective gas speed; C_f, the coefficient of skin friction; C_P, the coefficient of pressure and Pr is the Prandtl number.

2.27.3 One-Dimensional Models

Energy conservation equation is the usual starting point for one-dimensional heat transfer modelling. Han and Reitz (1997) based on one-dimensional energy conservation approach, developed a wall temperature function suitable for IC engines density variable turbulent flow. The formulation for wall heat flux is shown in equation 2.18. The model comprises a part for steady state solution of the conservation equation and a part corresponding to the unsteady state of the heat transfer.

$$q_W = \frac{\rho C_P U^* T \ln(T/T_W) - (2.1y^* + 33.4) Gv/U^*}{2.1 \ln(y^*) + 2.5}$$

$$-KT_o \left(\frac{P}{P_o}\right)^{\gamma - \frac{1}{\gamma}} \frac{k \rho_{oU^*}}{\mu_w} \left\{ \int_o^\tau \frac{1}{\sqrt{\pi(\tau - \theta)}} + 0.082 \left(1 - exp\left(-\frac{\sqrt{\tau - \theta}}{3}\right)\right) \frac{d\emptyset_{us}(0,\theta)}{d\theta} d\theta \right\} \tag{2.18}$$

where ρ is the density of the gas; C_P, the coefficient of pressure; U^*, dimensionless gas speed which is equal to $\sqrt{kC_u{}^{0.5}}$; y^+ is dimensionless distance; G is the source term in energy equation; K is the mean flow kinetic energy; T_o is the reference temperature and θ is dimensionless temperature;

ρ_o is the density of the gas at a reference point; τ is the transmittance; $\emptyset_{us}$ is unsteady dimensionless temperature; C_u is the gas tangential velocity due to swirl; μ_w is the dynamic viscosity at the wall and k is the thermal conductivity of the medium.

2.27.4 Multidimensional Models

These models numerically solve momentum equations, turbulent species, and conservation equations for reacting fluids. Numerical Computational Codes based on Multidimensional approach have become priceless tools for heat transfer modelling due to their ability of providing complete information of the in-cylinder flow pattern and behavior. The components of these models are: Mathematical models describing the flow process; discretization procedure used to transform the differential equations of the mathematical model into algebraic relations between discrete values of velocity, pressure and temperature that can be located on computing mesh, which conforms to the geometry of the combustion chamber; solution algorithms, whose function is to solve the algebraic equations and computer code which translates the numerical algorithm into computer language (Torregrosa *et al.,* 2008).

Mohammadi *et al*. (2008) used CFD code to compute the average heat flux at various locations of a spark ignition engine. Woschni correlation was used to compare with the computationally determined total heat flux on the combustion chamber. Close agreement was observed between the two results. Higher heat flux was recorded on the intake valves and the heat flux on the cylinder head was more than on the piston.

2.27.5 Radiative Heat Transfer Models

Models on Radiative heat transfer are intended for modelling heat transfer by radiation at a particular point. Radiative heat flux is a function of gas temperature in the near-wall region and the temperature of the combustion chamber walls. Soot is a major component of radiative heat

transfer that is why radiative heat flux in CI engines (about 10 %) is higher than those of SI engines (about 3-4 %) (Lounici *et al*. 2010).

2.28 Research Gaps

From what was presented so far, one may understand that many researchers worked on various vegetable oils. Some determined the tribological characteristics and physico-chemical properties of various vegetable oils; some formulated biolubricants, characterized and used them for low temperature applications. Some carried out chemical modifications such as epoxidation of some plant oils and determined their physical and chemical properties. After exhaustive search the following research gaps have been identified:

Research Gap 1: To the best of my knowledge, no available literature on physico-chemical properties of epoxidized jatropha biolubricant for spark ignition engine lubrication such as Total base number, foaming tendency, high-temperature-high-shear stability, evaporation loss, seal compatibility, elemental contents, etc;

Research Gap 2: Also, no data on thermal properties of epoxidized jatropha biolubricant such as coefficient of thermal conductivity and specific heat capacity;

Research Gap 3: Similarly, no work on performance parameters such as specific fuel consumption, brake mean effective pressure, thermal efficiency, etc. of epoxidized jatropha biolubricant on spark ignition engine;

Research Gap 4: Additionally, there is no work on heat transfer simulation of spark ignition engine lubricated with epoxidized jatropha biolubricant.

In this work, physico-chemical properties required for spark ignition lubricant base stock were determined and compared with those of mineral base oils. Furthermore, properties required for

spark ignition engine oil were determined for epoxidized jatropha biolubricant and its blends and compared with relevant standards. Also, thermal properties of epoxidized jatropha biolubricant and its blends were determined and used for the engine thermal analysis. In addition to that, the performance of the best biolubricant blend was tested on spark ignition engine and compared with a reference engine oil recommended by the engine manufacturer. The engine was modelled using GT software and heat transfer simulations were also carried out.

CHAPTER THREE

MATERIALS AND METHODS

3.1 Materials and Equipment

3.1.1 Materials

Jatropha oil was sourced at National Research Institute for Chemical Technology (NARICT), Basawa Zaria. Mineral SAE 30 automotive engine oil was sourced at Total blending Company, Kaduna. Other Materials used for the work include: formic acid, hydrogen peroxide, sulfuric acid, magnesium sulphate, anhydrous methanol, Sodium hydroxide, Potassium hydroxide, Sodium methoxide, Tetraoxosulphate (IV) acid, Hydrochloric acid, Trimethylolpropane (TMP), Isopropyl alcohol, Phenolphthalein, Calcium Oxide and a blend of B023232 (14.2 % wt) and B23333 (3.8 % wt) additive (Comprising anti-oxidant, anti foaming agent, detergent/ dispersant, pour point depressant and viscosity modifier) . The Apparatus used include: Beakers (50-500 mL), Burette (50 mL), Pipette (25 mL), Glass funnel, Measuring Cylinders (5-250 mL), Thermometers (Mercury-in-glass and thermocouples) and retort stand.

3.1.2 Equipment

Various equipment were used at various test centers all located in Nigeria. The following equipment were used during experimentation and testing of physico-chemical properties.

(i) Abbe's Refractometer (Range: 1.300-1.700) for measurement of Refractive Index available at College of Science and Technology Kaduna Polytechnic, Kaduna.

(ii) Beaker, measuring balance, etc for measuring Water Content (%) available at College of Science and Technology, Kaduna Polytechnic, Kaduna.

(iii) ASTM D150-1P 196 Colour Tester for measuring Colour available at Kaduna Refining and Petrochemical Company, KRPC.

(iv) Titration Set for measuring Iodine Value (mg I_2/g), Sap. Value, Base Number and Acid number (mgKOH/g) available at College of Science and Technology, Kaduna Polytechnic, Kaduna.

(v) Hydrometer, Fisher Brand (Size 0.795-0.910; 0.001 Accuracy) for measuring Density (kg/m^3) available at College of Science and Technology Kaduna Polytechnic, Kaduna.

(vi) Capillary Viscometer for measuring Viscosity available at College of Science and Technology Kaduna Polytechnic, Kaduna.

(vii) Cleveland Open Cup Tester, Stanhope-Seta for determining Flash Point (^oC) available at Kaduna Refining and Petrochemical Company, KRPC.

(vii) Pour Point/ Cloud Point Analyser – Stanhope for measuring Pour Point (^oC) available at Kaduna Refining and Petrochemical Company, KRPC.

(viii) Joule's Apparatus for determination of Specific Heat Capacity (kJ/kgk) available at College of Science and Technology Kaduna Polytechnic, Kaduna.

(ix) Lee's Apparatus for determination of coefficient of Thermal Conductivity (kW/mk) available at College of Science and Technology Kaduna Polytechnic, Kaduna.

(x) Copper Strip Corrosion Tester for measuring Copper Strip Corrosion available at Kaduna Refining and Petrochemical Company, KRPC.

(xi) Pressure Differential Scanning Calorimeter, STARe System by Mettler Toledo for determining Oxidation Induction Temperature (^oC) and Oxidation Induction Time (min) available at Faculty of Engineering, ABU, Zaria.

(xii) RionVT-03 Rotary Viscometer (Range: 1-330 mpa.s) for determination of High-Temperature High-Shear (HTHS) Viscosity @ 150^oC (cSt) available at College of Science and Technology, Kaduna Polytechnic, Kaduna.

(xiii) Noack Volatility Set for determination of Evaporation Loss (%) available at College of Science and Technology, Kaduna Polytechnic, Kaduna.

(xiv) Sulfated Ash Furnace for determination of Ash Content (%) available at OANDO, Kaduna.

(xv) FTIR, Cary, Agilent Technology (Range: 280 cm^{-1} to 4000 cm^{-1}) for measurement of FTIR Spectrum available at Faculty of Engineering, ABU, Zaria.

(xvi) X-ray Fluorescent, Spectrometer, 8000 Express, Version 1.99, Build 34 for determining Phosphorus/ Sulfur Content (ppm) available at Faculty of Engineering, ABU Zaria.

(xvii) Tribometer, Anton Paar Australia, serial: 0.001-0000.0000.0000 for determination of Coefficient of Friction/ Wear Rate available at Faculty of Engineering, ABU Zaria.

(xviii) Foaming Tendency Tester, N. Labo 76210 Lintot- France for determining Foaming Tendency for Sequence I, II, III available at Total Oil Blending Company, Lagos.

(xix) Demulsibility Tester Bath Ricaldo W 350 for determination of Demulsibility {ml-ml-ml (min)} available at Total Oil Blending Company, Lagos.

(xx) Hardness testing Machine for Seal Compatibility test available at College of Science and Technology, Kaduna Polytechnic, Kaduna.

(xxi) TecQuipment TD201 Engine Test Set for Engine Test available at Heat Engine Lab, Mech. Engineering Department, ABU Zaria.

3.2 General Methodology

The general methodology for this work is presented in figure 3.1.

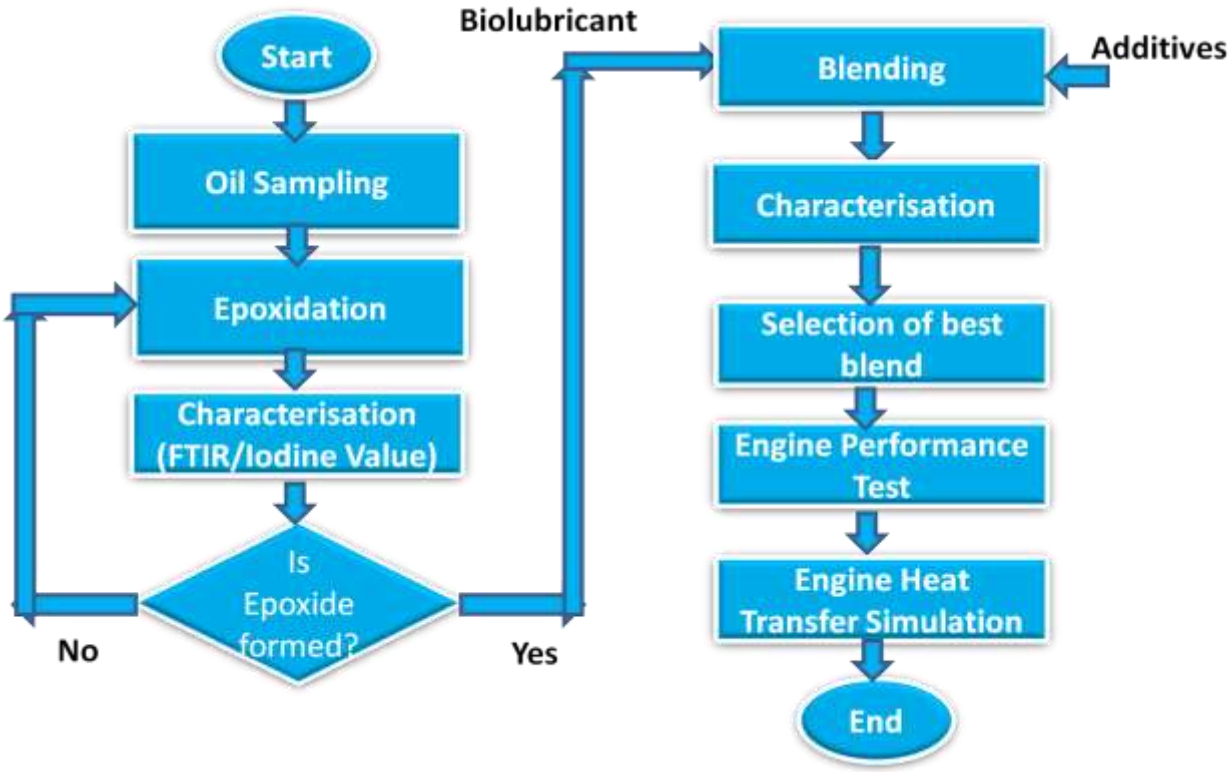


Figure 3.1: General Methodology

3.2.1 Epoxidation of Jatropha Oil

The production of epoxidized jatropha oil was done by reacting the jatropha oil with performic acid generated in-situ via the reaction of hydrogen peroxide with formic acid using sulfuric acid as catalyst as presented in figure 3.2.

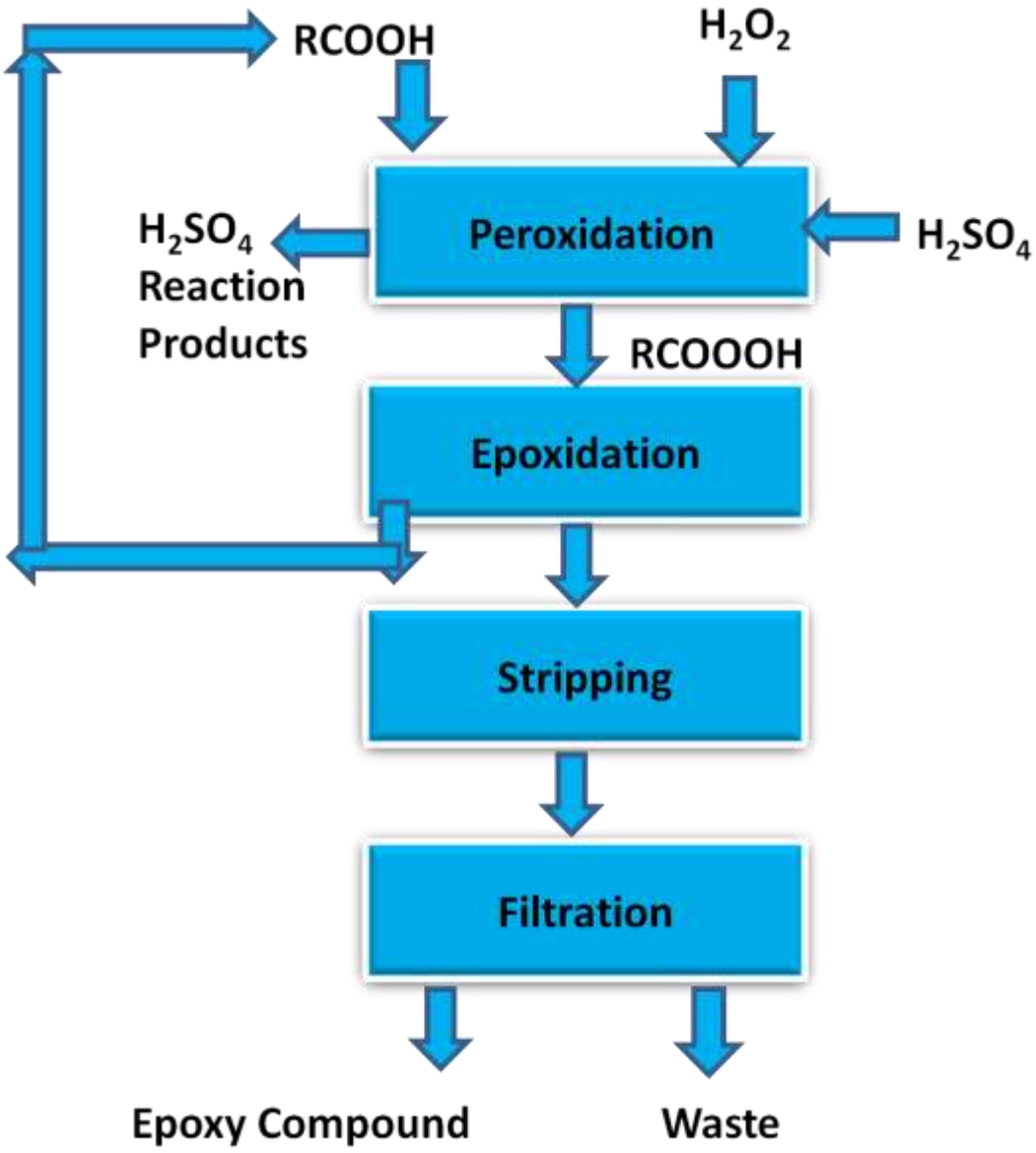


Figure 3.2: Epoxidation Process

A jatropha oil sample of 1000 g, 109 g of formic acid and 5 g of sulfuric acid were weighed and poured into a beaker and placed on a magnetic stirrer. The mixture was heated and agitated at a constant rate and the temperature was maintained at 60^{o}C. 754.8 g of hydrogen peroxide (H_2O_2) was added into the mixture drop wise and agitation of the mixture continued for further one hour. The mixture was poured into separating funnel allowed to settle. The sulfuric acid and hydrogen

peroxide were washed and the settled product dried overnight with magnesium sulphate. The theoretical oxirane oxygen content (OOC_t) of the product was calculated according to ASTM D1652-97 Standard using equation (3.1):

$$OOC_t\% = \left[\frac{\left(\frac{IV_O}{2A_i} \right)}{100 + \left(IV_O / 2A_i \right) A_O} \right] A_O \qquad (3.1)$$

where:

IV_O = Initial Iodine Value of the sample = 77.41 mg I_2/g

A_i = Atomic weight of iodine = 126.9

A_o = Atomic weight of oxygen = 16

Similarly, the experimental oxirane oxygen content (OOC_e) was determined using equation (3.2):

$$OOC_e = 1.6N(V - B)/W \qquad (3.2)$$

where V: consumed titrated solution; N: normality of the solution used; W: weight of oil sample used.

The degree of epoxidation (DOE) was calculated from equation (3.3):

$$DOE = \frac{OOC_e}{OOC_t} \qquad (3.3)$$

3.2.2 Confirmation of Epoxides Formation

The formation of epoxides in the oil sample was confirmed using Fourier-Transform Infrared (FTIR). The FTIR spectra were recorded using Agilent Technologies Cary 630 FTIR Spectrometer attached with a computer shown in Plate 3.1. The spectra were recorded from a frequency of 280 cm^{-1} to 4000 cm^{-1} using transmittance method. The crystal of the equipment

was cleaned with organic solvent. 10 mg of the sample was placed on the crystal. The transmittance was viewed on the computer and recorded.



Plate 3.1: Cary 630 Fourier Transform Infra red Spectrometer

3.2.3 Characterization of Crude and Epoxidized Jatropha Oils

The physico-chemical properties of the crude jatropha oil and epoxidized jatropha oil were determined in order to:

(i) Ascertain the quality of the crude jatropha oil;

(ii) Verify the suitability of epoxidized jatropha oil for biolubricant production;

(iii) Compare between the properties of crude jatropha oil, epoxidized jatropha oil and mineral base oils (SN 100, SN 150, SN 500 and BS 150).

The properties determined were refractive index, moisture content, iodine value, saponification value, density, viscosity, flash point and pour point.

3.2.4 Production Epoxidized Jatropha Biolubricant (EJBL)

Figure 3.3 shows the flow chart for the biolubricant production. Esterification was carried out to further reduce the free fatty acid contents of the oil so as to avoid high saponification of the oils.

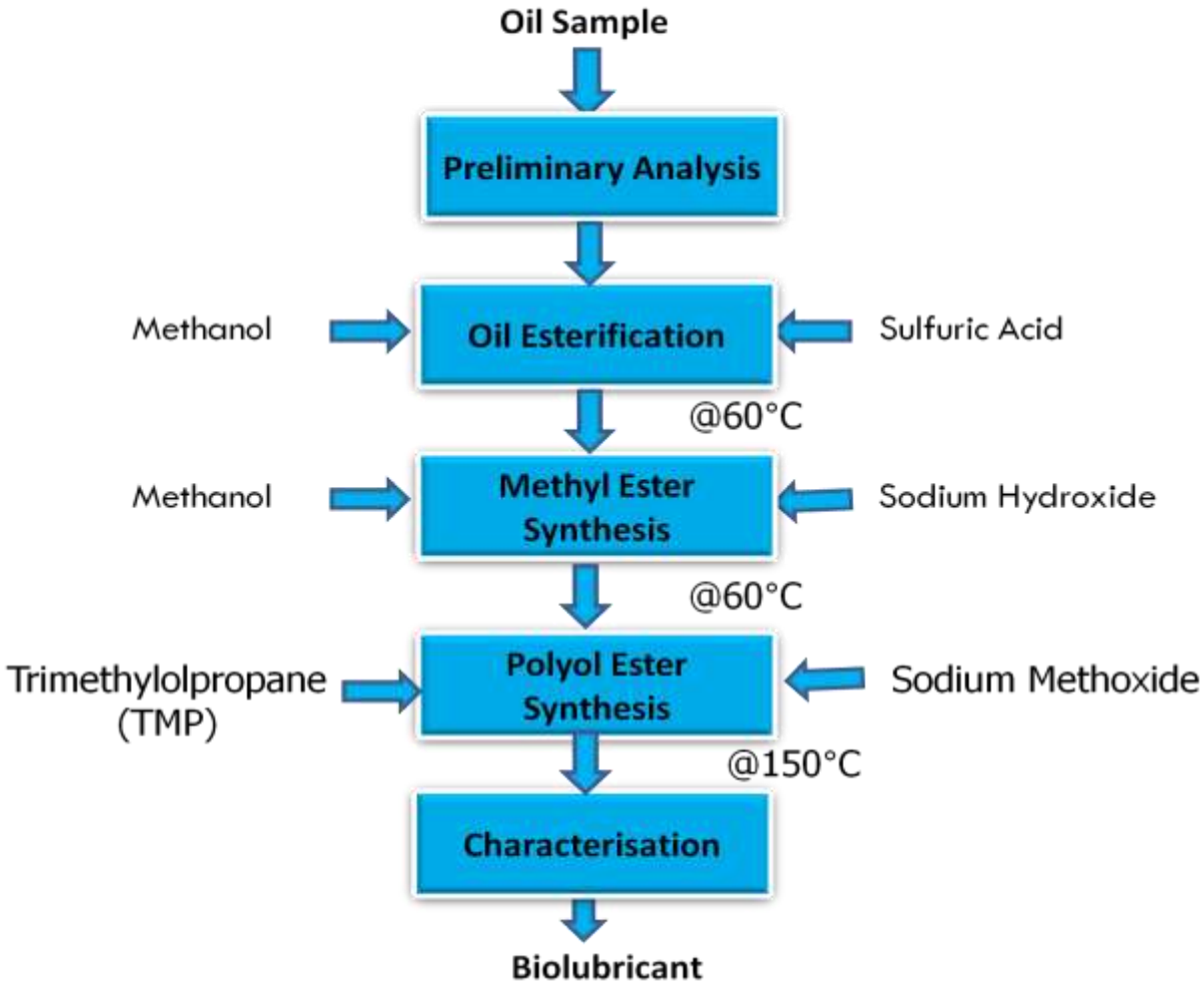


Figure 3.3: Biolubricant Production Process

This was achieved by reacting 89.4 g of the oil with methanol using sulphuric acid as catalyst. The weight ratio-to-methanol was 3:1; the amount of the catalyst used was 0.5 % w/w of the oil. Synthesis of biolubricant requires double transesterification; the first is done to produce an intermediate product that is the methyl ester of the oil. The second uses the methyl ester as the reactant to produce polyol ester of the oil which is the biolubricant. The methyl ester was

transesterified with trimethylolpropane (TMP) in 50 mL batches using sodium methoxide (comprising 30 % methanol) as catalyst. The quantity of sodium methoxide used was 0.8 % w/w of the total reactants. The weight ratio of epoxidized jatropha oil methyl ester-to-TMP was 3.5:1. The temperature of the reaction was 150^{o}C for 3 hr (Bilal *et al*., 2013).

3.2.5 Blending

The formulated biolubricant (EJBL) was blended with 1 % to 10 % automotive additive package (B023232/B23333) by volume using 1 % increments. Blends were prepared by mixing 495 mL of EJBL with 5 mL of the additive to form EJBL01; 490 mL of EJBL with 10 mL, to form EJBL02; 485 mL of EJBL with 15 mL to form EJBLO3, 480 mL of EJBL with 20 mL to form EJBL04; 475 mL of EJBL with 25 mL to form EJBL05; 470 mL of EJBL with 30 mL to form EJBL06; 465 mL of EJBL with 35 mL to form EJBL07; 460 mL of EJBL with 40 mL to form EJBL08; 455 mL with 45 mL to form EJBL09 and 450 mL of EJBL with 50 mL to form EJBL10.

3.2.6 Characterization of the Epoxidized Jatropha Biolubricants and the Refrence Oil

The epoxidized jatropha biolubricant, its blends and mineral base lubricant (SAE30) were characterized. The properties determined were refractive index, moisture content, iodine value, densities, viscosities @ 40^{o}C and 100^{o}C, viscosity indices, pour points, flash points, high-temperature high-shear viscosities, evaporation losses, foaming tendencies, total base numbers, acid numbers, elemental contents, seal compatibilities, oxidation stabilities, specific heat capacities, coefficient of thermal conductivities, ash contents, demulsibilities and copper strip corrosions. In Addition to that, Coefficient of friction and wear tests were carried out for the biolubricant chosen for the engine test and the reference engine oil. The test procedures are as follows:

3.2.6.1Refractive Index

The Refractive Index RI of the sample was determined according to ASTM D 1747 using Abbe's refractometer shown in Plate 3.2. The glass prism was thoroughly cleaned and two drops of the oil sample were applied on the surface. The reading was obtained through the telescope.



Plate 3.2: Abbe's Refractometer

3.2.6.2Moisture Content

Moisture content deactivates catalyst and reacts with fats to form fatty acids; hence the need for the oils to be dry. ASTM D890 method was used as adopted by Manji *et al*. (2013).

3.2.6.3 Iodine Value

The ASTM D 2078 was used to determine the Iodine values (IV) of CJO and EJO. First, to re-ascertain formation of epoxides; secondly to know the level of conversion of double bonds to epoxy rings. 0.20 g of each of the samples was weighed and poured into a conical flask. Carbon tetrachloride and 25 mL wig's reagent were added shaked and placed in the dark for 1 hr. A 20 mL of 10 % KI and 150 mL distilled water were added and titrated against 0.1 M sodium thiosulfate using 1 % starch solution as indicator. A blank test was carried out simultaneously under same condition. The IV was determined using equation (3.4).

$$IV = \frac{(B-S)X12.69XT}{W} \qquad (3.4)$$

where: B = Titre Value of Blank (mL) , S = Titre value of sample (mL), T= Normality = 0.1 mL and W = Weight of oil (g).

3.2.6.4 Saponification Value

This was carried out based on ASTM D 94 Standard. Other equivalent standards are: IP 136, ISO 6293, DIN 51559, JIS K2503, and AFNOR T60-110. A 2 g of the sample was weighed into a conical flask and 25 mL of 0.5M of alcoholic potassium hydroxide solution was added. A reflux condenser was attached and the flask was heated in boiling water for 30 min. The mixture was titrated against 0.5M Hcl using phenolphthalein indicator. A blank titration was also carried out under the same condition. The Saponification Value SV was calculated using equation (3.5):

$$SV = \frac{(B-S)X25.5}{W} \qquad (3.5)$$

where: B = Titre Value of Blank (mL), S = Titre value of sample (mL), W = Weight of oil (g).

3.2.6.5 Density

The densities of the samples were determined using ASTM D 1298 Standard. Other equivalent test methods include: IP 160, ISO 3675, DIN 51757H, JIS K2249H and AFNOR T60-101. A Fisher brand hydrometer was used for the measurement. The hydrometer was lowered into the sample and allowed to settle. When the content and the hydrometer all attained thermal equilibrium, the scale of the hydrometer was read.

3.2.6.6 Viscosity

The viscosities of the samples were determined at 40^{o}C and 100^{o}C using ASTM D 445 Standard. Other equivalent test methods are: IP 71-1, ISO 3104, DIN 51562, JIS 2283, and AFNOR T60-100. The time taken by 50 mL of the oil sample to flow inside the capillary of a calibrated viscometer between two marks was recorded. The kinematic viscosity was the product of the measured time and the viscometer constant. The sample was tested at 40^{o}C and 100^{o}C. This is

in conformity with the work of Bilal *et al.* (2013) and Aji *et al.* (2015). The viscosity indices were then computed using ISO Online Viscosity Index Calculator.

3.2.6.7 Pour Point

The pour points (PP) of the oil samples were determined using ASTM D 97 Standard. Other equivalent test methods are: IP 15, ISO 3016, DIN 51597, JIS K 2269, and AFNOR T60-105. During the test, 5 mL of the sample was placed into a test tube and a thermometer was inserted into the test tube through a cork and heated to 50^{o}C and placed in a refrigerator. The sample was examined for flow characteristics after every 3^{o}C temperature drop. The lowest temperature at which the sample still flowed in the test tube was recorded as its pour point.

3.2.6.8 Flash point

This was determined using ASTM D 92 Standard for Flash Point of automotive oils using Cleveland Open Cup Tester as recommended by NIS. The test set up is shown in Plate 3.3.



Plate 3.3: Cleveland Open Cup Tester

Other equivalent test methods are: IP 36, ISO 2592, DIN 51376, JIS K 2265, and AFNOR T60-118. The test cup was filled with the sample and continuously heated at constant rate and stirred. Flame was regularly directed into the cup. The lowest temperature at which the vapors above the sample ignited was recorded as the flash point.

3.2.6.9 Thermal / Shear Stability (High-Temperature High-Shear Test)

The ASTM D 4683 Standard for determining high-temperature high-shear apparent viscosity was used. Totten (2006) stated that the type of viscometers used to study high-temperature high-shear viscosity included rotary (ASTM D 4683, ASTM D 4741) and capillary (ASTM D 4624 ASTM D 5481). Nigerian Industrial standard specified ASTM 4683 and ASTM D 4741. The High-temperature high-shear viscosity test was determined by heating 200 cm^3 of the oil sample to 170^oC and the value of the viscosity was recorded when the oil temperature dropped to 150^oC (Humphrey, 2016).

3.2.6.10 Evaporation Loss

Noack Evaporation Loss ASTM D5800 was used for this test. Other equivalent test methods are: IP 421, DIN 51581 and CEC-L14-A88. During the test, 0.25 L of the sample was poured into an evaporation crucible and heated to 250^oC for 1 hr the loss in mass of the oil sample was determined.

3.2.6.11Foaming Tendency

The ASTM D892 standard method for determining foaming characteristics of automotive lubricants was used for this test. Other equivalent test methods include: IP 146, ISO 6247, DIN 51566 and JIS K2518. Oil foaming can have severe consequences in an automobile engine; foaming can cause inadequate lubrication, collapse of valve lifters, cavitations, loss of oil pump pressure and finally mechanical failure. Plate 3.4 shows the foaming tendency apparatus used.



Plate 3.4: Foaming Tendency Apparatus

The test was conducted on three sequences:

Sequence I: a constant flow of air at the rate of 94 ± 5 mL / min was blown on 190 mL of the oil sample maintained at 24^{o}C for 5 min, timed from the appearance of first bubble. The air supply was shut off. The volume of the foam formed, which is the difference between oil level and the top of the foam, was recorded.

Sequence II: The Sequence I procedure was repeated at a temperature of 93^{o}C.

Sequence III: After Sequence II test, the oil sample was cooled down to 24^{o}C and the procedure of sequence I, repeated.

Foam Stability in each case, is the volume of foam left after 10 min.

3.2.6.12 Total Base Number (TBN)

The Titrimetric Method (ASTM D974) for TBN determination of fresh oil was used. 0.1 g of methyl orange was dissolved in 5 mL of distilled water in a 1 L conical flask. 8.9 mL of concentrated hydrochloric acid was added into a 1 L volumetric flask containing 500 mL of 2-

propanol, mixed thoroughly and then made up to the 1 L mark with 2-propanol. 495 mL of 2-propanol and 500 mL of Toluene were added to the 5 mL of aqueous methyl orange solution in the 1 L conical flask. The mixed solvent-indicator solutions were mixed thoroughly by shaking until well homogenized. 80mL of mixed solvents-indicator solution was added into 250 mL conical flask. One gram of the sample was added into the flask and mixed thoroughly. The mixture was then titrated with 0.1M Hcl to the methyl orange end point (A). A blank titration was also carried out for the mixed solvent-indicator solution (B). TBN was calculated from equation (3.6):

$$\text{TBN (mg KOH/g)} = \frac{(A-B)XCXD}{W} \qquad (3.6)$$

where: A = Titre volume for sample (mL)

B = Titre volume for blank (mL)

C = Molecular weight of KOH

D = Molarity of Hcl

W = weight of sample (g)

3.2.6.13Total Acid Number (TAN)

This was determined using ASTM D974, other equivalent test methods include: IP 139, ISO 6618, DIN 51558T1, JIS K2501 and AFNOR T60-112. Total acid number is the quantity of KOH in mg required to neutralize 1 g of the oil sample. The test was similar to the method used by Bilal *et al.* (2013) and Manji *et al.* (2013). 1g of the oil sample was put into a 250 mL conical flask and warmed. 25 mL of methanol was added and stirred thoroughly. 2 drops of phanalphthalein indicator were applied and a drop of 0.1 M KOH solution was added until a light pink colour was seen. The end point was observed and recorded. The acid value AV is given by equation (3.7):

$$AV = \frac{\text{MM of KoH X Titre Value X 0.1 M of KoH}}{\text{Weight of Sample}} \quad (3.7)$$

3.2.6.14 Elemental Content Test

There are various elemental analyses used to detect presence of elements, additives or wear of engine components. These tests include Atomic Absorption Spectroscopy AAS, Inductively Coupled Plasma Atomic Emission Spectroscopy ICP-AES, X-ray Fluorescence XRF, Micro Elemental Technique, etc. ASTM D 4927 for XRF Spectrometer was used in this work to determine Phosphorus content and sulfur content of the oil samples. Other equivalent test methods are: IP 407 and DIN 51391-T2. Plate 3.5 shows the XRF Spectrometer used for the tests.



Plate 3.5: XRF Spectrometer

3.2.6.15 Seal Compatibility

The ASTM D 4289 elastomer compatibility test was used to investigate the compatibility of the epoxidized jatopha biolube with the oil seals. Three samples of oil seals were chosen as per API/ ILSAC Standards. The seals were measured for initial volume using displacement method and hardness using durometer A. They were then immersed in the lubricating fluid which was

maintained at 100^{o}C for 70 hr the resulting change in volume and hardness were determined in percentage (%).

3.2.6.16 Oxidation Stability

The oxidation induction time (OIT) which is an indicator of oxidation stability was determined based on ASTM D6186 Standard using differential scanning calorimetry (DSC 2) STARe System by Mettler Toledo shown in Plate 3.6.



Plate 3.6: Differential Scanning Calorimeter (DSC)

The test commenced by weighing 3 mg of the oil sample into a standard open aluminium pan and placed in the measuring cell. The cell temperature was increased from room temperature, 32^{o}C to 200^{o}C and allowed to reach equilibrium. Oxygen at 3.5 MPa was used to pressurize the cell and the flow rate of the purge gas adjusted to 0.1 L/min. The OIT was measured from the time the oxygen valve was opened. OIT was detected using extrapolation of the DSC signal when a strong exothermic reaction (oxidation) was detected as described by Černý and Zelinka (2004).

3.2.6.17 Specific Heat Capacity

The specific heat capacities of the lubricating oil samples were determined by electrical method using Joule's apparatus as shown in Plate 3.7. The set up consists of copper calorimeter, stirrer, mercury-in-glass thermometer, weighing balance, milli-ammeter, milli-voltmeter, variable resistor, stop-clock and retort stand.



Plate 3.7: Joule's Apparatus

The empty calorimeter was weighed and recorded; sample of the oil was poured into the calorimeter and weighed again. The initial temperature of the calorimeter and its content was recorded. The calorimeter was connected to the electrical circuit and the stop clock was started. After 10 min of heating, the current, voltage and final temperature were recorded. The specific heat capacity of the oil sample was determined from equation 3.8:

$$C = \frac{Ivt}{m(\theta_2 - \theta_1)} - \frac{m_c C_c}{m} \qquad (3.8)$$

where:

I = Current (A);

v = Voltage (v);

t = Time (sec);

m = Mass of oil sample (kg);

m_c = Mass of Calorimeter (kg);

C_c = Specific heat capacity of the calorimeter (kJ/kgk);

θ_1 = Initial temperature of the calorimeter and the content (K);

θ_2 = Final temperature of the calorimeter and the content (K);

3.2.6.18 Coefficient of Thermal Conductivity

The coefficients of thermal conductivities of the samples were determined by the ASTM D 2717 Standard using Lee's apparatus shown in Plate 3.8. The set up consists of a heating source, steam jacket, a circular disc with steam chest and two chambers separated by a gap for the specimen. . The heating source was ignited ad steam generated to the steam chest. Heat was transferred from the steam chest through first brass disc with thermometer to indicate T_1, then to the oil sample which was confined in a very tiny space such that only heat conduction can occur to the second brass disc chamber.



Plate 3.8: Lee's Apparatus

The brass chamber is equipped with another thermometer to register T_2. The temperatures of the two thermometers were recorded after every two minutes for 30 minutes using a timer. The

cooling rate dT/dt was determined from a plot of T_2-T_1 against t. The coefficient of thermal conductivity of the sample is determined from equation (3.9):

$$k = \frac{mc_b dTx}{Adt(T_2 - T_1)} \qquad (3.9)$$

Where m is the mass of the lower disc (kg), c_b is the specific heat capacity of the lower disc (kJ/kgk); dT/dt is the cooling rate ($^oC/s$), A the cross sectional area of the hole for the specimen (m^2) and T_2-T_1 the temperature difference (^oC).

3.2.6.19 Ash Content

The ASTM D874 method was used for this test. Other equivalent test methods are: IP 163, ISO 3987, DIN 51575, JIS K 2272, and AFNOR T60-143. During the test, 0.1 kg of the oil sample was ignited and burned to ash and carbon. The residue was cooled to room temperature and treated with 0.1 L of H_2SO_4 acid and heated at 775^{o}C for 60 min. the ash was then cooled and re-treated with H_2SO_4 and heated again at 775^{o}C for another 60 min and allowed to cool to room temperature. The sulfated ash content was determined from equation (3.10):

$$\text{Ash Content} = \frac{W_1 - W_2}{W_2} \qquad (3.10)$$

where W_1 and W_2 are the respective initial and final weights of the sample in mg.

3.2.6.20 Demulsibility

Demulsibility test determines the ability of oil sample to separate from water. The ASTM D 2711 was used for the test. Plate 3.9 shows the demulsibility tester. A 100 mL graduated cylinder maintained at 54 ± 1^oC in a large heating bath was used for the test. 40 mL of distilled water was poured into the cylinder. The oil sample was added up to 80 mL mark. The bath and the content were allowed to attain uniform temperature, 54^{o}C.



Plate 3.9: Demulsibility Tester

The cylinder was clamped up directly under a string paddle dipped into the content. The stirrer was started to a speed of 1500 ± 15 rpm and allowed to properly stir the mixture for 5 min. the stirrer was removed, allowing the liquid to drop back to the cylinder and inspected for separation after every 5 min.

3.2.6.21 Copper Strip Corrosion Test

The ASTM D 130 method was used for this test. Other equivalent test methods are: IP 154, ISO 2160, DIN 51759, JIS K 2513, and AFNOR M07-015. A polished copper strip was immersed in 100 mL of the oil sample and heated to 100^{o}C. The strip was kept at that temperature for 5 hr. after which, the strip was removed, cleaned and compared with ASTM Copper Strip Corrosion Standard.

3.2.6.22 Coefficient of Friction and Wear Test

The coefficient of friction and wear characteristic of the oil samples were evaluated using aluminium and mild steel test pieces on Anton Paar Tribometer 8054 shown in Plate 3.10. The tests were carried out at oil temperatures 40^{o}C and 100^{o}C.



Plate 3.10: Tribometer

3.2.7 Engine Performance Test

The optimized biolubricant blend was tested on spark ignition engine. Parameters such as brake power, specific fuel consumption, operating temperature and pressure, indicated mean effective Pressure and brake thermal efficiency were determined.

3.2.7.1 Equipment and Engine Test

Heat transfer modeling for a spark ignition engine lubricated with the epoxidized jatropha biolube requires a suitable SI engine equipped with the necessary tools for determining operating temperatures and pressure.

3.2.7.2 The Test Engine

The engine used for the work is TecQuipment TD201 small engine test set located at the heat engine laboratory, Mechanical Engineering Department, Ahmadu Bello University, Zaria. The engine is naturally aspirated four-stroke, single cylinder and air-cooled with specifications as outlined in Table 3.1. The engine is coupled with a hydraulic dynamometer. A bench- mounted instrument frame is provided for instrumentation.

Table 3.1 Test Engine Technical Details

Items	**Specifications**
Dimensions	Width 500 mm Height 430 mm Depth 400 mm
Net Weight (With Base Plate)	22 kg
Fuel Type	Unleaded Petrol Minimum 90 RON Also allowed are: Ethanol mix of 90 % Unleaded Petrol and up to 10 % Ethyl Alcohol Methyl tertiary butyl ether (MTBE) mix of up to 15 % MTBE by volume
Absolute Max Power	5.2 kW (7 hp) at 3600 $rev.min^{-1}$
Net Power	4.5 kW at 3600 $rev.min^{-1}$ 2.2 kW at 1800 $rev.min^{-1}$
Engine Type	Single Cylinder
Engine Cycles (strokes)	4
Engine Capacity	208 cm^3 (0.208 L)
Bore	70 mm
Stroke/Crank Radius	54 mm/ 27 mm
Connecting Rod Length	84 mm
Compression Ratio	8.5: 1
Oil Type	SAE 30 or Multigrade 10W-30
Oil Capacity	0.6 L

Source: TecQuipment TD201 engine manual.

3.2.7.3 The Hydraulic Dynamometer

A trunnion mounted hydraulic dynamometer fitted to the test bed is used to determine the performance of the engine under test. The dynamometer applies load according to the water flow rate and the water level in its casing. The flow rate/level is controlled by an accurate valve. The engine torque is determined by an electronic load cell. The rotational speed is measured by a proximity sensor.

3.2.7.4 Instrumentation of the Test Engine

Plate 3.11 shows the engine instrument frame. The frame comprises four display units: the Torque, Speed, Engine inlet air and the Exhaust Displays. Power is calculated from the modules that display torque and speed. The frame has been equipped with Versatile Data Acquisition System (VDAS) which is connected to a computer. The VDAS automatically calculates values such as thermal efficiency, mean effective pressure, specific fuel consumption, etc, from the signals it receives from other modules.



Plate 3.11: Engine Instrument Frame

The exhaust module uses K-type thermocouple mounted at the exhaust manifold. Additional Four K-type thermocouples were used to measure the steady- state temperatures of the outside lower surface of the engine wall, outside upper surface of the engine wall, oil temperature, and exhaust valve temperature. The K-type thermocouples offer measurement ranges from –270^{o}C to +1372^{o}C and temperature tolerance of ± 2.2^{o}C or 0.75 %. The thermocouple installed to measure the oil temperature was inserted into the oil inlet hole through the oil hole cover and sealed to prevent oil leakage as presented in Plate 3.12.



Plate 3.12: Locations of Thermocouples for Oil and Outer Surface Temperature Measurements on the Engine

The tip of the thermocouple probe was aligned with the tip of the dip stick to avoid possible contact with moving parts of the engine. The thermocouple installed to measure exhaust valve temperature was inserted through the

valves cover and fixed to the exhaust valve spindle as shown in Plate 3.13. The additional instrumentations proved to be adequate and safe throughout the engine tests. No oil leakage or thermocouple contact with engine moving parts was noticed.



Plate 3.13: Location of Thermocouple for Exhaust Valve Temperature Measurement on the Engine

3.2.7.5 Engine Test Procedure

To start the engine for test, water tank for the dynamometer was filled; volumetric fuel gauge was also filled with petrol. 0.6 L of the engine reference oil was poured into the engine oil sump. The power supply to the equipment was on. Additional temperature sensors used were also powered. The computer and the VDAS hardware were powered. The VDAS icon on the computer desktop was double clicked to open the VDAS window. The test engine was then started using the ignition key and allowed to warm up for 5 min. The timer on the VDAS window was set to record engine parameters (speed, torque, temperatures, etc,) every 2 min. Inlet

valve to the dynamometer was opened and actual engine tests commenced. The readings on the temperature sensors were continually recorded every 2 min. The results were tabulated and used with the recorded data on the VDAS output. Similar test procedure was repeated for the formulated biolubricant.

3.2.8 Modelling and Engine Heat Transfer Simulation

The purpose of this modeling and simulation was to predict the engine oil temperatures, engine outer surface temperatures and exhaust valve temperatures at various engine speeds and validate the results with experimental results. The model used here is GT-Suite in-built heat rejection model for naturally aspirated four-stroke, four cylinder and water cooled engine. The model is used to predict quantity of heat rejected to engine oil, coolant, and to the ambient. It consists of detailed engine structures, oil and coolant circuits. The model was modified in this work to four-stroke, single cylinder and air cooled. Plate 3.14 shows the simplified GT-Suite model.

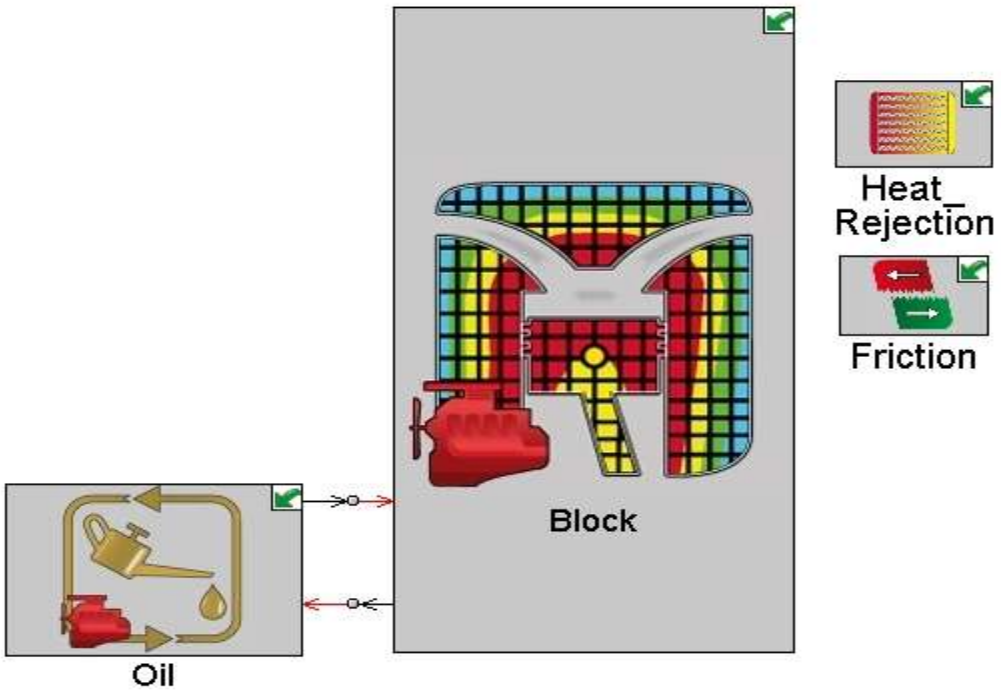


Plate 3.14: Modelled 1Cyl, 4-stroke Engine on GT-Suite

To launch the file on the PC, the following path was followed: Start → Programs→Application Group → GTise v7.4.0 → File→ Open →1-Cyl-Jaafar.gtm.

The oil circuit was modeled with all pressure losses of internal bearings and other oil consumers lumped into a single pressure restriction. All internal oil holes were simplified into one volume that provides a temperature boundary condition for the cylinder structure. The finite element structure template 'EngCylstrucCon' was used to model the cylinder structure with all its accessories including piston, ports and head. This model is thermally linked to the engine cylinder gas side, the oil and the valves. Figure 3.4 shows the procedure for launching the simulation of GT software.

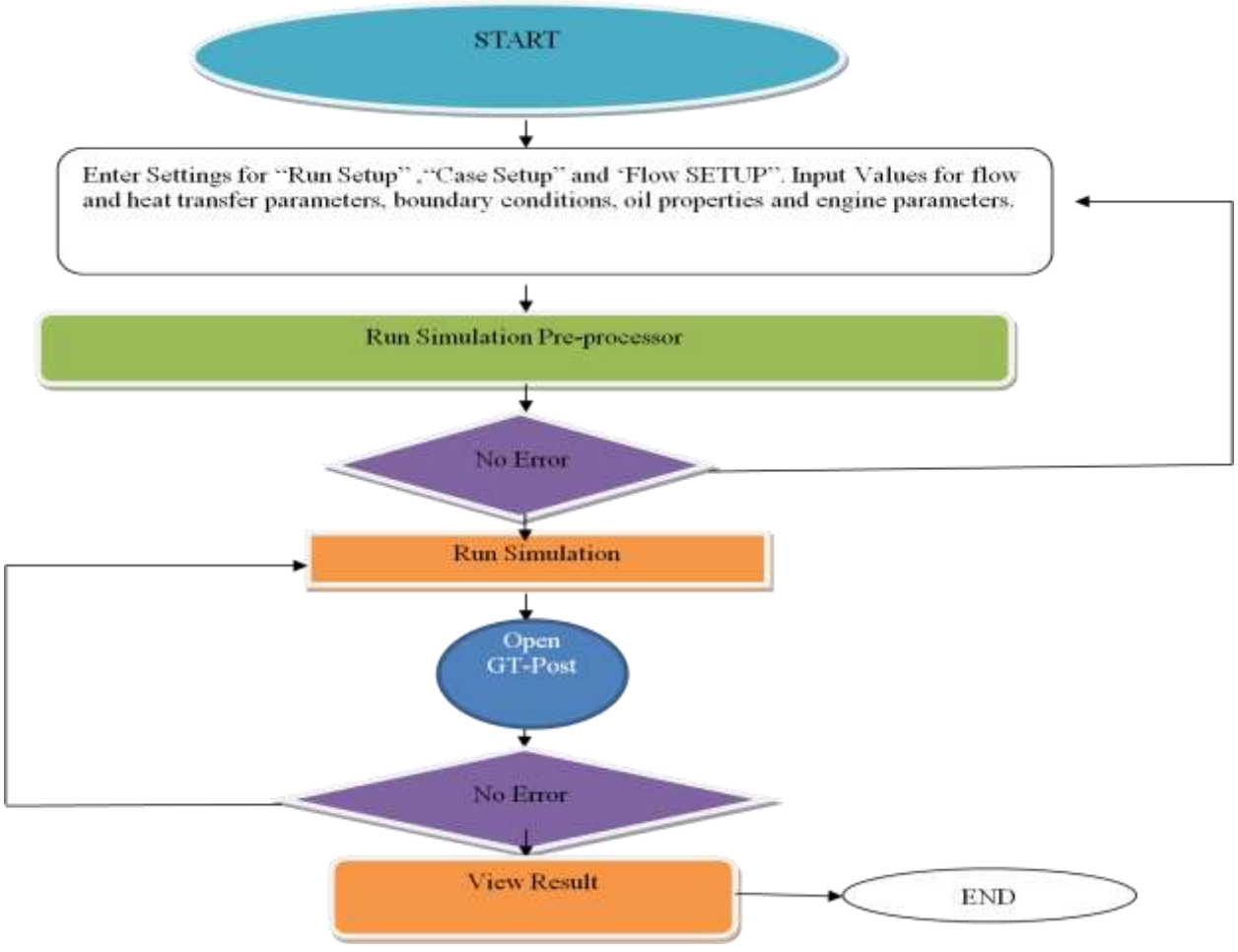


Figure 3.4: Flow Chart for Running the Simulation on GT-Suite

The engine block, head structure and oil pan were modeled using 'thermal masses' and were interconnected via 'conductance objects' which transfer heat by convection to the ambient. 'Controls' were used in the model to relevant heat source and heat rejection. Convective heat rejection rates were calculated by sensing mass flow rates and enthalpies in and out of a control volume.

3.2.8.1 Engine Heat Transfer Simulation Parameters and Equations

Figure 3.5 shows a simplified illustration for all the energy interactions between the engine and its surroundings. The heat generated from the chemical energy of the fuel in the combustion chamber is partly converted to useful work (W_b) some rejected as heat through the exhaust gases (Q_{ex}), some rejected as heat ($Q_{L)}$ to the surroundings (engine oil, engine parts and ambient air).

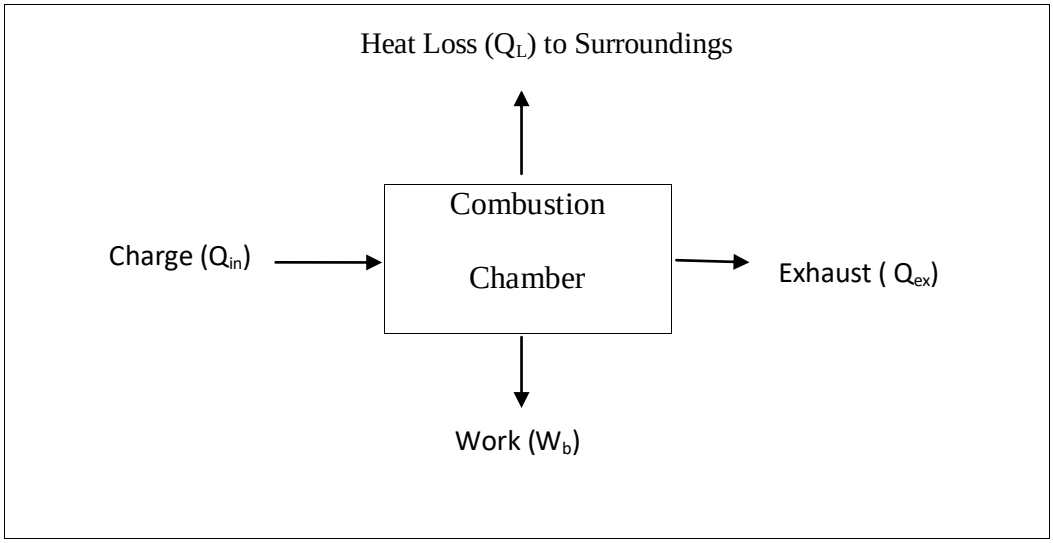


Figure 3.5: Engine Energy Balance

Applying mass conservation principle on the system,

$$\dot{m}_{in} = \dot{m}_{out} \tag{3.10}$$

The chemical energy is partly converted to useful work; partly absorbed by the engine components and partly rejected to the surroundings. The 'surrounding' of the combustion

chamber refers to the engine components surrounding the combustion chamber; the engine oil and the immediate environment of the engine which are affected by the changes in the engine. Therefore Q_L comprises heat loss to immediate environment and heat absorbed by the engine oil. Heat Transfer from the combustion chamber to the immediate environment occurs first by forced convection from the combustion gases to the piston head and cylinder wall; conduction through the engine body to the outer surface of the engine then by mixed convection (due to presence of fan on one side of the engine) from the outer surface of the engine to the ambient air. Similarly the engine oil transfers heat by forced convection to boundary layer oil.

The crankcase has an irregular geometry as shown in Plate 3.15. For simplicity, the crankcase was assumed to be made up of plane surfaces joined together. The areas of the plane surfaces were lumped together as $A_{k;}$ x is the thickness of the crankcase wall.

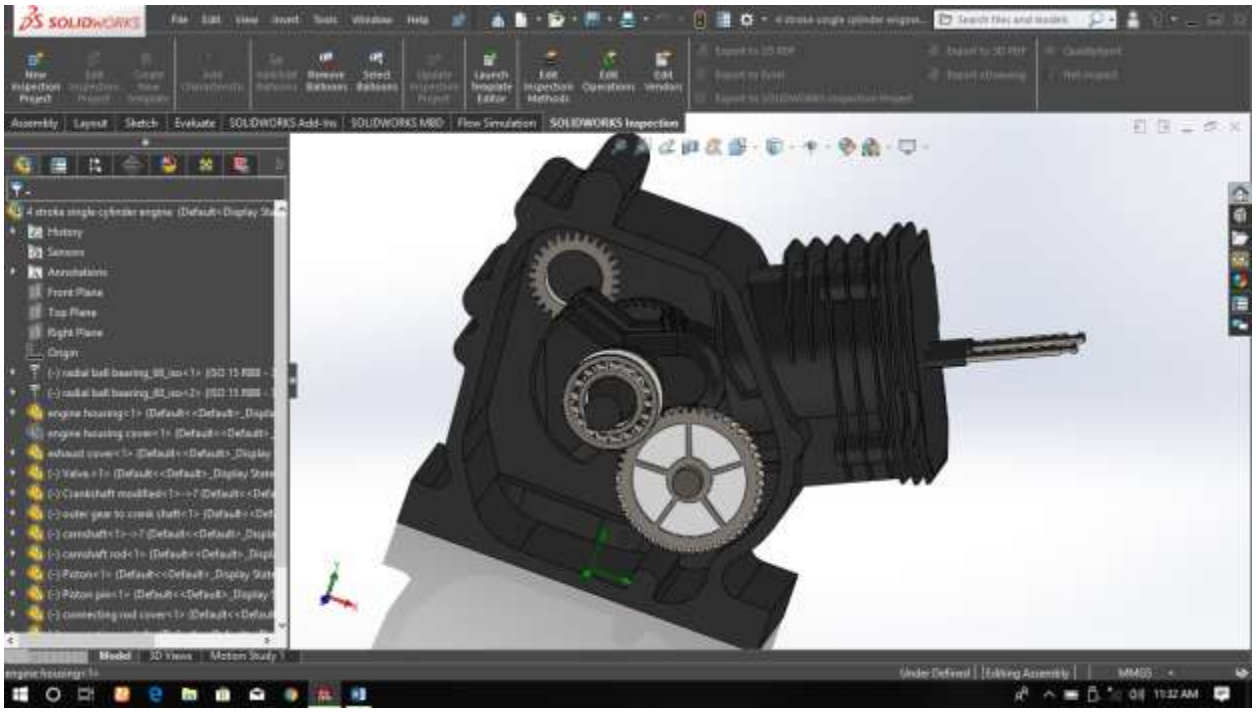


Plate 3.15: The Engine Crankcase

The flow model solver used in this work is 'Explicit'. It solves Navier-Stokes equations namely, continuity, energy and conservation equations in one-dimension. In the Explicit, mass flow rate, density and internal energy are the primary solution variables. Some of the equations the Explicit solves to predict flow and heat transfer variables are given in equations (3.11) to (3.18):

Continuity: $$\frac{dm}{dt} = \sum_{boundaries} \dot{m} \tag{3.11}$$

where $$\dot{m} = \rho A du \tag{3.12}$$

Energy: $$\frac{d(me)}{dt} = -p\frac{dv}{dt} + \sum_{boundaries}(\dot{m}H) = hA_S(T_f - T_w) \tag{3.13}$$

and,

Momentum: $$\frac{d\dot{m}}{dt} = \frac{1}{dx}\left[dpA + \sum_{boundaries}(\dot{m}u) - 2C_f \rho u|u|\frac{dxA}{D} - C_p(0.5\rho u|u|)A\right] \tag{3.14}$$

where $\dot{m}$ is the boundary mass flux (kg/s) into descretized volume; m is mass (kg) of the volume; V is the volume (m^3), p is pressure (N/m^2), ρ, density (kg/m^3), A_S is heat transfer surface area (m^2), e is total internal energy (kJ), H is total enthalpy (kJ), h is heat transfer coefficient (W/m^2k), T_f is fluid temperature (K), T_w is wall temperature (K), U is velocity at the boundary (m/s), C_f is coefficient of skin friction, C_p is pressure loss coefficient, D is equivalent diameter (m), dx is length of mass element in the flow direction, i.e descretization length (m), dp is pressure differential acting across dx.

The Conservation of Energy Equation solved by the GT 'Explicit' is expressed as in equation (3.15):

$$\int \frac{\partial(\rho C_v T)}{\partial t} dV = \int (-\nabla q) dV \tag{3.15}$$

from which,

$$\rho C_v \frac{\Delta T}{\Delta t} = \sum_{faces}(-qA) \tag{3.16}$$

where C_v is specific heat capacity at constant volume (kJ/kg), q is heat flux (kJ/m^2)

Heat flux q at the conduction face is expressed in equation (3.17):

$$q_{conduction} = -k\nabla T \tag{3.17}$$

where k is the thermal resistance calculated from the coefficient of thermal conductivity of the material at the nodal temperature; T is the nodal temperature.

Heat flux q at convection face is expressed in equation (3.18):

$$q_{convection} = h(T_g - T_w) \tag{3.18}$$

'User defined' was checked on for external convection as such it was determined manually and inputted. This is because mixed convection heat transfer prevailed at the engine surroundings during the engine test.

In GT software, 'EngCylHeatTr' and 'EngCylTwall' reference objects are used to model heat transfer in the combustion chamber and crankcase. Desired heat transfer model is selected and the heat transfer coefficient is calculated. Various types of heat transfer models are available in the 'EngCylHeatTr' template.

3.2.8.2 Wall Temperatures

The inner surface temperatures of the cylinder and temperatures of the piston and the head were imposed using 'EngCylTWall'. The template has typical values which are used when the temperatures are not known:

Piston Temperature 277^{o}C – 327^{o}C

Head Temperature 277^{o}C – 327^{o}C

Cylinder temperature 127^{o}C

Since the ranges are for both spark ignition and compression ignition engines, the lower values were used for the engine considering the fact that spark ignition engines normally have lower engine temperatures than compression ignition engines.

The average engine surface temperatures and average oil temperatures used for the simulations were: 72.5^{o}C for SAE 30 and 70^{o}C for EJBL05 and 78^{o}C for SAE 30 and 73^{o}C for EJBL05 respectively. The minimum and maximum working temperatures of the SAE 30 and EJBL05 were respectively 261 K, 478 K and 259 K, 491 K.

3.2.8.3 Determination of Engine Gas Side Heat Transfer Coefficient h_g

The heat transfer coefficient h_g was determined using modified Woschni correlation by Hohenberg available in the GT software as suggested by many researchers such as Wang and Berry (1985), Lounici *et al.* (2010) and Rashedul *et al.* (2014) .

Thus, Hohenberg correlation is written as in equation (3.22):

$$h_g = C_1 . V_c^{-0.06} P^{0.8} . T_g^{-0.4} \left(1.4 + V_P\right) \qquad (3.22)$$

Where $C_1 = 130$, V_P = mean piston speed and V_c is instant cylinder volume.

3.2.8.4 Determination of Coefficient of Thermal Conductivity

For simplicity, the cylinder, engine block and the crankcase and piston rings were assumed to be of the same material: grey cast iron. This is because these engine parts are mostly produced from it (Gill, 2013). The piston was assumed to be of aluminium alloy. The values of coefficient of thermal conductivities used for these materials in the setup are as presented in appendix D.1.

3.2.8.5 Determination of Engine Outer Surface Heat Transfer Coefficient h_a

The Heat Transfer Coefficient h_a was manually calculated and inputted into the GT settings. Mixed convection heat transfer exists between the outer surface of the engine and the ambient because there is a fan that cools the engine at one side and the remaining sides are cooled by

natural convection. Hence the heat transfer coefficient h_a was determined by modeling the situation as mixed convection over a vertical cylinder with longitudinal evenly distributed straight fins of 'convection-off-the-end' type.

Equations (3.19) to (3.24) give the expressions for determining convective heat transfer coefficient for combined natural and forced convection:

$$\overline{N}u_D = 0.332\,\mathrm{Re}_D^{\frac{1}{2}}\,\mathrm{Pr}_D^{\frac{1}{3}} \tag{3.19}$$

If,

$$\frac{Gr_D}{Rr_D^{\,2}} < 4, \quad \text{and}$$

$$\overline{N}u_D = 0.508\,\mathrm{Pr}_D^{\frac{1}{2}}(0.952 + \mathrm{Pr})^{\frac{-1}{4}} Gr_D^{\frac{1}{4}} \tag{3.20}$$

If,

$$\frac{Gr_D}{Rr_D^{\,2}} > 0.6 \text{ for Pr} < 10 \text{ and } \frac{Gr_D}{Rr_D^{\,2}} > 1.0 \text{ for Pr} = 100.$$

where:

$$Nu_D = \frac{hD}{K} \tag{3.21}$$

$$Rr_D = \frac{\rho c D}{\mu} \tag{3.22}$$

$$\mathrm{Pr}_D = \frac{c_p \mu}{k} \tag{3.23}$$

$$Gr_L = \frac{\beta g(T_S - T_\infty)L^3}{\upsilon^2} \tag{3.24}$$

It was found that for this system,

$$Gr_D / Rr_D^{\,2} > 0.6 \text{ for Pr} < 10$$

Therefore, Equation (3.20) was used to calculate h_a. The properties of air used for the simulations are presented in appendix D.2.

The heat transfer from the fins was calculated using equation (3.25) to (3.28)) as suggested by Sachdeva, 2008:

$$Q_{fin} = \sqrt{h_a pkA}\theta_0 . \frac{\tanh(mL) + \left(h/mk\right)}{1 + \left(h/mk\right)\tanh(mL)} \qquad (3.25)$$

where L is the length of the fin; θ_0 is the excess temperature at base of the fin and:

$$m = \sqrt{hp/kA} \qquad (3.26)$$

$$p = 2(w + t) \qquad (3.27)$$

$$A = wt \qquad (3.28)$$

3.2.8.6 Determination of Engine Oil Heat Transfer Coefficient h_{eo}

The heat transfer for the engine oil h_{eo} was manually determined and inputted in the GT setup. This was done by modeling the oil flow as a liquid undergoing turbulent flow in a cylindrical enclosure. Modified Dittus-Boelter equation by Sieder and Tate was used as shown in equation (3.29):

$$\overline{N}u_d = 0.027\,\mathrm{Re}_d^{\,0.8}\,\mathrm{Pr}_d^{\,0.33}\left(\frac{\mu}{\mu_s}\right) \qquad (3.29)$$

All properties were evaluated at mean bulk temperature except μ_s which was taken at inner surface temperature of the cylinder.

3.2.8.7 Oil Splash Velocity

The velocity of the oil was determined as used in the setup from the fact that the scoop (dipper) that splashes the oil is attached to the crankshaft; it therefore rotates at the engine speed, N. The oil is assumed to move with a velocity equal to the tangential velocity of the scoop. Therefore oil splash velocity c was calculated from equation (3.30):

$$c = \frac{2\pi N r_d}{60} \quad (3.30)$$

where:
$r_d = r_c$ (radius of the crankshaft) + dipper length

3.2.9 Simulation Settings

A number of settings are required for the heat transfer simulation. These include 'Run Setup' where settings for maximum duration of simulation in cycles, solution method, flow type, wall temperature calculation intervals, etc, were entered; 'Case Setup', in this settings, parameters such as initial "oil Temperature", "ambient Temperature", "Ambient Pressure" among other things were entered. The Engine Speed for case 1 was set at 1118 rpm, for case 2, 1500 rpm, for case 3, 2200 rpm and for case 4, 3450 rpm as presented in Plate 3.16. The engine speeds were selected so as to coincide with that of the experiment. Flow parameters such as flow velocity, density, kinematic viscosity and boundary condition settings, etc, were entered. "Run Simulation" menu was launched and the results were viewed with GT-Post. The windows of some of the settings are presented in Plates 3.16 to 3.20.

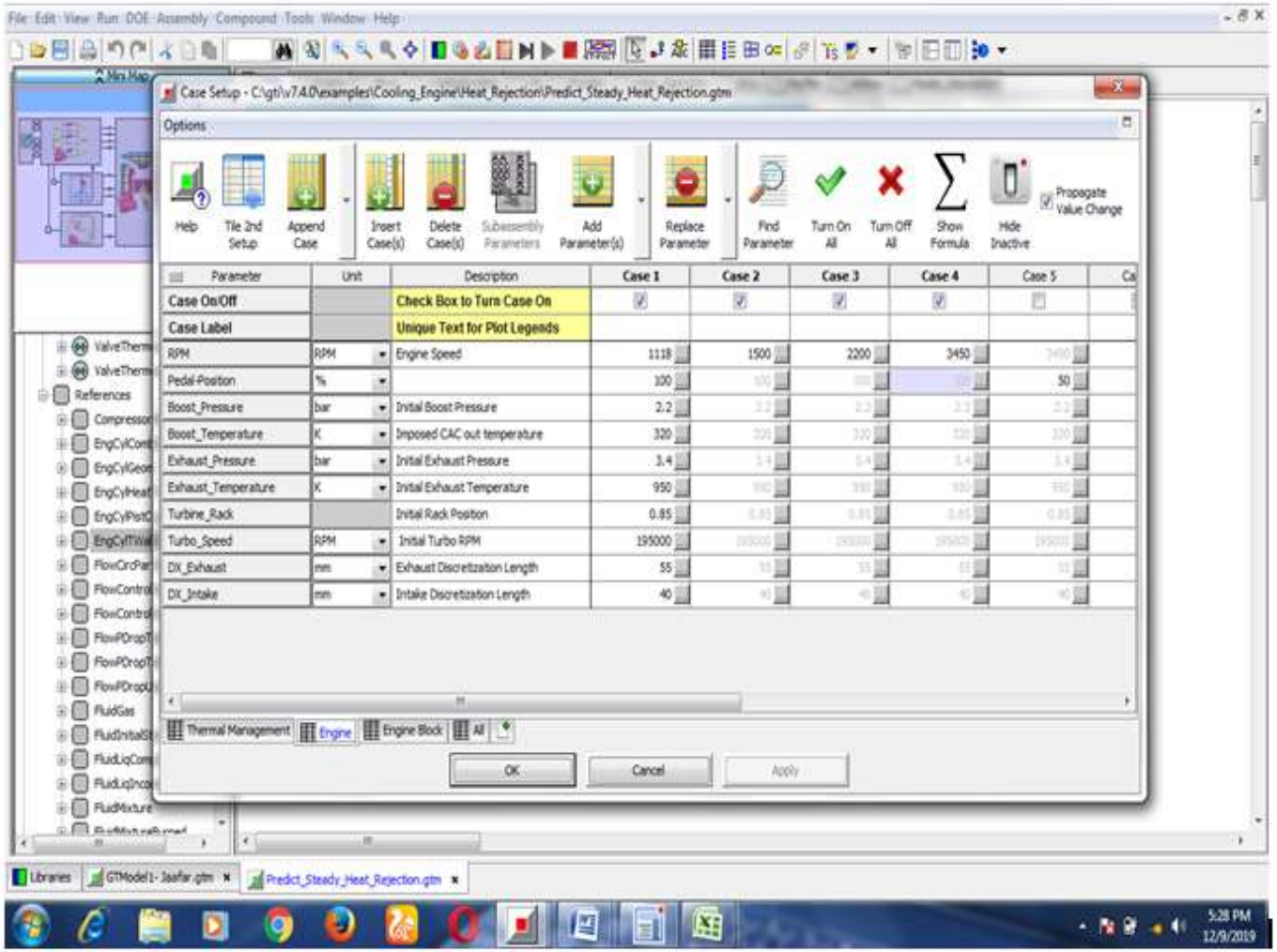


Plate 3.16: GT Case Setup

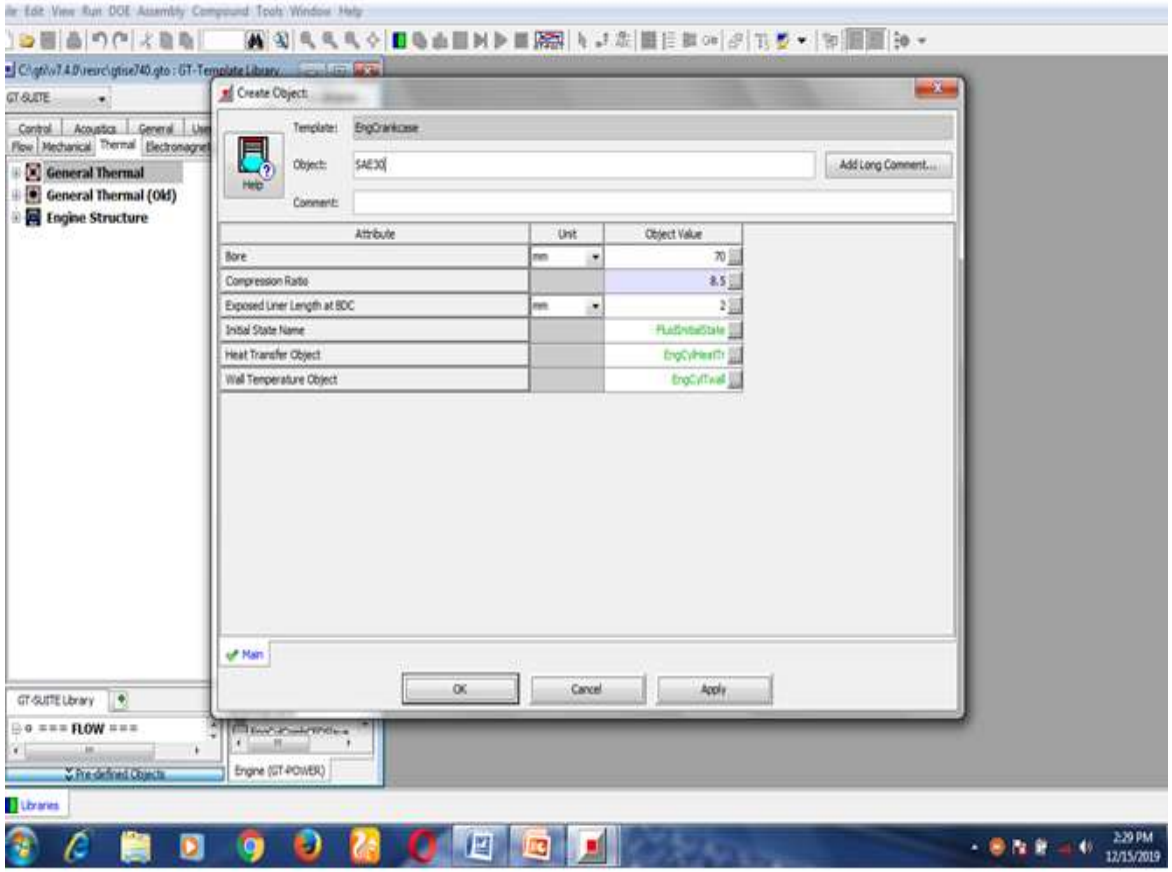


Plate 3.17: GT Crankcase Setup for SAE30

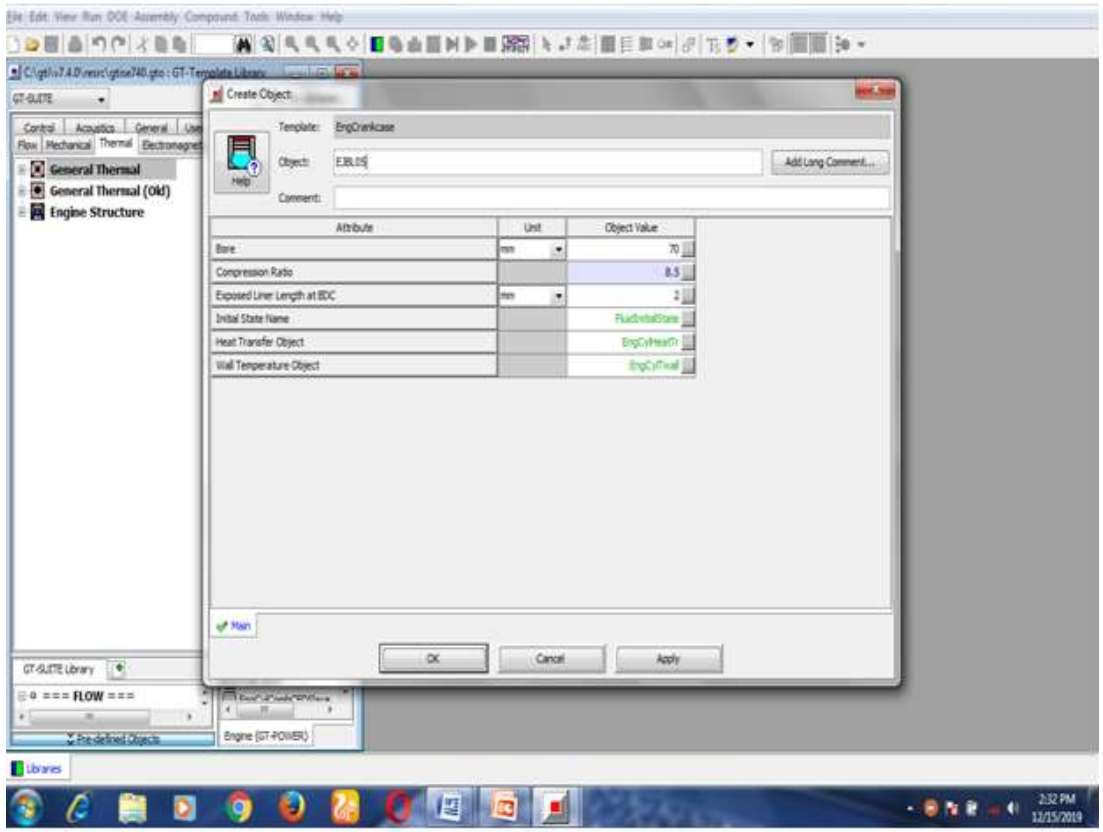


Plate 3.18: GT Crankcase Setup for EJBL05

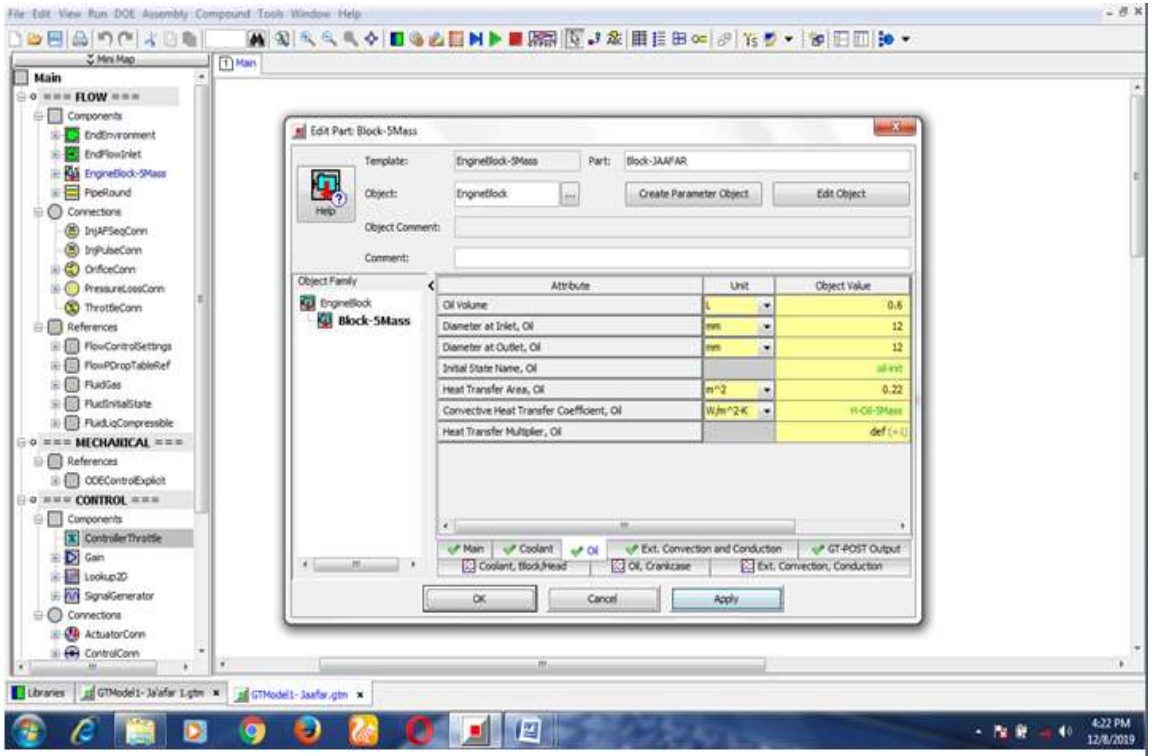


Plate 3.19: GT Oil Flow Setup

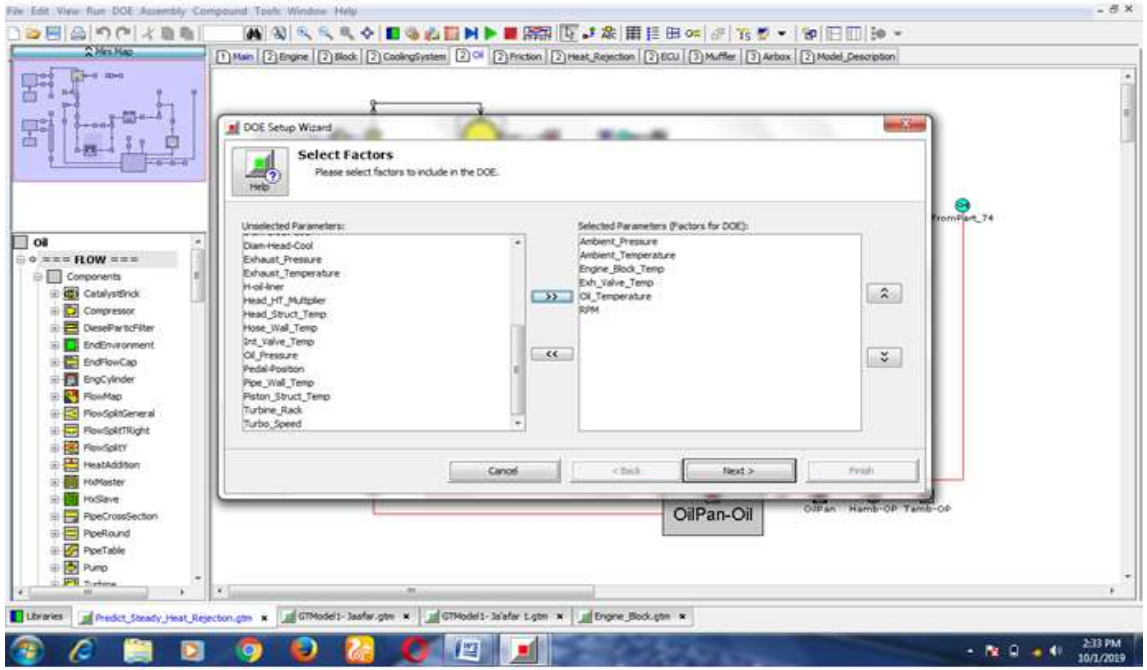


Plate 3.20: GT Settings for the experiment

CHAPTER FOUR

RESULTS AND DISCUSSIONS

4.1 Fourier Transform Infrared (FTIR) Spectrum of CJO and EJO

The infrared spectra of crude jatropha oil (CJO) and that of epoxidized jatropha oil (EJO) are presented in figure 4.1 and 4.2 respectively. The EJO spectrum showed clear doublet vibration at (819-838) cm^{-1} characteristic of C-O-C oxirane stretch. This is a confirmation of epoxide formation in the sample.

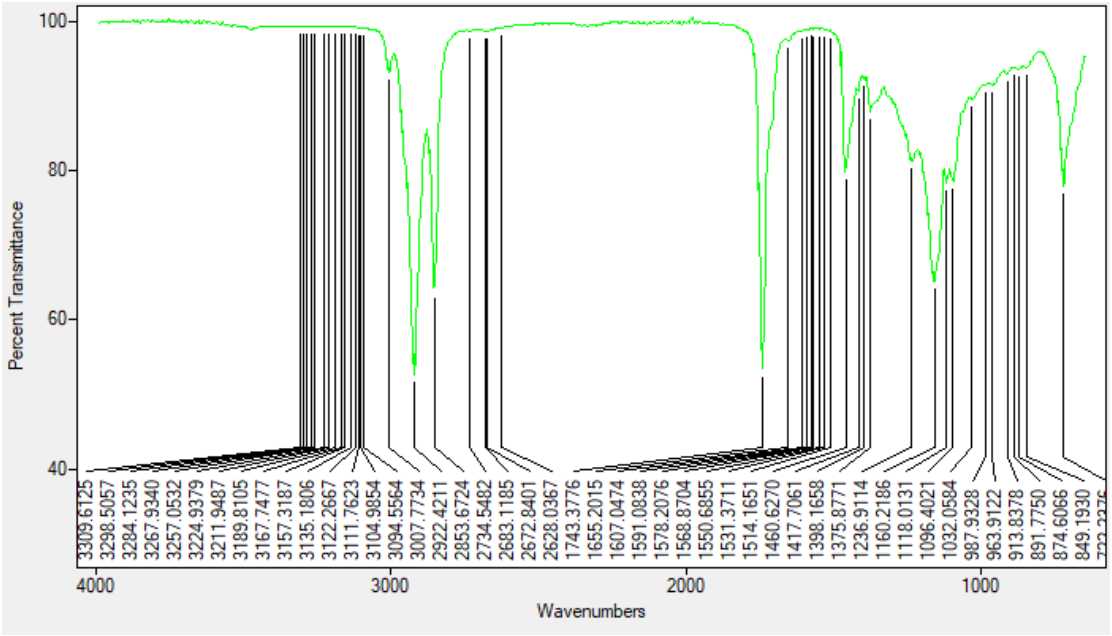


Figure 4.1: Infrared Spectrum of CJO

This is in conformity with the findings of Sammaiah *et al.* (2014), Wong *et al.* (2017), and Cheing *et al.* (2017) on epoxidation of jatropha oil. Sammaiah *et al.* established the formation of epoxides at 823 cm^{-1}; Wong *et al.* at 830-850 cm^{-1}. Similarly Nykulyshyn *et al.* (2017) carried out epoxidation of soybean oil and confirmed the formation of epoxides at 830-850 cm^{-1}. The EJO also showed characteristics of C-H stretching at 2922.57 cm^{-1}, carbonyl absorption at 1739.65 cm^{-1}, triglyceride ester triplet at 1237.13, 1164.32 cm^{-1} and 1096.92 cm^{-1} as shown in

appendix I. There is an indication of epoxy ring opening characteristics at 3454.97 cm^{-1} – 3235.44 cm^{-1}.

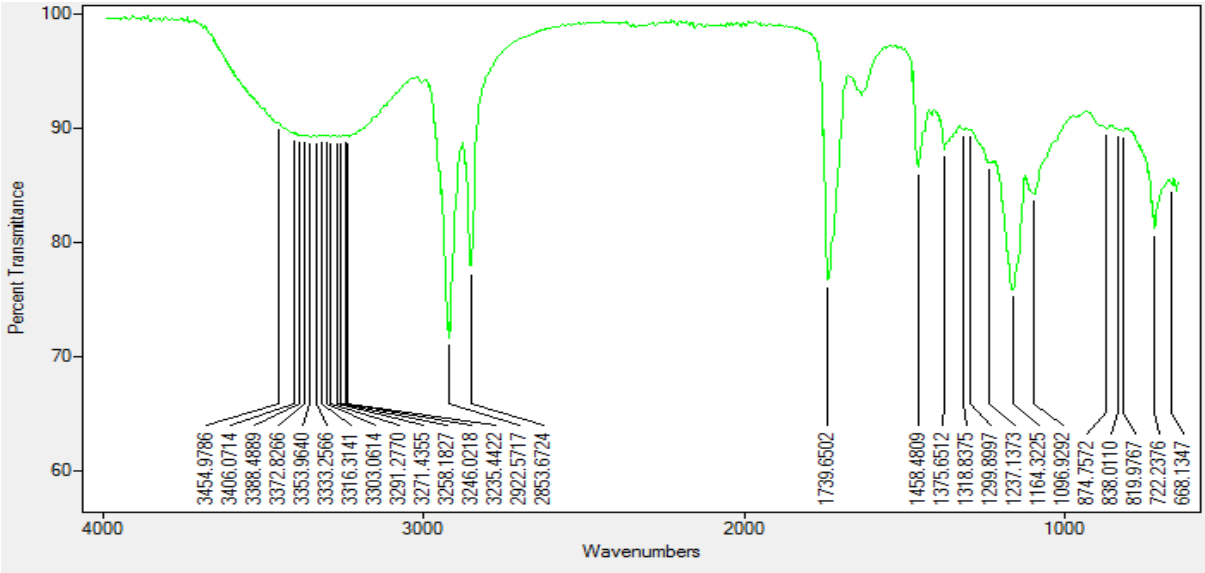


Figure 4.2: Infrared Spectrum of EJO

It is clear that there are many structural differences between the spectrum of CJO and that of EJO due to the effects of epoxidation to the crude jatropha oil as shown in Figure 4.3.

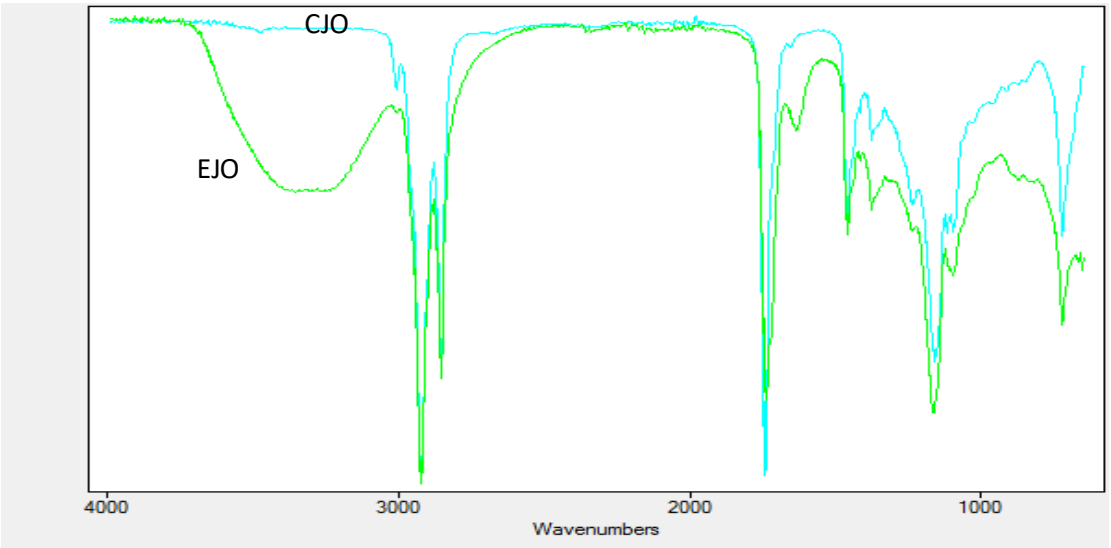


Figure 4.3: Superimposed Infrared Spectrum of CJO and EJO

The theoretical oxirane oxygen content and experimental oxirane oxygen contents from equation (3.1) and (3.2) were calculated to be 4.65 % and 2.76 % respectively. Hence the degree of epoxidation from equation (3.3) gave: 59.35 %. This means that only 59.35 % of the unsaturated bonds were converted to oxirane rings.

4.2 Confirmation of Epoxides Formation Using Iodine Value

Figure 4.4 presents the result for the Iodine Value (IV) of CJO and EJO and compares it with EN Standard for Iodine Value.

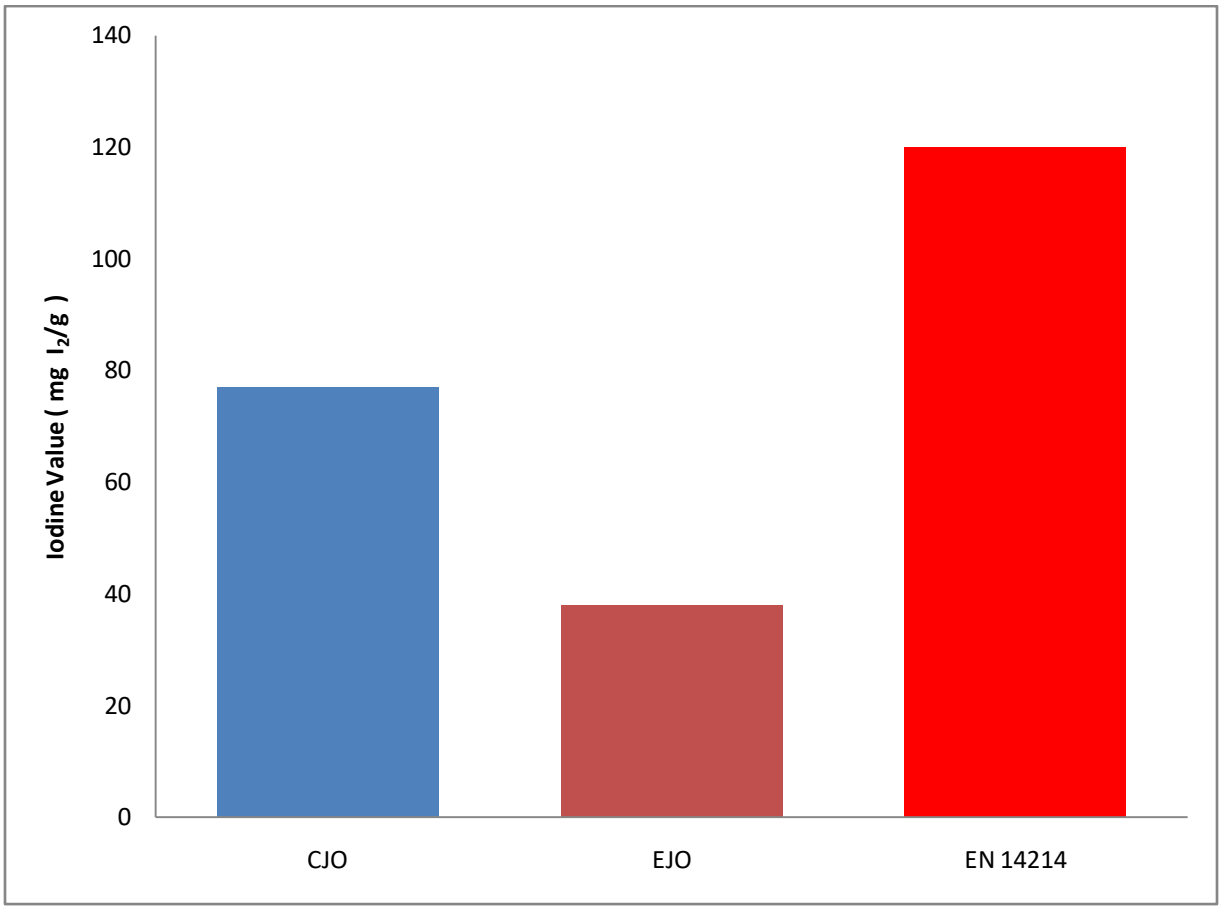


Figure 4.4: Iodine Values of CJO, EJO and EN 14214 Standard

Iodine value gives insight to the physical and chemical stability of oil. The higher the Iodine value the more unsaturates present in the oil and therefore the less stable the oil is. It was

observed that the IV dropped significantly from 77 mg I_2/g to 38.45 mg I_2/g when the oil was epoxidized. Therefore significant conversion of the fatty acids double bonds to oxirane has been achieved. Sammaiah *et al., (*2014) recorded a remarkable Iodine value decrease from 92 mg I_2/g to 2 mg I_2/g. Reduction in Iodine Value after epoxidation is a clear indication that epoxidation has occurred.

4.3 Effect of Epoxidation on Oxidation Stability

Figure 4.5 shows the Oxidation Induction Time (OIT) for CJO. The OIT indicates the potential of the oil sample to fight oxidation. The result shows that the CJO has week resistance to oxidation; it starts oxidation at a temperature just about 76^{o}C after 4 min, 30s. This is contrary to the findings of Yang, *et al.* (2014) who reported that Nigerian Jatropha oil starts oxidation at 110^{o}C.

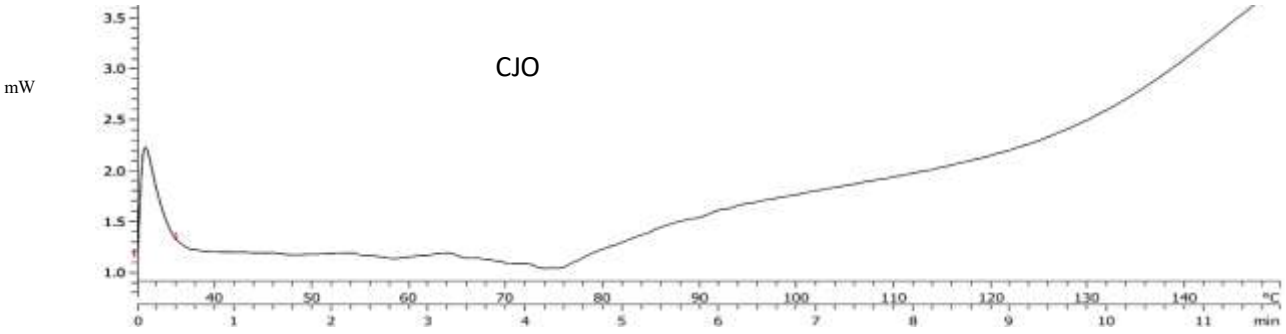


Figure 4.5: Oxidation Induction Time for Crude Jatropha Oil (CJO)

Figure 4.6 shows that the epoxidized jatropha oil, EJO, starts oxidation at about 130^{o}C after about 10 min of the test. This shows that the epoxidation carried on the crude jatropha oil (CJO) has significantly improved its oxidation stability. The findings are close to those of Sammiah *et al.* (2014) who reported OIT of 5 min for Jatropha oil and 20 min for epoxidized jatropha oil. The improvement of oxidation stability after epoxidation is due to conversion of carbon-carbon double bonds to saturated epoxy rings (Sammaiah *et al.*, 2014).

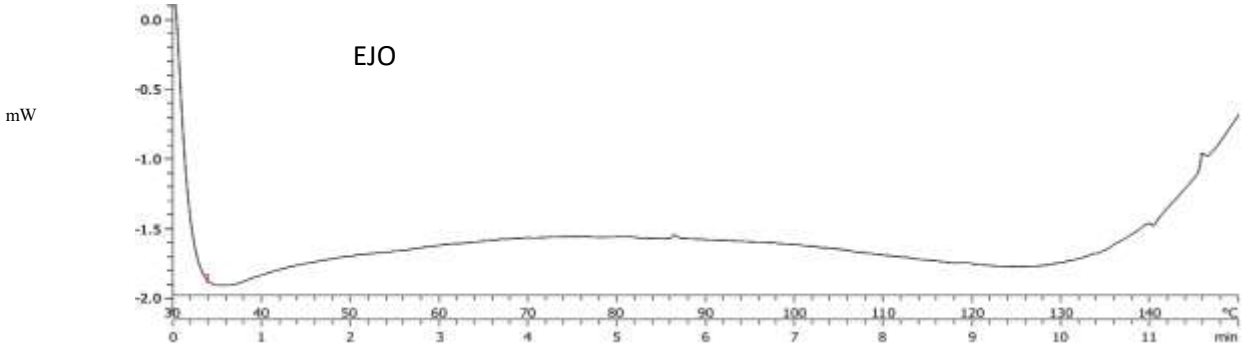


Figure 4.6: Oxidation Induction Time for Epoxizided Jatropha Oil (EJO)

4.4 Assessment of Crude Jatropha Oil and its Epoxy for Automotive Biolubricant Formulation

The quality of the jatropha oil was assessed by using Refractive Index, Water Content, Saponification and Iodine Values.

4.4.1 Refractive Index

The refractive Index of the CJO and EJO are presented in figure 4.7. Refractive Index (RI) is used to investigate purity of a substance. Pure liquid substances have RI in the range 1.3000 and 1.7000 as stipulated by ISO 6320 (Aji *et al.*, 2015). The refractive Index of the CJO was found to be 1.4583. This agrees with the results obtained by Salimon *et al.* (2008) and Aji *et al.* (2015) of 1.469 and 1.4689 respectively. Since the value falls within the normal range of 1.3000 and 1.7000, the CJO sourced for the work was pure.

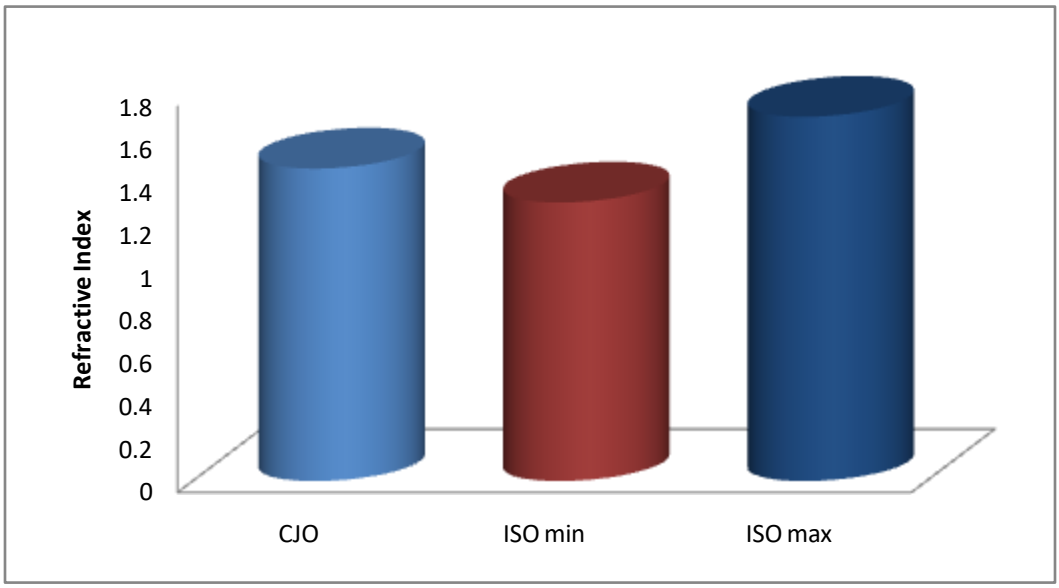


Figure 4.7: Refractive Index of CJO and ISO Standard for Refractive Index

4.4.2 Moisture Content

Figure 4.8 shows the moisture content result for CJO and EJO and the NIS Standard for engine lubricants base oil moisture content. The maximum permissible Water content for Internal Combustion engine base oil as specified by API and NIS is 0.025 %. The moisture contents of the CJO and EJO were obtained to be 0 %. Therefore the oil samples were dry enough for lubricant formulation. Moisture in oil deactivates catalyst and converts fat to fatty acid thereby increasing saponification of the oil.

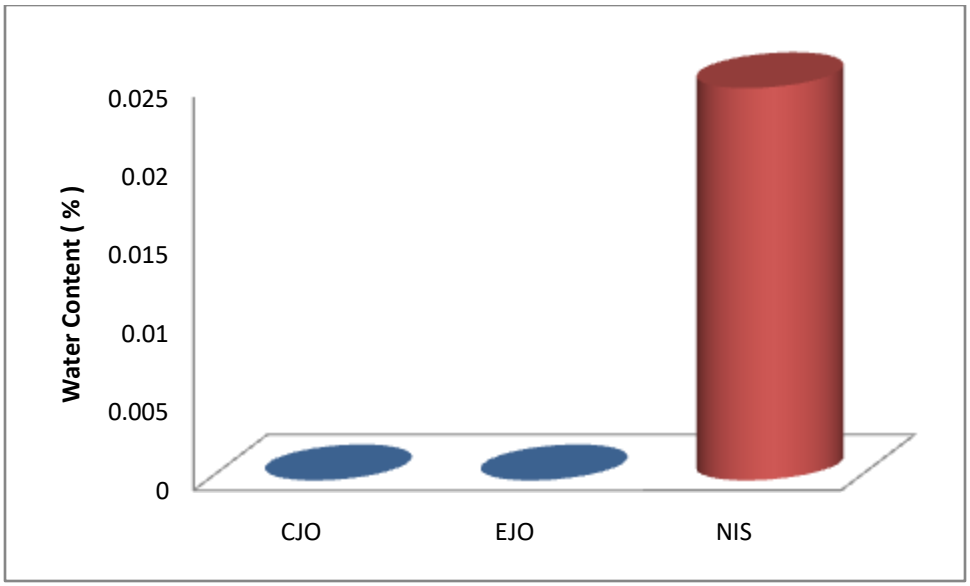


Figure 4.8: Water Content of CJO, EJO and the NIS max Water content limit for Engine Oils

4.4.3 Saponification Value (SV)

Figure 4.9 presents the Saponification value for CJO and EJO. The SV obtained for the CJO was 195.86 mg / g. This agrees with the values obtained by Zaku *et al.* (2012); Bilal *et al.* (2013) and Salimon and Abdullah (2008) of 191.8; 198.76 and 198.85 mg / g respectively. Oils with high saponification value consume more alcohol during esterification with fewer yields. The standards used for bio-based products such as ASTM D7467, EN 14214, DIN E51606, OECD did not specify SV for vegetable oils. However some researchers such as Joshua (2013) reported that SV of (188 - 198) is required for jatropha biodiesel and biolubricant production. The saponification value for the EJO dropped significantly to 96.77 mg/g. This was due to the reduction of the oil's FFA through chemical modification.

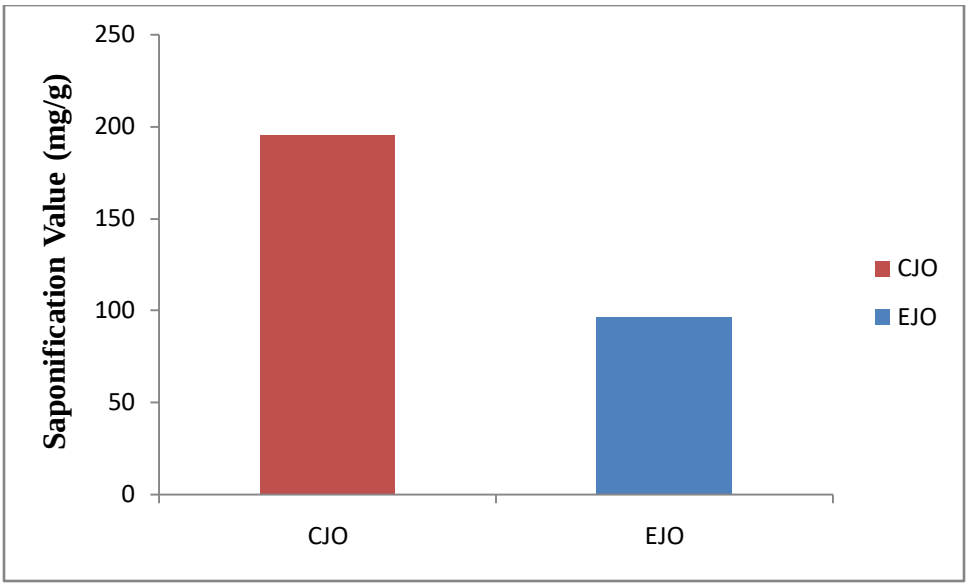


Figure 4.9: Saponification Values of CJO and EJO

4.4.4 Iodine Value (IV)

The results for the Iodine value has been presented in figure 4.4. The IV of the CJO was 77 mg I_2/g and below the 120 mg I_2/g stipulated by EN 14214 as max Iodine Value for biodiesel and biolubricant production. This agrees with the result obtained by Zaku *et al.* (2012) who got Iodine value of 62.12 mg I_2/g for crude jatropha oil. However, Salimon and Abdullah (2008) reported IV of 105.20 ± 0.70 mg I_2/g for a Nigerian specie of jatropha seeds oil and 135.15 ± 1.44 mg I_2/g for a Malaysian specie of jatropha seeds oil. Similarly, Arbain and Salimon (2009) reported the IV for an Indian jatropha oil to be 13 mg I_2/g. The values differ due to differences in the specie found in different places. Since the IV is within the EN limit, the CJO can be used for biolubricant production.

4.5 Minimum Requirements of Lubricant Base Stock for SI Engine Oil Formulation

The basic properties of lubricant base stock for SI engine oil formulation are presented for CJO and EJO and compared with those of Mineral base oil. The values for mineral base oil are as reported in Totten (2006).

4.5.1 Viscosity / Viscosity Index

The viscosities of CJO at 40^{o}C and 100^{o}C were determined to be 34.06 cSt and 7.5 cSt respectively. Whereas for EJO, 170.63 cSt and 17.6 cSt respectively. There is a remarkable increase in viscosity after epoxidation. Sammaiah *et al.* (2014) ascribed viscosity and density increase of epoxides to increase in molecular weight of the epoxides due to conversion of carbon-carbon double bonds to saturated epoxy group, and more polar structure and stronger interactions between molecules of the epoxides than the virgin oil.

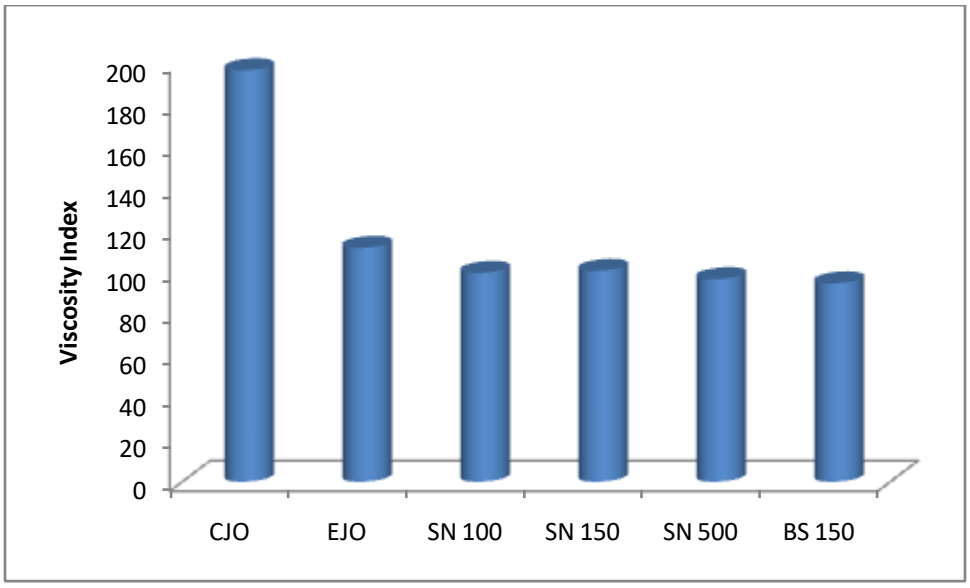


Figure 4.10: Viscosity Index of CJO & EJO Compared to Mineral Base Oils

However the VI of CJO (197) is much higher than that of EJO (112). This finding is consistent with the work of Anjana *et al.* (2013) who reported that chemical modification of vegetable oils

lowers its viscosity index. The result implies that the rate of viscosity change with temperature is higher for EJO than CJO. It can be seen in figure 4.10 that, the VI of EJO is higher than that of SN 100, SN 150, SN 500 and BS 150. Viscosity decrease with temperature is not desirable due to risk of mechanical failure at elevated temperatures, though it offers better fuel economy (Humphrey, 2016). According to API Viscosity Index classification, the CJO viscosity (197), falls within Super High range (160 - 200). However VI of 112 for EJO falls within very high range (110 - 125). Thus EJO has excellent VI and can therefore be an excellent candidate for high temperature applications.

4.5.2 Flash Point

The flash points of CJO and EJO were found to be 192^{o}C and 249^{o}C respectively as presented in figure 4.11. This means that the epoxidation has positively enhanced the flash point of the virgin oil. The results agree with that of Sammaiah *et al*. (2014), who got Flash points for jatropha oil to be 186^{o}C and for epoxidized jatropha oil 288^{o}C. The Flash Point of EJO is much higher than that of SN 100, SN 150, SN 500 and BS 150. Therefore in terms of flash point, EJO can be said to be good base oil for engine oil formulations.

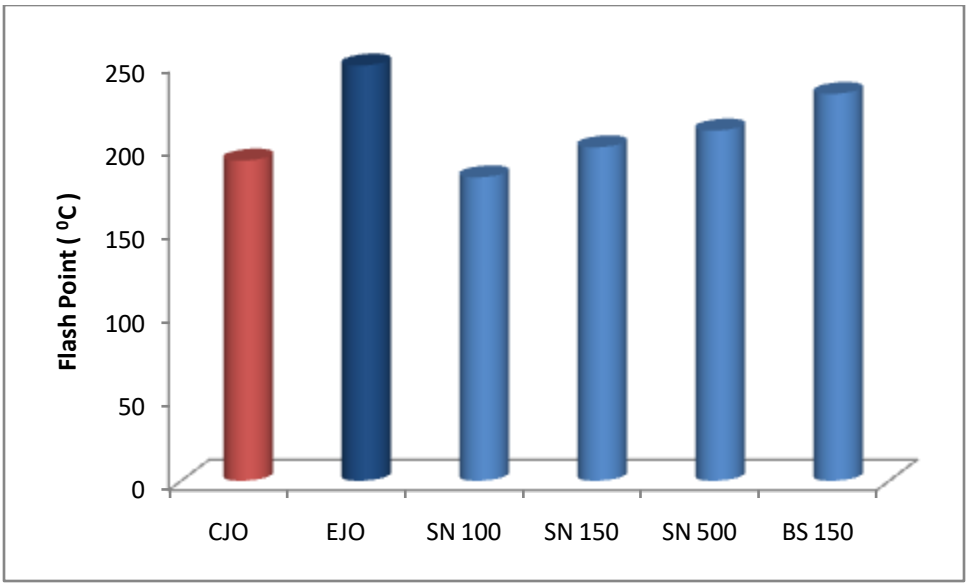


Figure 4.11: Flash Points of CJO & EJO Compared to Mineral Base Oil

4.5.3 Pour Point

The Pour Points were found to be -2°C for CJO and -5°C for EJO as shown in figure 4.12. This is contrary to the findings of Sammaiah *et al*. (2014), who reported that epoxidation improves all the properties of vegetable oil except the pour point. The lower the pour point, the better the lubricant protection to engine parts at low temperature services. The pour point of EJO (-5°C) is close to that of SN 500 (-6°C) and that of BS 150 (-6°C). Therefore the Pour Point of EJO can be said to be acceptable for internal combustion engine base oil because it is very close to the pour points of SN 500 and BS 150 base oils.

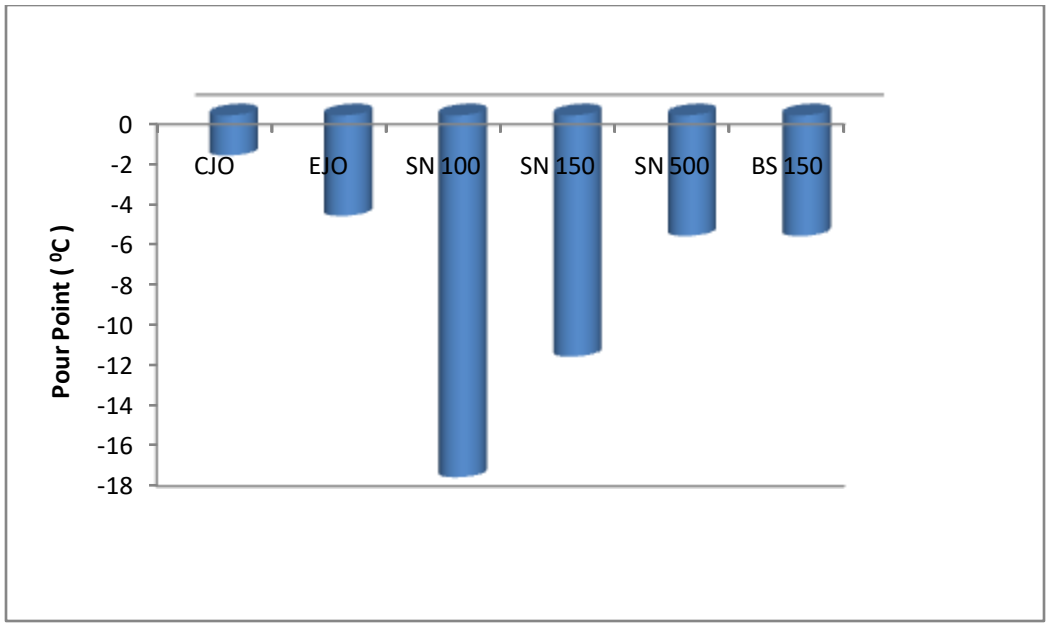


Figure 4.12: Pour Points of CJO & EJO Compared to that of Mineral Base Oils

4.6 Performance Parameters of EJBL and its Blends

The Nigerian Industrial Standard (NIS) specifies the minimum performance requirements for spark ignition engine oils and compression ignition engine oils. The results for the performance parameters of epoxidized jatropha biolube (EJBL), and blends of epoxidized jatropha biolube with 1 % to 10 % additives (EJBL01, EJBL02. EJBL03, EJBL04, EJBL05, EJBL06, EJBL07, EJBL08, EJBL09 and EJBL10) are compared and presented below. The purpose of which, was to get the best blend that could be safely used for engine performance test in the test engine. NIS specified nine parameters: Density, Viscosity @ 40^{o}C, Viscosity @ 100^{o}C, Viscosity Index, Pour Point, Flash Point, Viscosity at High Temperature High Shear @ 150^{o}C, Evaporative Loss and Foaming Tendency.

4.6.1 Density

The densities of EJBL and its blends @ 15^{o}C are presented in figure 4.13. The density increased with increased additive concentration. This result agrees with the findings of Obasi *et al.* 2014

who used B0 23233/ B 23333 additive on NS 150 and NS 500 base oils. EJBL and all the blends have passed the minimum density requirement of NIS for SAE 30, SAE 40, SAE 50 and 15W-40. However NIS does not impose maximum density limit for engine oil.

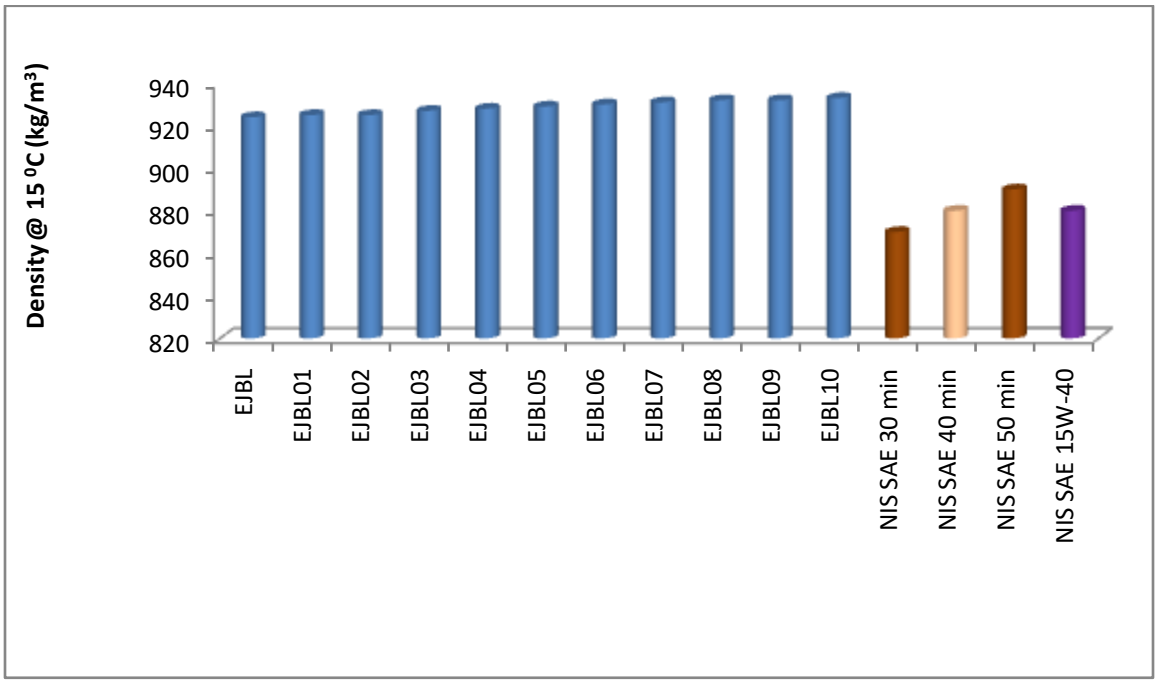


Figure 4.13: Density @ 15°C of EJBL and its Blends Vs NIS min Standards for Density @ 15°C for Various Engine Oil Grades

4.6.2 Viscosities / Viscosity Index

The results of viscosities @ 40°C and 100°C and also the Viscosity Indices for EJBL and its blends are depicted in figures 4.14, 4.15 and 4.16 respectively. EJBL, EJBL01, EJBL02, EJBL03 and EJBL04 have viscosities @ 40°C below the NIS minimum requirements for SAE 30, SAE 40, SAE 50 and 15 SAE 40. EJBL05 meets the minimum requirement for SAE 30 viscosity @ 40°C. EJBL06, EJBL07 and EJBL08 have met the requirements for SAE 40. Also EJBL10 has satisfied the requirement for 15W-40. EJBL, EJBL01, EJBL02, EJBL03 and EJBL04 have viscosities @ 100°C below the range for SAE30, SAE40, SAE50 and 15SAE40 as shown in figure 4.13. The viscosity of EJBL05 is within SAE30 range. EJBL06, EJBL07, EJBL08 and EJBL09 fall within SAE40 and 15 SAE 40 range. Similarly EJBL10 falls within SAE 50 range.

The VI of EJBL and all its blends are higher than the NIS minimum requirements for SAE 30, SAE 40, SAE 50 and 15 SAE 50 as shown in figure 4.14. Therefore all the blends have passed the NIS minimum requirement for engine oil Viscosity Index.

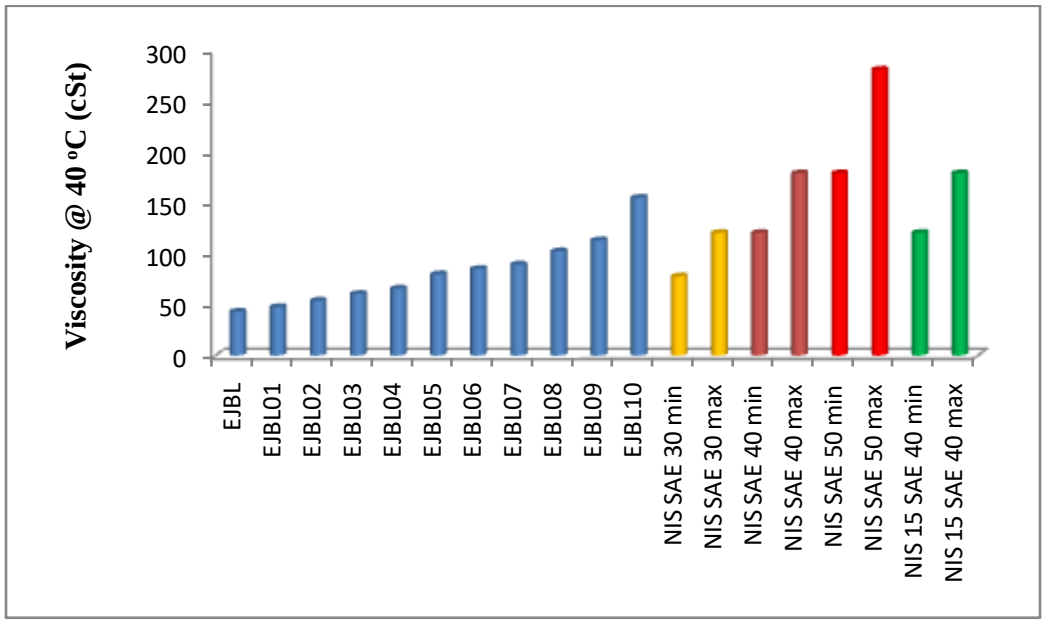


Figure 4.14: Viscosity @ 40°C of EJBL and its Blends Vs NIS min Standards for Viscosity @ 40°C for Various Engine Oil Grades

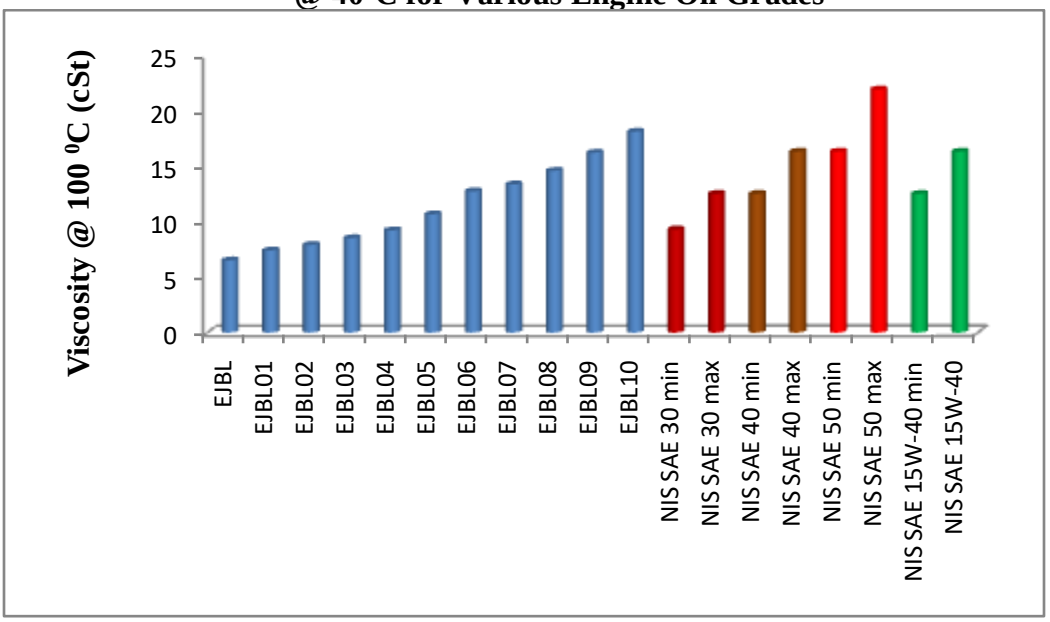


Figure 4.15: Viscosity @ 100°C of EJBL and its Blends Vs NIS min Standards for Viscosity @ 100°C for Various Engine Oil Grades

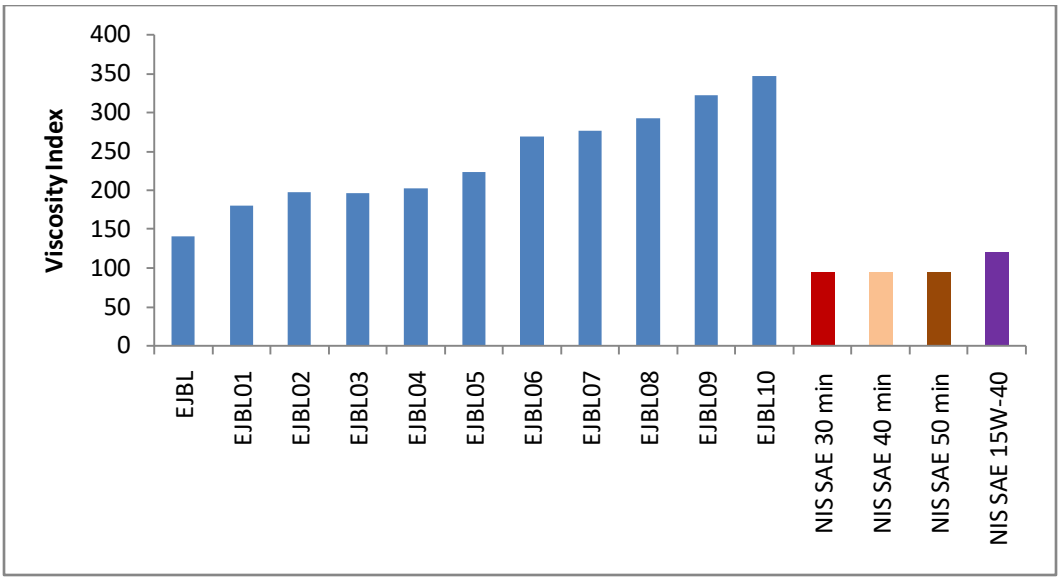


Figure 4.16: Viscosity Index of EJBL and its Blends Vs NIS Viscosity Index Standards for Various Engine Oil Grades

4.6.3 Pour Point

Figure 4.17 shows the pour points for EJBL and its blends and the minimum NIS pour point limits. The pour point of a lubricant marks the lowest temperature the lubricant can still be used. EJBL, EJBL01, EJBL02. EJBL03 and EJBL04 do not meet the minimum NIS pour point requirements for SAE 30, SAE 40, SAE 50 and SAE 15W-40. Whereas EJBL05, EJBL06, EJBL07, EJBL08, EJBL09 and EJBL10 have met the minimum requirements for SAE 30, SAE 40 and SAE 50. This finding agrees with Erhan *et al*. (2006), who reported that cold flow properties of biolubricants improve by using non-biobased additive.

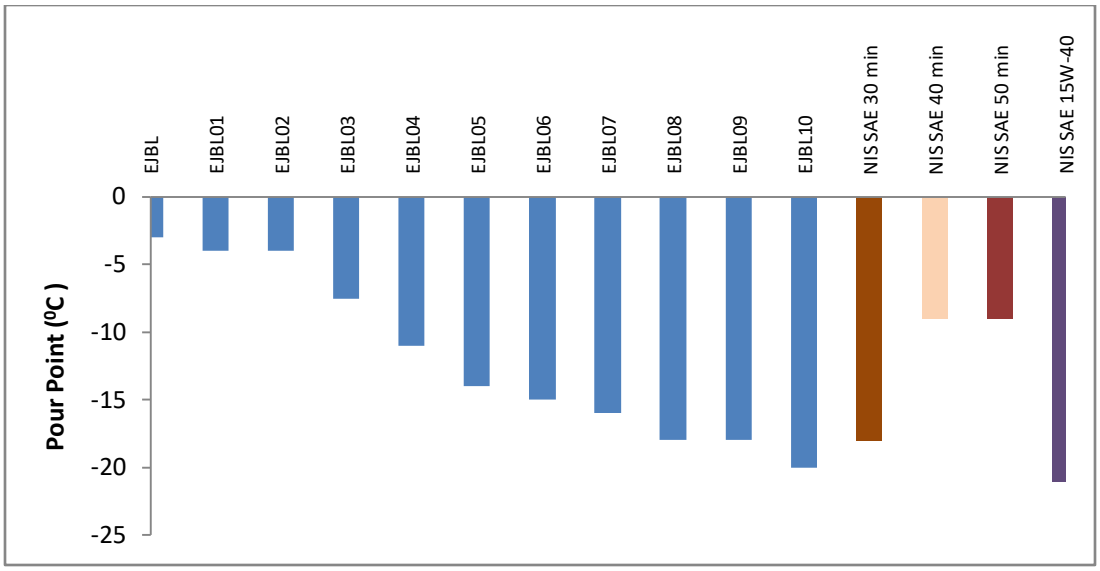


Figure 4.17: Pour Point of EJBL and its Blends Vs NIS min Pour Points Standards for Various Engine Oil Grades

A rule of thumb commonly used in lubricant selection is to ensure that the lubricant has a pour point at least 10^{o}C below the lowest anticipated temperature of the use location (Mohammed, 2015).

4.6.4 Flash Point

The results of the flash points for the various biolubricant blends are presented in figure 4.18. The Flash point gives an idea of the volatility of the lubricant and its tendency of explosion hazards during usage. EJBL, EJBL01, EJBL02, EJBL03, EJBL04, EJBL05 were found to meet the NIS minimum requirement for Flash Point of SAE 30. Also, EJBL06, EJBL07, EJBL08, EJBL09 and EJBL10 have flash points above the NIS minimum requirement for SAE 30, SAE 40, SAE 50 and SAE 15W-40. Gill, (2013) reported that the minimum flash point for internal combustion engine lubricants varies from 174^{o}C to 260^{o}C. Similarly, ILSAC GF-1 and ILSAC GF-2 engine oil minimum performance standard specifies 185^{o}C as the minimum flash point for ASTM D93 method and 200^{o}C for ASTM D92 as shown in appendices B6 and B7. Therefore

Flash Points of all the biolubricant blends are within the acceptable limits of internal combustion engine lubricants.

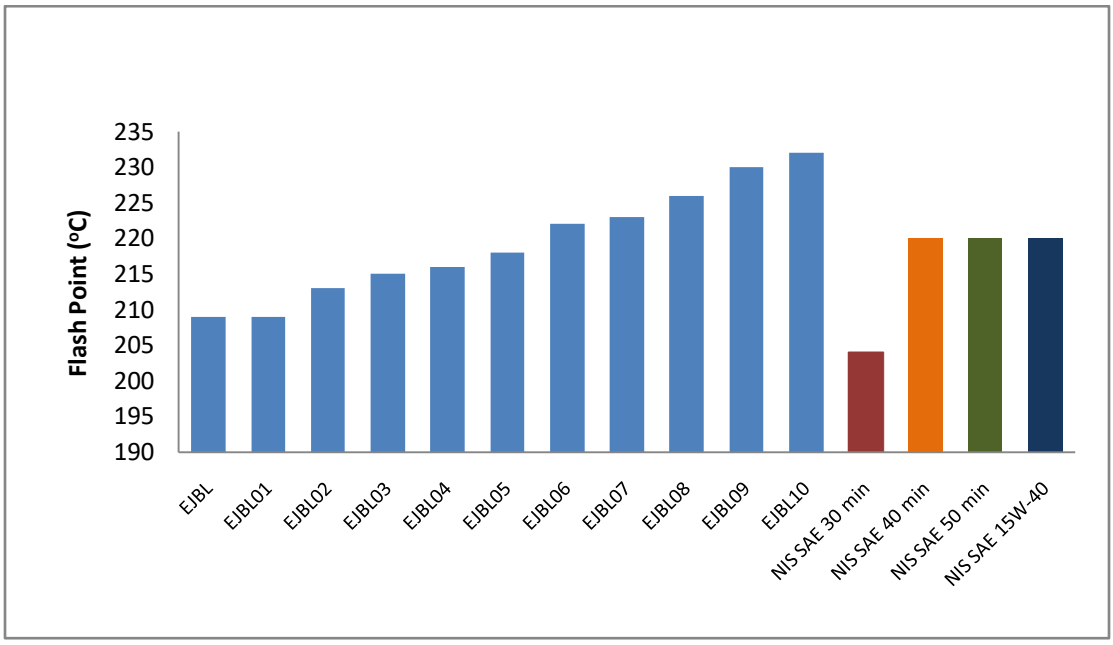


Figure 4.18: Flash Point of EJBL and its blends Vs NIS min Flash Points Standards for Various Engine Oil Grades

4.6.5 High-Temperature High-Shear (HTHS) Viscosities

The High-Temperature-High-Shear (HTHS) Viscosities of EJBL and its blends are presented in figure 4.19. HTHS Viscosity @ 150^{o}C is used to determine the thermal stability of a lubricant (Ja'afar *et al*. 2018). EJBL, EJBL01, EJBL02 and EJBL03 were found to have HTHS Viscosities below the NIS minimum HTHS standard for SAE 30, SAE 40, SAE 50 and SAE 15W-40 as shown in figure 4.18. Whereas, EJBL04, EJBL05, EJBL06, EJBL07, EJBL08, EJBL09 and EJBL10 have satisfied the standard.

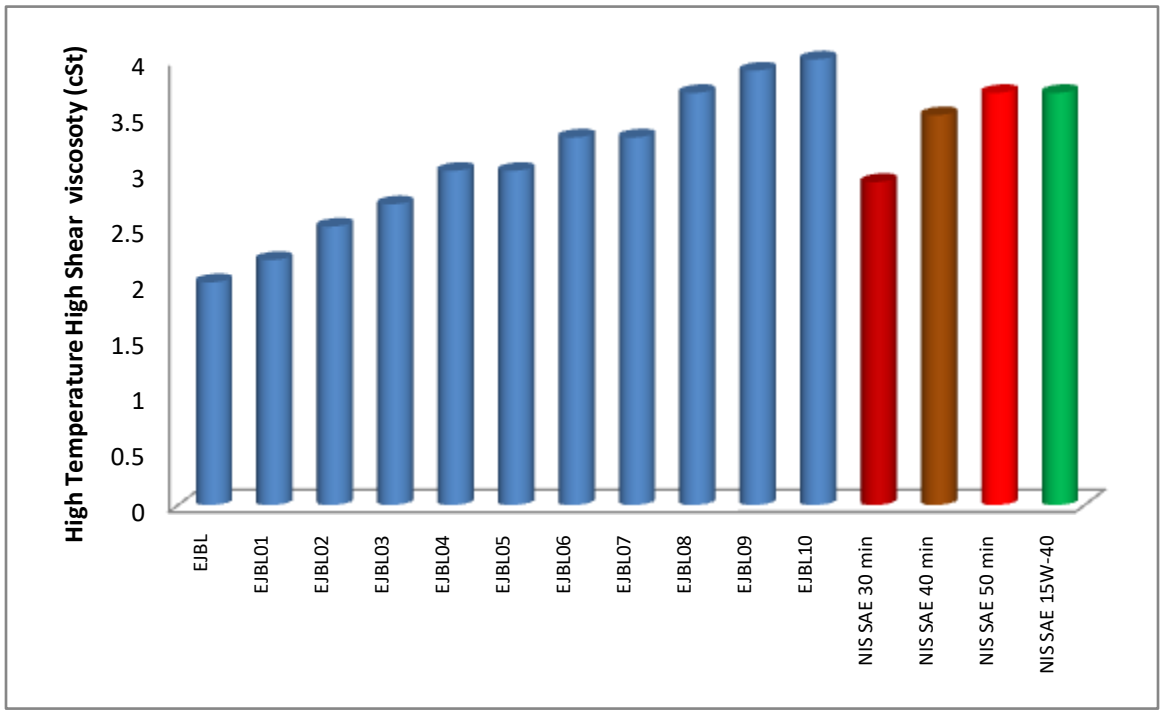


Figure 4.19: HTHS Viscosity @ of 150^{o}C of EJBL and its Blends Vs NIS min HTHS Viscosity for Various Engine Oil Grades @ of 150^{o}C

It can be seen that the NIS Minimum HTHS viscosity requirement @ 150^{o}C for SAE 30 is lower than that of SAE 40, SAE 50 and SAE 15W-40. According to Humphrey (2016), sufficient HTHS viscosity creates enough protective oil film between engines. This is critical for prevention of wear at ring/liner interface and lower HTHS viscosities ensure better fuel economy. Therefore, SAE 40, SAE 50 and 15 SAE 50 with higher values of HTHS viscosity @ 150^{0}C are designed to have better engine protection at elevated temperature, than SAE 30.

4.6.6 Evaporation Loss

The results for evaporation loss of EJBL and its blends are presented in figure 4.20. The evaporation loss of EJBL and all its blends are below the NIS maximum evaporation limit permissible for SAE 30, SAE 40, SAE 50 and SAE 15 W-40 of 22 % as shown. The evaporation

loss was observed to decrease with increase in the additive concentration due to increase in viscosity. The findings agree with Hsien *et al.*, 2015 reported that, bio-based lubricants have lower evaporation loss than mineral base lubricants due to the high molecular weight of their triglycerides. Also, API and ILSAC have set maximum Evaporation loss (Noack) limit of 15 % for SN, SM, GF-5 and GF-4 (Appendices B3 and B4). Similarly, the maximum evaporation loss for SJ, SL, GF-2 and GF-3 is 22 % as shown in appendix B5 and Appendix B6. Therefore EJBL and all the remaining blends, have also met the API maximum evaporation standard for SJ, SL, GF-2 and GF-3.

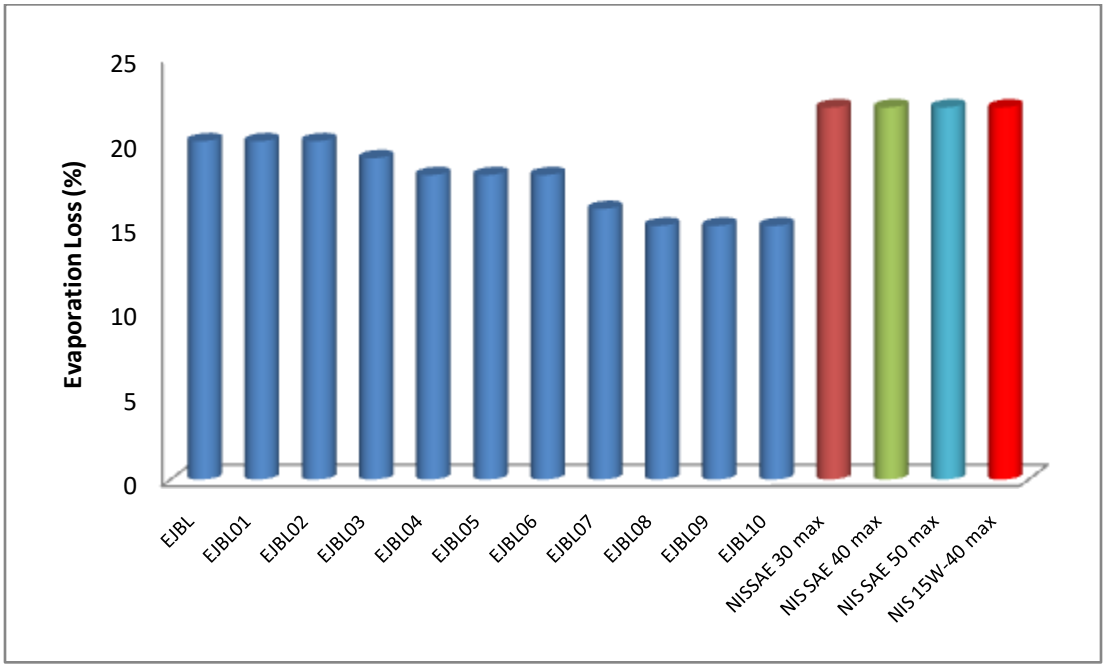


Figure 4.20: Evaporation Loss of EJBL and its Blends Vs NIS Max Evaporation Loss for Various Engine Oil Grades

4.6.7 Foaming Tendency

The results of foaming stabilities for the EJBL and all its blends for Sequence I, II and III are presented in figure 4.21. The foaming stabilities after 10 min were observed to be within the acceptable limits for API SN, SM, SJ and SL and ILSAC GF-5, GF-4 and GF-3 as shown in

appendices B3, B4, B5 and B6. API stipulates max foaming/settling volume for sequence I and III at 10/0 and for sequence II at 50/0. Therefore the EJBL and all its blends have satisfied the NIS (API and ILSAC) requirements for engine oil foaming characteristics. Older versions of API Standards, such as SF, SG and SH, have no foaming tendency specifications.

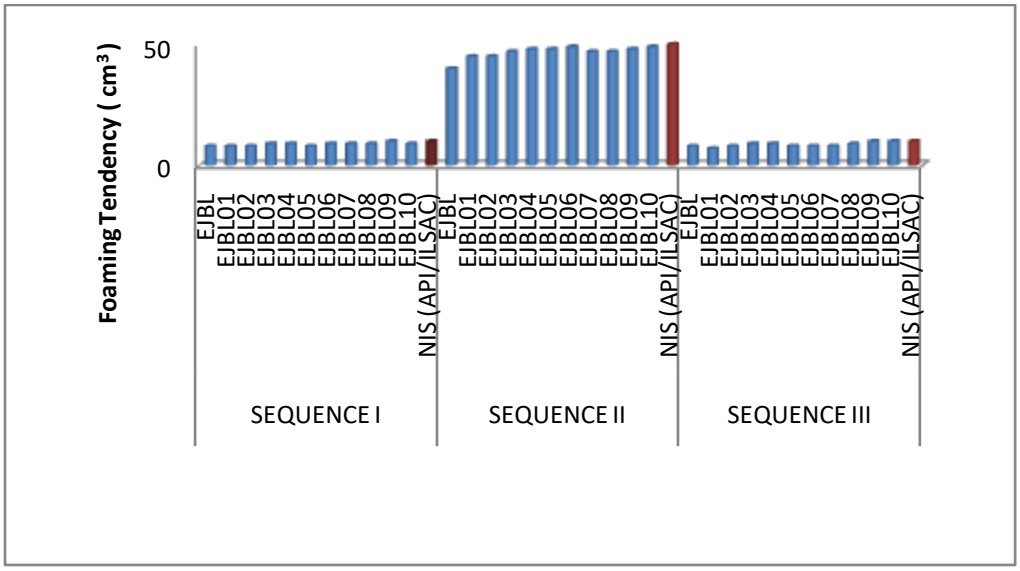


Figure 4.21: Foaming Tendency Limit

4.7 Additional Requirements not Specified by NIS

Other Spark Ignition Engine oil requirements not specified by NIS but specified by ASTM, ISO or API/ILSAC include: Total Base Number, Phosphorus and Sulfur, Seal Compatibility, etc.

4.7.1 Total Base Number (TBN)

The results of the TBN for EJBL and its blends are depicted in figure 4.22.The Total Base Number (TBN) or simply the Base Number (BN) is the reserved alkalinity which is responsible for fighting lubricants oxidation. When oil oxidizes it becomes thick and eventually causes seizure of moving parts hence mechanical failure. The ASTM D2896 and ISO 3771 standards

stipulate a minimum TBN value of > 8 mgKOH/g for automotive engine oils. It can be seen that EJBL, EJBL01, EJBL02, EJBL03 and EJBL04 did not meet the ASTM minimum requirement. EJBL05, EJBL06, EJBL07 and EJBL08 meet the minimum requirement. Whereas EJBL09 and EJBL10 are below the standard. All the mineral base engine oil grades satisfied the minimum TBN requirement.

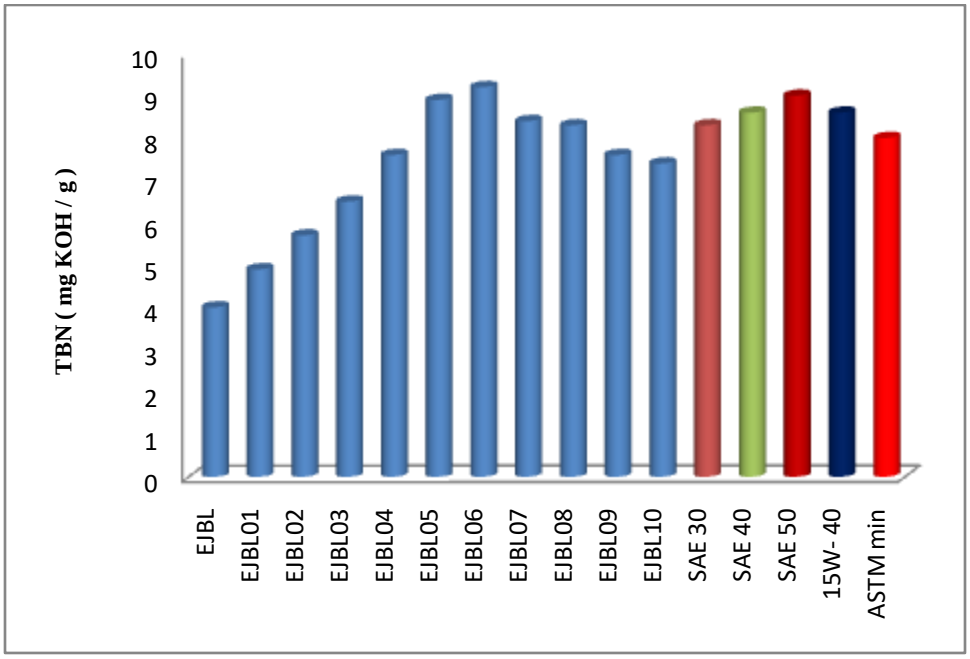


Figure 4.22: TBN of EJB its Blends and Various Engine Oil Grades Vs ASTM Min TBN Standard for Spark Ignition Engine

4.7.2 Phosphorus / Sulfur Content

The Phosphorus and sulfur contents of EJBL and its blends are presented in figure 4.23 and figure 4.24 respectively. Phosphorus content in engine oil is a non-critical parameter and is not required for non ILSAC GF-4 lubricants (API/ILSAC, 2015). Therefore API SN, SM, SJ and SL do not have phosphorus limit. Some latest vehicles with catalytic converters have specifications for max. phosphorus content of engine oils. API/ILSAC imposes phosphorus content limits of 0.06 % - 0.08 %. The EJBL and all its blends have phosphorus contents below the ILSAC phosphorus content requirement as shown. Similarly the mineral base lubricants, SAE 30, SAE

40, SAE 50 and 15 SAE 40 used for this study all couldn't meet the ILSAC minimum phosphorus content requirement of 0.06 %.

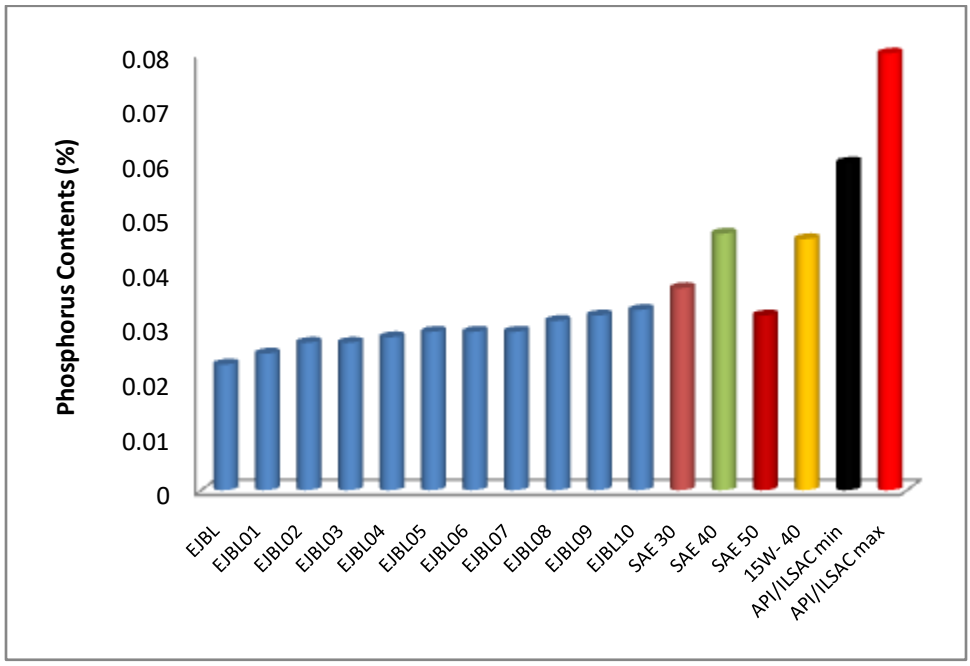


Figure 4.23: Phosphorus Contents of EJBL, its Blends, Various Engine Oil grades and API/ILSAC Min and Max Phosphorus Limits

Just like Phosphorus, Sulfur content is also a non-critical parameter and is not required for non ILSAC GF-5 and GF-4 lubricants as shown in appendices B3, B4, B5 and B6. ILSAC imposes a sulfur content limit of 0.5 % max as shown in figure 4.24. The EJBL and all its blends have sulfur contents far below 0.5 % therefore satisfy the ILSAC sulfur content requirement. Similarly the mineral base lubricants, SAE 30, SAE 40, SAE 50 and 15 SAE 40 used for this study all met the ILSAC maximum sulfur content requirement.

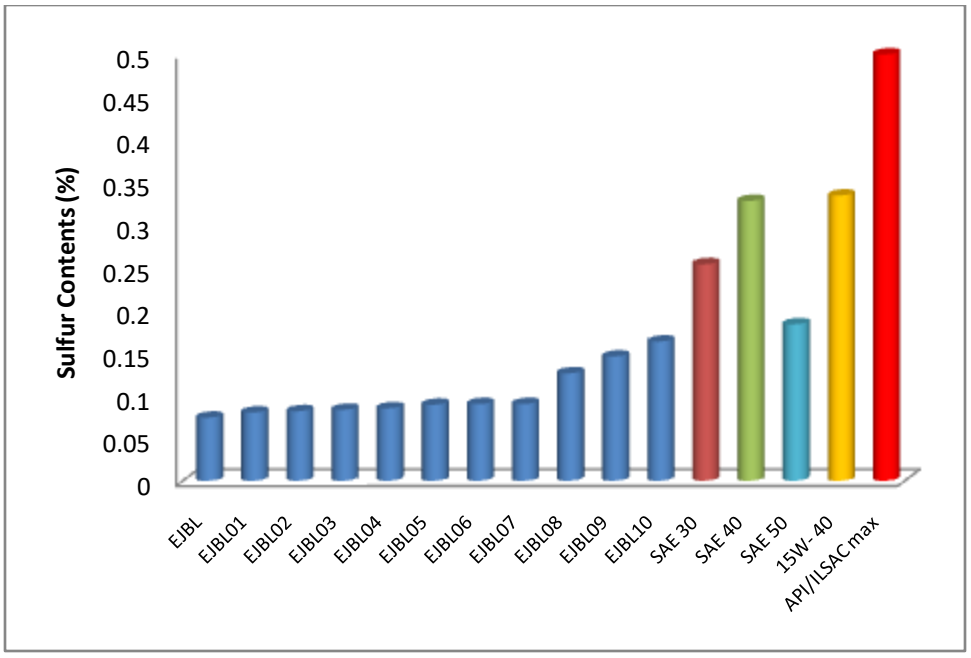


Figure 4.24: Sulfur Content of EJBL, its Blends, Various Engine Oil Grades and API/ILSAC Max Sulfur Limit

4.7.3 Seal Compatibility

The results of seal compatibility test for EJBL and its blends are shown in figure 4.25a and 4.25b. The seals used for this test were Silicone rubber (SR), Fluorocarbon Rubber (FKM) and Ethylene Acrylic rubber (AEM). The volume and hardness change after the test for EJBL and all its blends were within API limits for SN-RC/GF-5 class as shown in appendix B3. Therefore EJBL and all its blends are very compatible with elastomers. Vidovic (2014) reported that standard elastomers such as Fluorocarbon Rubber (FKM), Silicone Rubber (Q, MQ, VMQ, and PVMQ), Hydrogenated Nitrile (HNBR), Ethylene Acrylic Rubber (AEM) and Polyacrylate Rubber (ACM) are highly compatible to biolubricants. This agrees with the report of Srivastava and Sahai (2013).

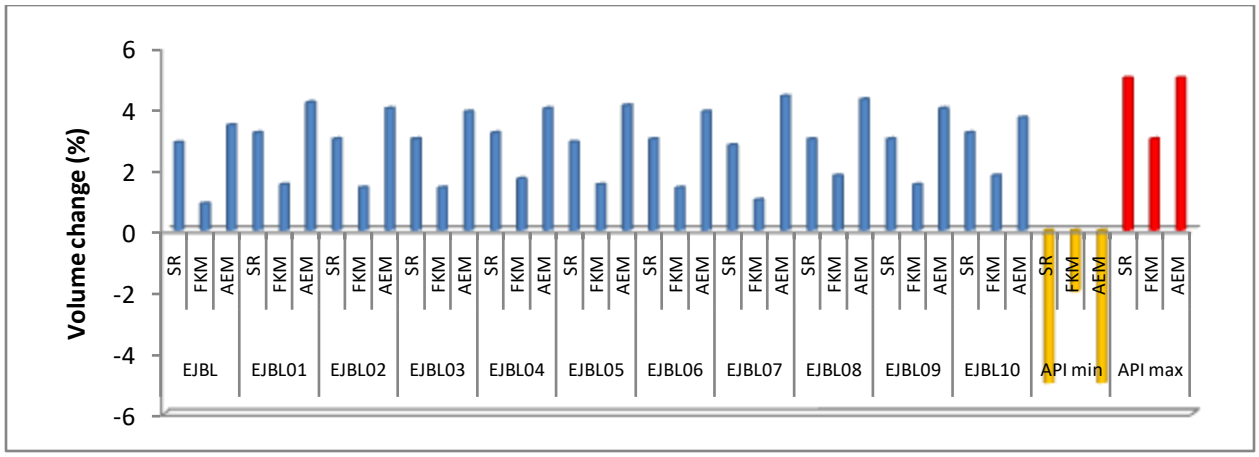


Figure 4.25a: Seal compatibility of EJBL, its Blends and API Standards

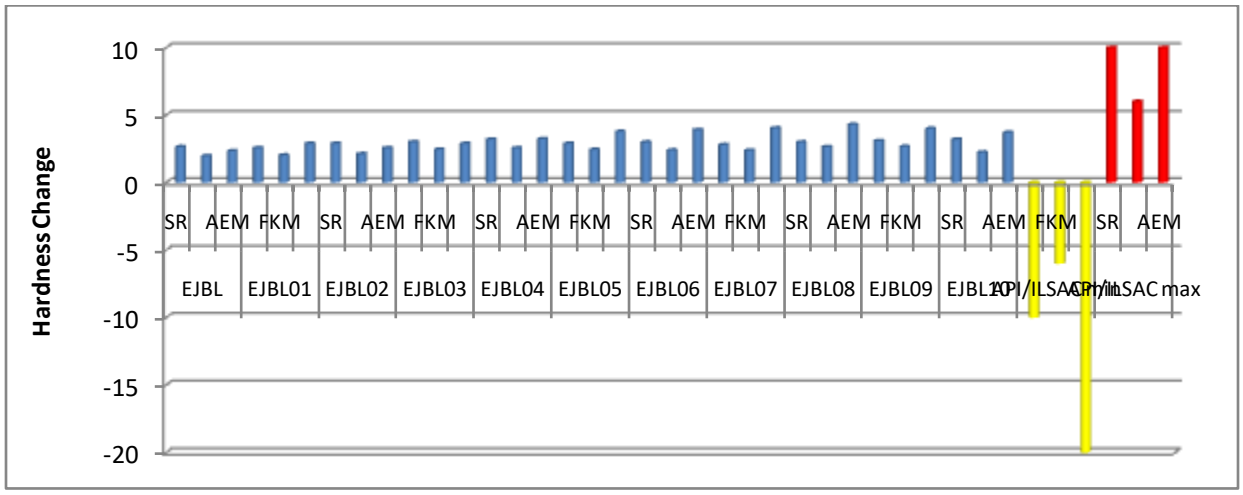


Figure 4.25b: Seal Compatibility of EJBL, its Blends and API Standards

4.7.4 Oxidation Induction Temperature (OIT)

The Oxidation Induction Temperature of EJBL and its blends and that of some mineral base engine oils are presented in figure 4.26. Minimum OIT of 122^{o}C was obtained for EJBL and EJBL10 and maximum OIT of 142^{o}C for EJBL06 and EJBL07. The mineral base lubricant recorded very high OIT with minimum of 240^{o}C for SAE30 and maximum of 260^{o}C for SAE50. This shows that the mineral base engine oils will offer better resistance to oxidation at higher temperatures than the epoxidized jatropha biolubricant.

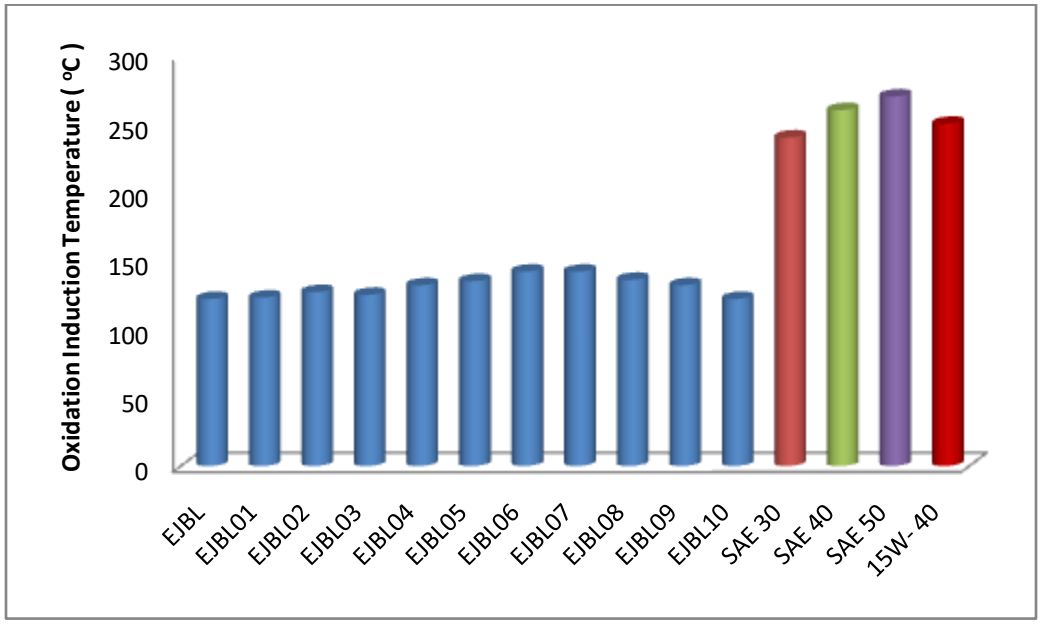


Figure 4.26: Oxidation Induction Temperature of EJBL, its Blends and Various Engine Oil Grades

4.7.5 Oxidation Induction Time (OIT)

The Oxidation Induction Time indicates the time taken for oxidation to commence under such operation conditions. The OIT of EJBL and its blends and that of some mineral base engine oils are presented in figure 4.27. A minimum OIT of 9 min was obtained for EJBL10 and maximum OIT of 11 min for EJBL06 and EJBL07. The mineral base lubricants have better OIT with minimum of 18 min for SAE30 and maximum of 21 min for SAE50. This means that the mineral base lubricants used for this research have superior oxidation resistance than their biolubricants counter parts.

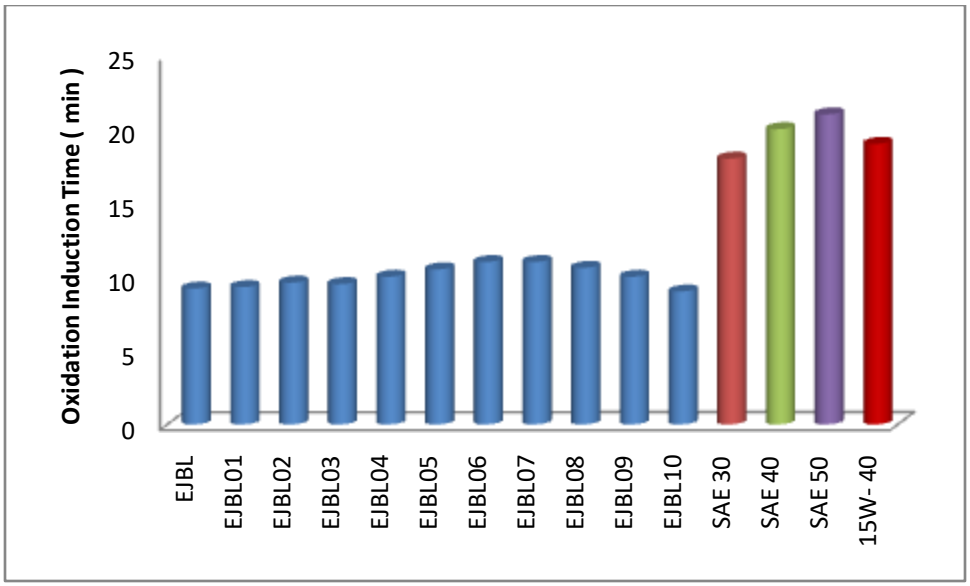


Figure 4.27: Oxidation Induction Time of EJBL, its Blends and Various Engine Oil Grades

4.7.6 Specific Heat Capacity (SHC)

The results of Specific heat capacities for the EJBL and its blends are presented in figure 4.28. SHC was observed to increase slightly with the additive concentration. This implies that the coefficient of thermal conductivity of the additive is higher than that of the biolubricant. It can be seen that the EJBL, EJBL01and EJBL02 have specific heat capacities similar to that of SAE 30. Also, EJBL03 and EJBL04 have specific heat capacities similar to that of SAE 40, SAE 50 and 15 SAE 40. The specific heat capacities of EJBL05, EJBL06, EJBL07, EJBL08, EJBL09 and EJBL10 were all above those of the mineral base engine oil. Since specific heat capacity is a measure of the ability of substance to absorb thermal energy, by this, EJBL05, EJBL06, EJBL07, EJBL08, EJBL09 and EJBL10 will absorb more heat than SAE 30, SAE 40, SAE 50 and 15W-40 for the same temperature difference. The findings agree with report by Scott *et al*. (2005) on heat transfer properties of engine oils.

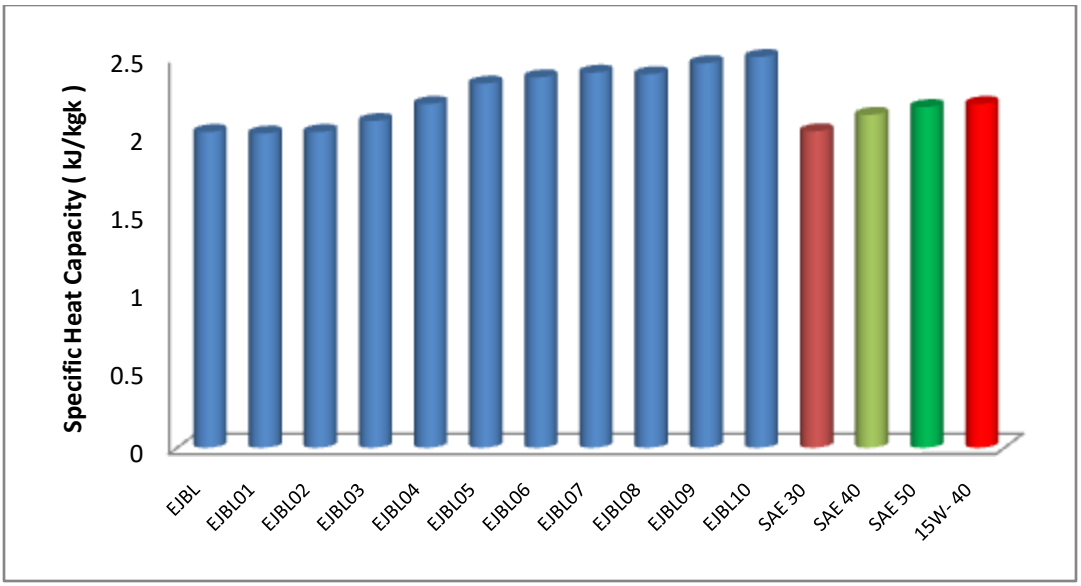


Figure 4.28: Specific Heat Capacity of EJBL, its Blends and Various Engine Oil Grades

4.7.7 Coefficient of Thermal Conductivity

The coefficient of thermal conductivities for EJBL and its blends were found to decrease with additive concentration as shown in figure 4.29. Therefore biolube with less additive will transfer heat by conduction more efficiently. Ja'afar and Mohammed (2018) reported that the larger the thermal conductivity and specific heat capacity, the more efficiently the oil will transfer heat. The reduction in coefficient of thermal conductivity with additive concentration is most likely that the additive has lower coefficient of thermal conductivity than the biolubricant. This can only be established if the coefficient of thermal conductivity of the additive is separately determined.

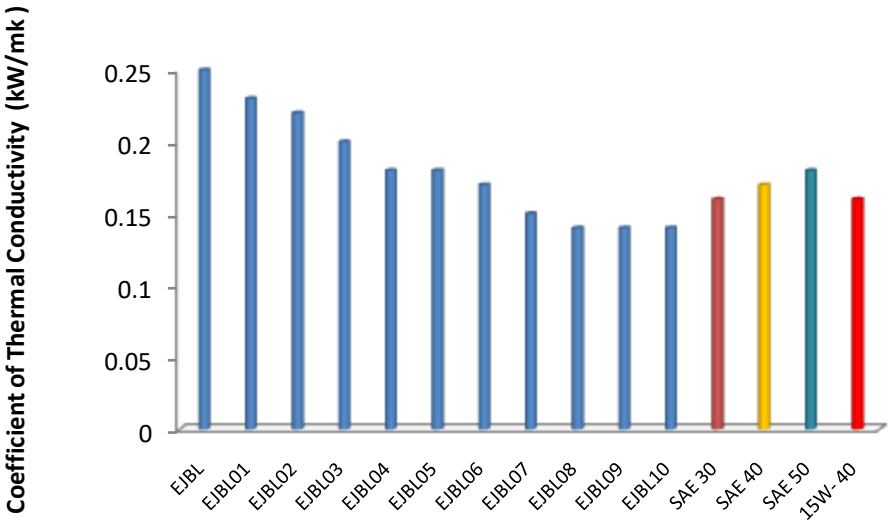


Figure 4.29: Coefficient of Thermal Conductivity of EJBL, its Blends and Various Engine Oil Grades

4.7.8 Ash Contents

The Ash Contents of EJBL and its blends and mineral base engine oils are presented in figure 4.30. EJBL and all its blends recorded very low ash contents compared to the mineral base engine oils. Slight increase in ash content with additive concentration was observed. Unlike the mineral base engine oils, the low ash content of biolubricants is ascribed to low organo-metallic constituents present in the oil. API did not specify ash contents for SI engines. It however specified 1.0 % max for CI engines and 35 mg as the max total engine deposits for SM and SL service classes.

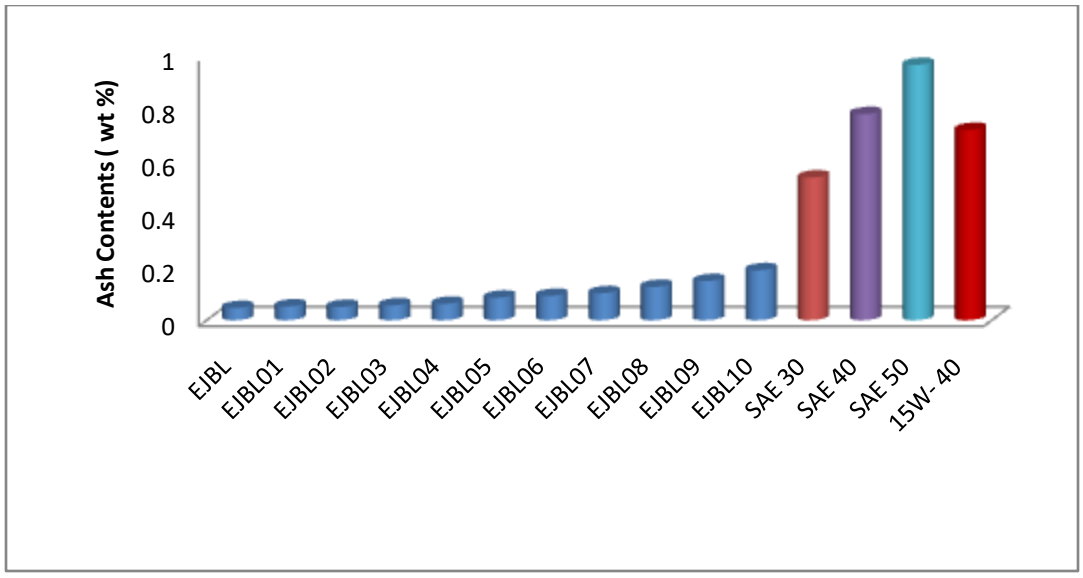


Figure 4.30: Sulfated Ash of EJBL, its Blends and Various Engine Oil Grades

4.7.9 Demulsibility

The results of demulsibility test for EJBL and its blends are presented in figure 4.31.The time taken for complete separation of water-oil emulsions of EJBL and all its blends occurred between 18 and 24 min. Whereas, the emulsions of the other grades (SAE 30, SAE 40, SAE 50 and 15W-40) separated completely in 25 to 26 min.

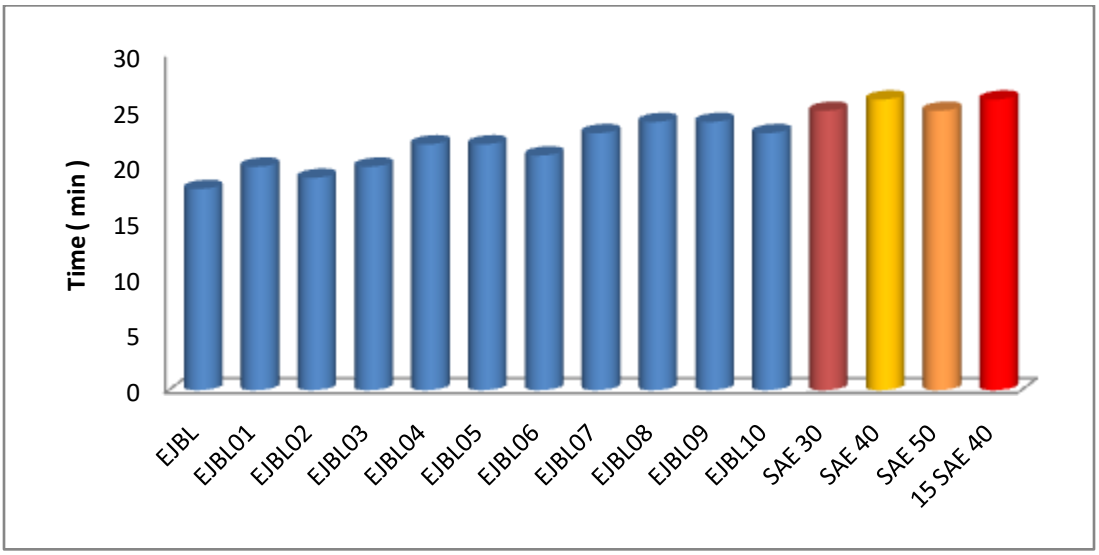


Figure 4.31: Demulsibility of EJBL, its Blends in Water and that of Various Engine Oil Grades

This shows that biolubricants have better demulsibility in water than mineral base lubricants. Lubricating oils are expected to have good demulsibility in the event of water contamination due to leakage or water vapour condensation in the crankcase (Gill, 2013).

4.7.10 Copper Strip Corrosion

The Copper Strip Corrosion test showed that EJBL and all its blends have 1a as presented in table Appendix B2. This shows that EJBL and all its blends will not cause corrosion of the engine parts on usage.

4.8 Choice of Blend for Engine Test

Internal combustion engines are designed to operate optimally with specific engine oil grade (Singh, 2004 and Gill, 2013). The manufacturer of the engine (TecQuipment, TD 201) used for the biolubricant test, recommended SAE 30 or 10W- 30 engine oil grade for the engine. Therefore SAE 30 has been chosen as the reference oil for this work. It is worth noting that SAE 30 and 10W-30 have same physical properties, only that 10W-30 has better fluidity at low temperature. Table 4.1 compares between the critical parameters of EJBL and its blend with SAE 30.

Table 4.1: Choice of Biolubricant Blend for TecQuipment TD201 Engine

	Density (kg/m^3)	**Viscosity @ 40°C (cSt)**	**Viscosity @ 100°C (cSt)**	**TBN (mgKOH/g)**	**Flash Point (° C)**	**Pour Point (° C)**	**Remarks**
SAE30	907	46.6	10.6	8.3	205	-12	Reference oil
EJBL	941	35	6.5	4.0	209	-3	NS-Low PP, low TBN, low HTHS Viscosity
EJBL01	942	35.6	7.4	4.9	209	-4	NS-Low PP, low TBN, low HTHS

							Viscosity
EJBL02	942	36.3	7.9	5.7	213	-4	NS-Low PP, low TBN, low HTHS Viscosity
EJBL03	944	40.2	8.5	6.5	215	-7.5	NS-Low PP, low TBN, low HTHS Viscosity
EJBL04	945	43.4	9.2	7.6	216	-11	NS- low TBN
EJBL05	946	47.2	10.7	8.9	218	-14	S
EJBL06	947	49.1	12.7	9.2	222	-15	NS- High Viscosity above Engine requirement
EJBL07	948	50.3	13.3	8.4	223	-16	NS- High Viscosity above Engine requirement
EJBL08	949	52.4	14.6	8.3	226	-18	NS- High Viscosity above Engine requirement
EJBL09	949	53.2	16.2	7.6	230	-18	NS- High Viscosity above Engine requirement and low TBN
EJBL10	950	55	18.10	7.4	232	-20	NS- High Viscosity above Engine requirement and low TBN

Source: TecQuipment TD201 engine manual.

Key: HTHS- High Temperature High Shear, PP- Pour Point, NS- Not Suitable, S- Suitable

It can be seen that the properties of EJBL05 are very close to that of SAE 30. Also EJBL05 has the required TBN for SI Engines. Gill, (2013) and Humphrey, (2016) noted that, using engine oil with viscosity below the recommended value causes engine wear; also using oil with higher viscosity above the recommended value adds more loads to the engine and results in decreased power output and low fuel economy.

4.9 Engine Performance Results

4.9.1 Engine Torque

At low and medium engine speeds (1000-1500 rpm), EJBL05 recorded lower engine torque than SAE30. This is because EJBL05 has higher viscosity (47.2 cSt) at low temperature than SAE 30 (46.6 cSt). Lubricant viscosity plays a major role in reducing total engine friction. Gill (2013) reported that, the torque developed by an engine is affected by the lubricants viscosity. Taylor, (1997) established that base oil viscosity, viscosity and viscosity index modifiers contribute immensely in reducing the total engine friction. The higher the engine friction, the lower the torque available at the flywheel. It can be seen from figure 4.32 that, at higher speeds (2500-3500 rpm), when the engine was hotter, the torque developed by the engine for both EJBL05 and SAE 30 increased due to reduction of viscosity. The torque increase for EJBL05 was higher than that for SAE 30. The maximum torque recorded for EJBL05 and SAE 30 were respectively 10.9 Nm and 11.5 Nm at 2850 rpm.

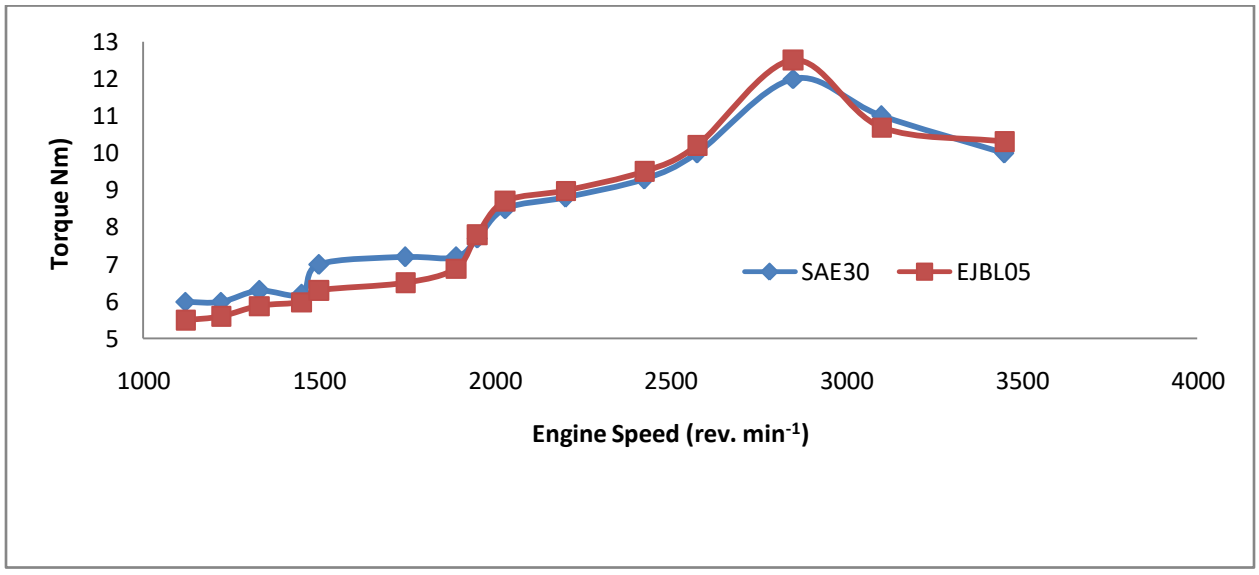


Figure 4.32: Engine Speed and Engine Torque

4.9.2 Engine Brake Power

Figure 4.33 shows the graph of Engine Brake Power against Engine Speed for EJBL05 and SAE30. The brake power is the available power at the flywheel for work. The maximum brake

powers recorded for EJBL05 and SAE30 within the test range were 3577 W and 3396 W respectively. This is equivalent to 5 % increase in favour of EJBL05. At low and high speeds the values are close to each other. SAE 30 has better brake power at medium speed (2000-2500 rpm) than EJBL05.

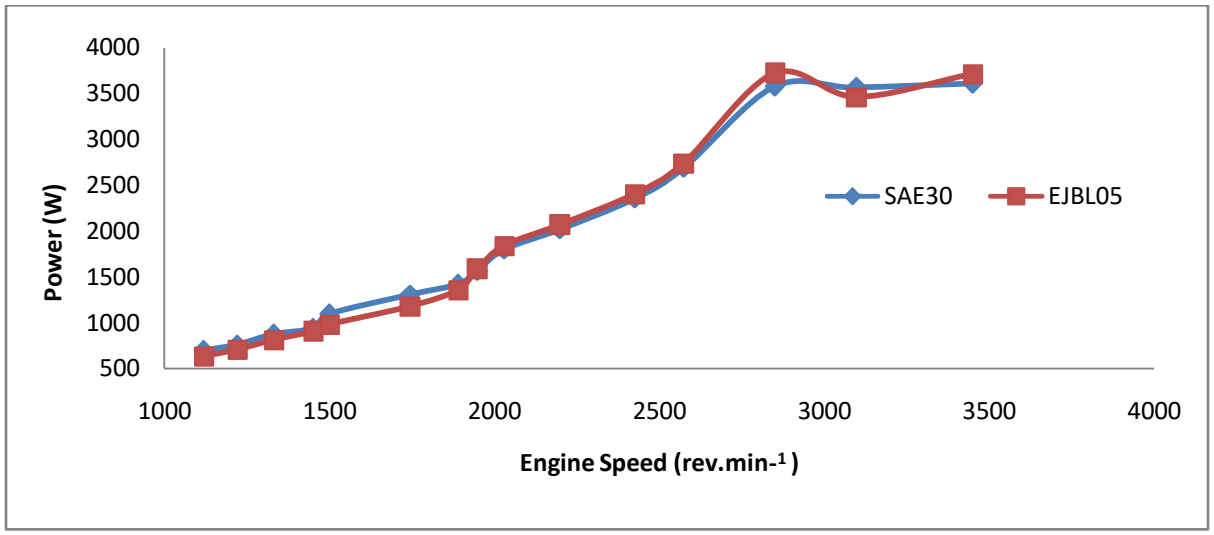


Figure 4.33: Engine Speed and Engine Power

4.9.3 Brake Mean Effective Pressure (BMEP)

Figure 4.34 presents the BMEP for EJBL05 and SAE30. The BMEP graph for both oils, show similar patterns to the Engine Speed and Engine Torque graph and Engine Speed and Brake Power graph shown in figure 4.32 and 4.33 respectively. BMEP increased with engine speed for both oils. Peak BMEP of 6.84 bars for SAE30 and 7.22 bars for EJBL05 were attained at a speed of about 2850 rev.min^{-1}. High BMEP means high temperature and stress for the engine parts.

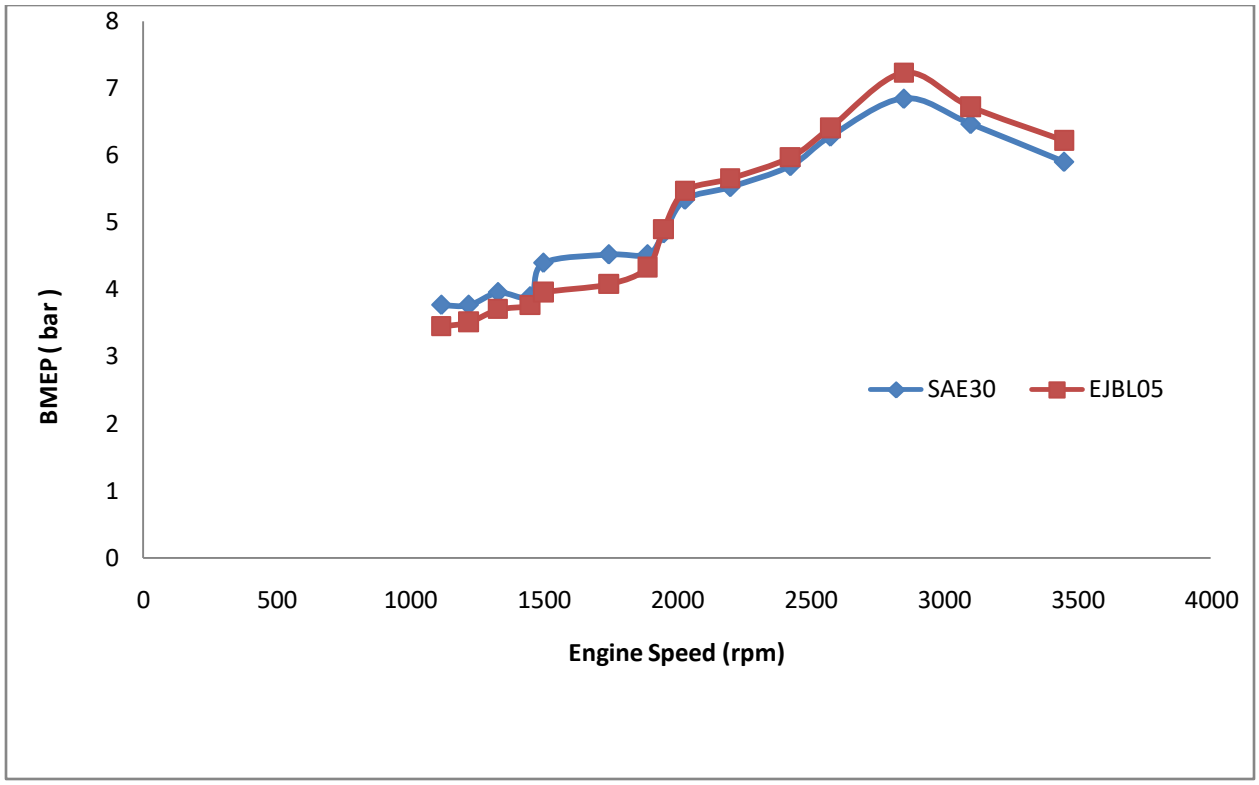


Figure 4.34: Engine Speed and Brake Mean Effective Pressure

4.9.4 Brake Specific Fuel Consumption (BSFC)

The brake specific fuel consumption indicates the amount of fuel consumed for a given power output. Lower BSFC means better engine efficiency due to lower total engine friction. It can be seen that from figure 4.35, maximum BSFC of 0.905 kg/kWh for EJBL05 and 0.671 kg/kWh for SAE 30 were observed at 1118 rpm indicating high fuel consumptions at the beginning of the engine operations due to high oil viscosities at low temperatures. EJBL05 at lower speeds (1000-1500 rpm) has higher BSFC than SAE30 due to its higher viscosity at low temperature. Minimum BSFC was recorded at 3450 rpm of 0.3492 kg/kWh for EJBL05 and 0.3762 kg/kWh for SAE 30. The BSFC of EJBL05 reduced substantially at higher speeds than that of SAE 30 because EJBL05 has lower viscosity at higher temperatures than SAE 30.

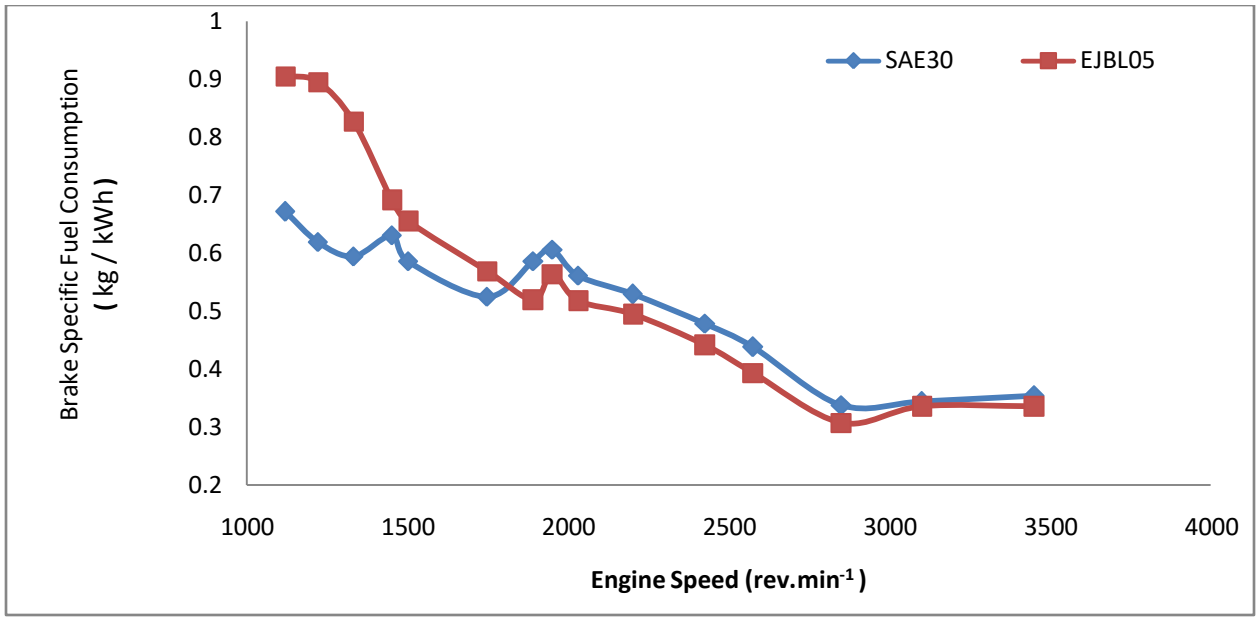


Figure 4.35: Engine Speed and Brake Specific Fuel Consumption

4.9.5 Thermal Efficiency

The results for thermal efficiency are presented in figure 4.36. Thermal efficiency indicates the percentage of the energy present in the fuel which is converted to useful output at the crankshaft. The rests of the energy are wasted through heat losses (via exhaust gases, coolants, etc) and parasitic loads. SAE30 offered better thermal efficiency at lower speeds (1000-1500 rpm) than EJBL05. The trend changed at higher speeds (2500-3500 rpm) in favor of EJBL05.

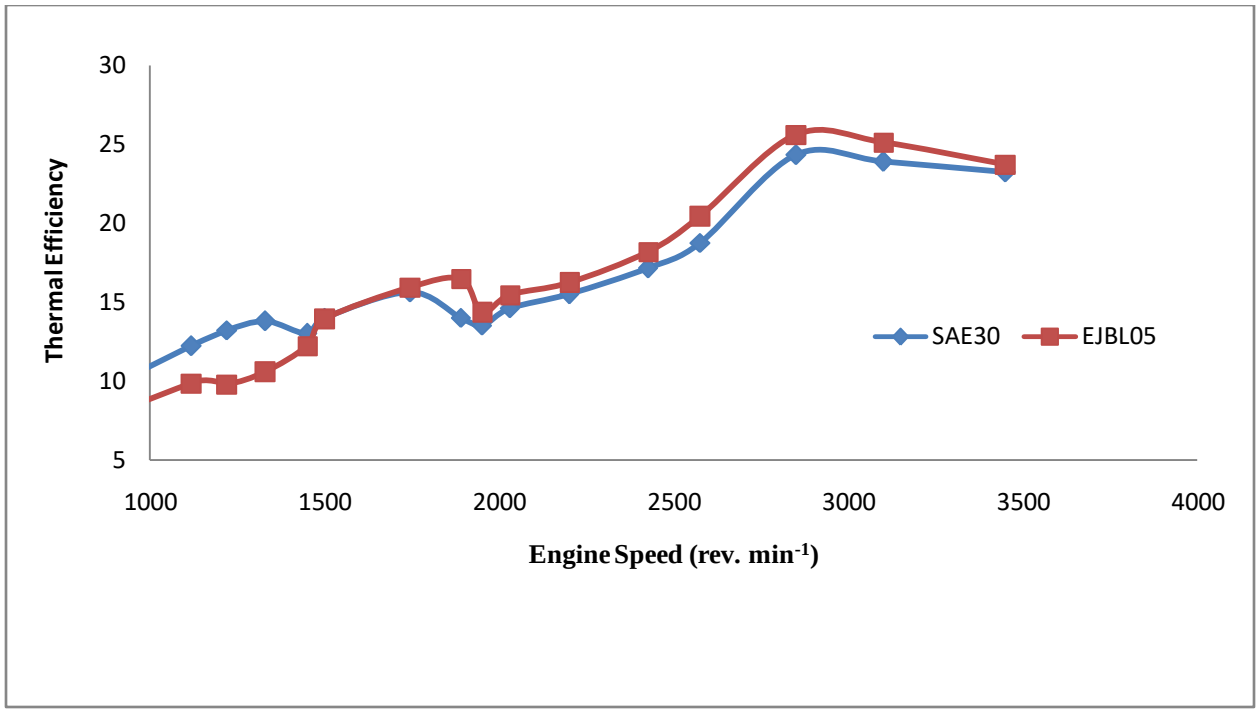


Figure 4.36: Engine Speed and Thermal Efficiency

4.9.6 Oil Temperature

Lower engine oil temperatures were recorded for EJBL05 than SAE 30 under all engine speeds range used for the test as shown in figure 4.37. The maximum temperatures observed for EJBL05 and SAE30 were 115^{o}C and 110^{o}C respectively. This is because EJBL05 has higher specific heat capacity, and coefficients of thermal conductivity than SAE30. Consequently EJBL05 absorbs more heat than SAE30 thus reducing the overall temperature rise.

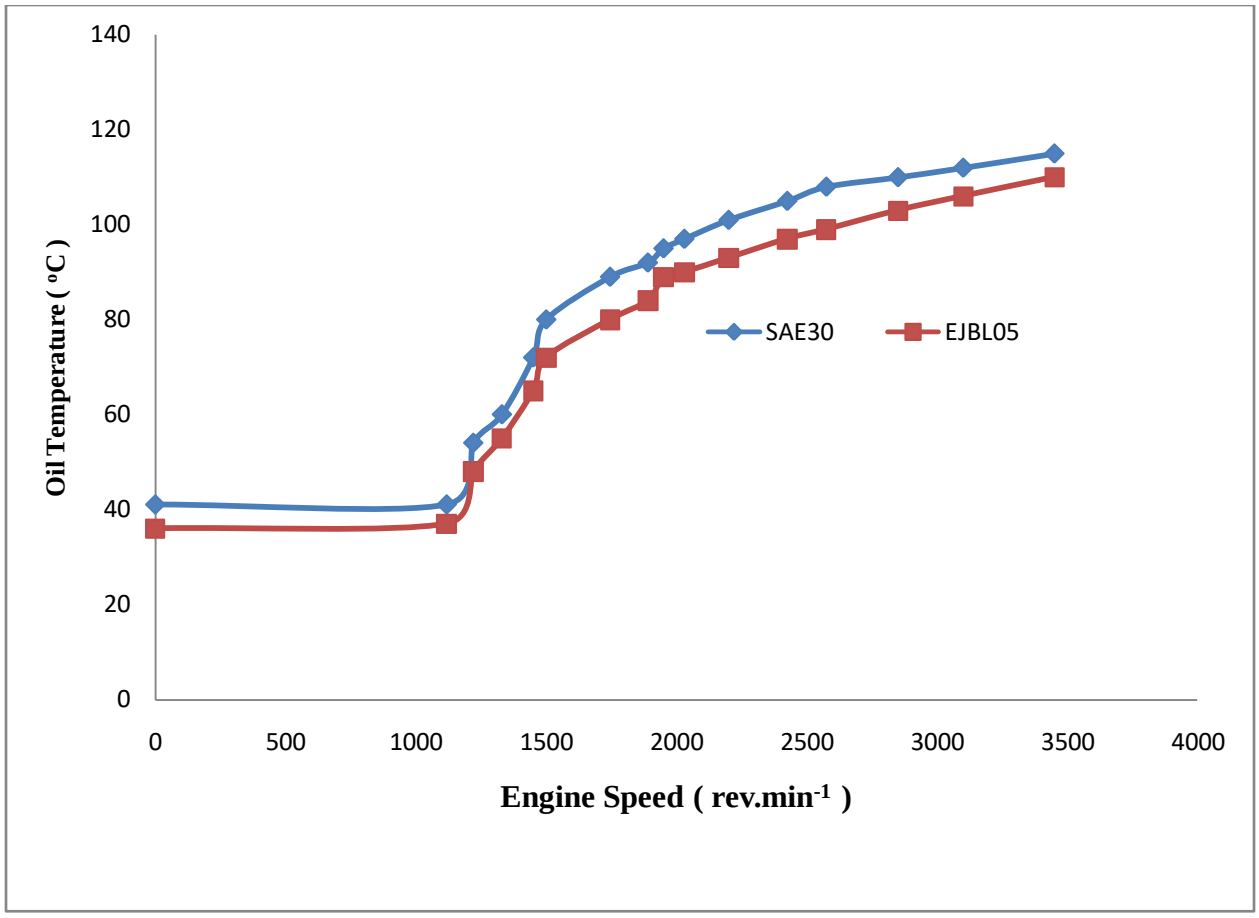


Figure 4.37: Engine Speed and Engine Oil Temperature

4.9.7 Exhaust Valve Temperature

At low and medium temperatures there are no much difference between the exhaust valve temperatures for SAE 30 and EJBL05 as presented in figure 4.38. The maximum exhaust valve temperatures recorded for EJBL05 and SAE 30 were 176^{o}C and 180^{o}C respectively. Lower exhaust valve temperatures were recorded for EJBL05 at higher speeds. This means that EJBL05 cools the exhaust valve more efficiently than SAE 30 at higher speeds due to increase in the oil's heat transfer coefficient at higher speed. The average heat transfer coefficient of EJBL05 at the exhaust valve was calculated to be 32,890 W/m^{2}k and that of SAE 30 was 31,020 W/m^{2}k. The high convective heat transfer coefficients were as a result of high Reynolds's numbers

characterized by splash lubrication system. Similar patterns of exhaust valve temperatures were observed for both EJBL05 and SAE30 at low and medium speeds. SAE30 recorded temperatures slightly higher than EJBL05 at higher speeds.

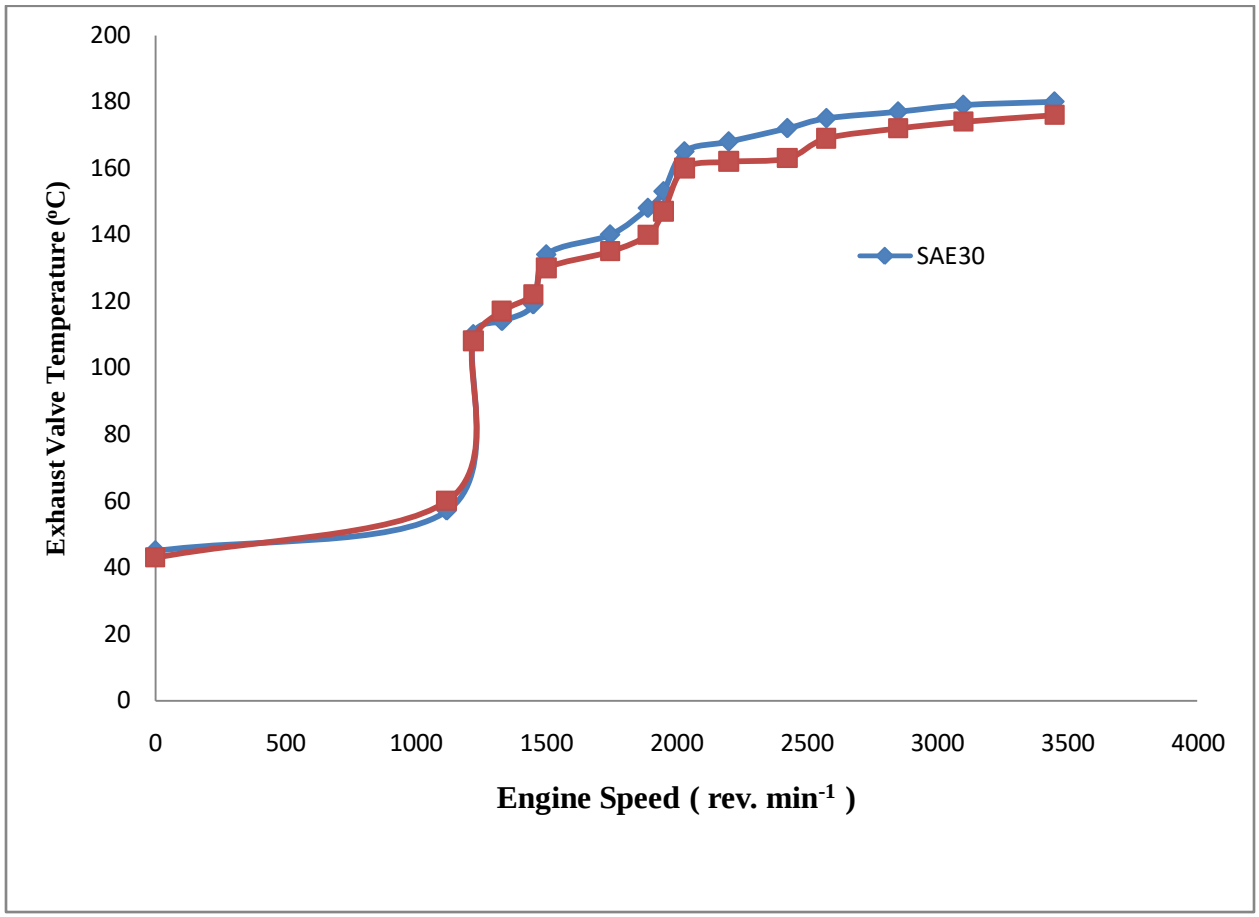


Figure 4.38: Engine Speed and Exhaust Valve Temperature

4.9.8 Engine Outer Surface Temperature

Lower surface temperatures were recorded for EJBL05 at lower and higher speeds as shown in figure 4.39. The outer surface temperature depends on the oil temperature inside the engine and ambient condition. Combined natural and forced convections prevailed at the engine surroundings during the tests. The convective heat transfer recorded by EJBL05 was lower

(0.654 W/m^{2}K) than that of SAE 30 (0.664 W/m^{2}K).The lower surface temperatures recorded for EJBL05 has further reaffirmed the result for oil temperature in section 4.7.6.

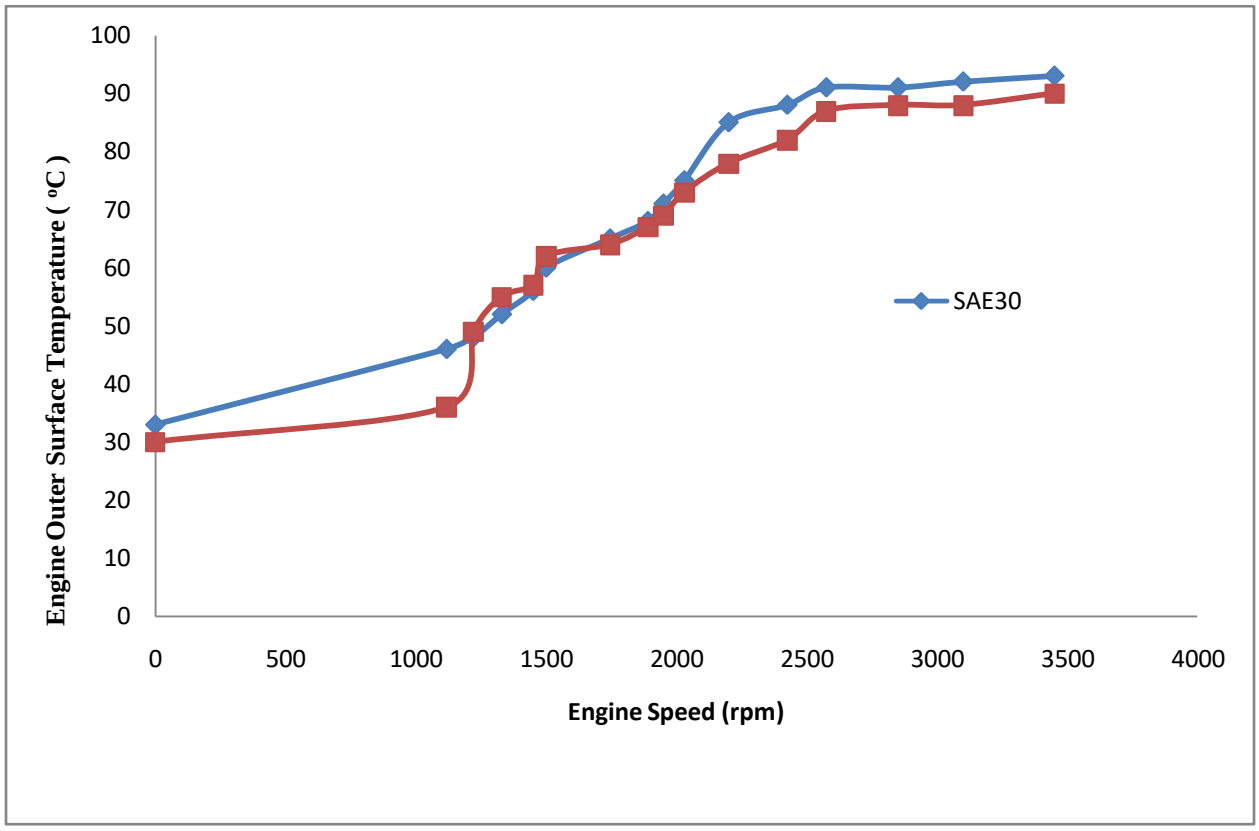


Figure 4.39: Engine Speed and Engine Outer Surface Temperature

4.10 Coefficient of Friction/Wear Rate

The results for coefficient of friction/Wear Rate tests carried out on mild steel and aluminium specimens showed that EJBL05 has lower coefficients of friction of 0.074 (mild steel) and 0.0271 (aluminium) than SAE30, which has 0.0923 (mild steel) and 0.076 (aluminium) under similar conditions. This means EJBL05 has better lubricity and will offer lower energy loss due to friction than SAE30. Bongfa (2015) reported that the molecular structure of oil and the thin lubricating film formation ability on the surfaces of contacting mechanical components determine the friction reduction efficiency of the oil. However SAE30 has better wear protection

ability than EJBL05 as indicated by their wear rate results of 0.02539 $mm^3/n/m$ (mild steel) and 0.03909 $mm^3/n/m$ (aluminium) for EJBL05 and 0.02115 $mm^3/n/m$ (mild steel) 0.04659 $mm^3/n/m$ (aluminium) for SAE30.

4.11 Simulation Results

The simulation results obtained was validated using the experimental results obtained for Oil Temperatures, Engine Surface Temperatures and Exhaust Valve Temperatures for SAE30 and EJBL05 engine oils. The engine speeds used for the simulation were selected in order to coincide with the values used for the experiments.

4.11.1 Oil Temperature

Figure 4.40 shows the results of the engine oils temperatures obtained during the experiment against the values obtained for the simulation. The simulated results showed consistent increase of temperature with engine speed for both the engine oils.

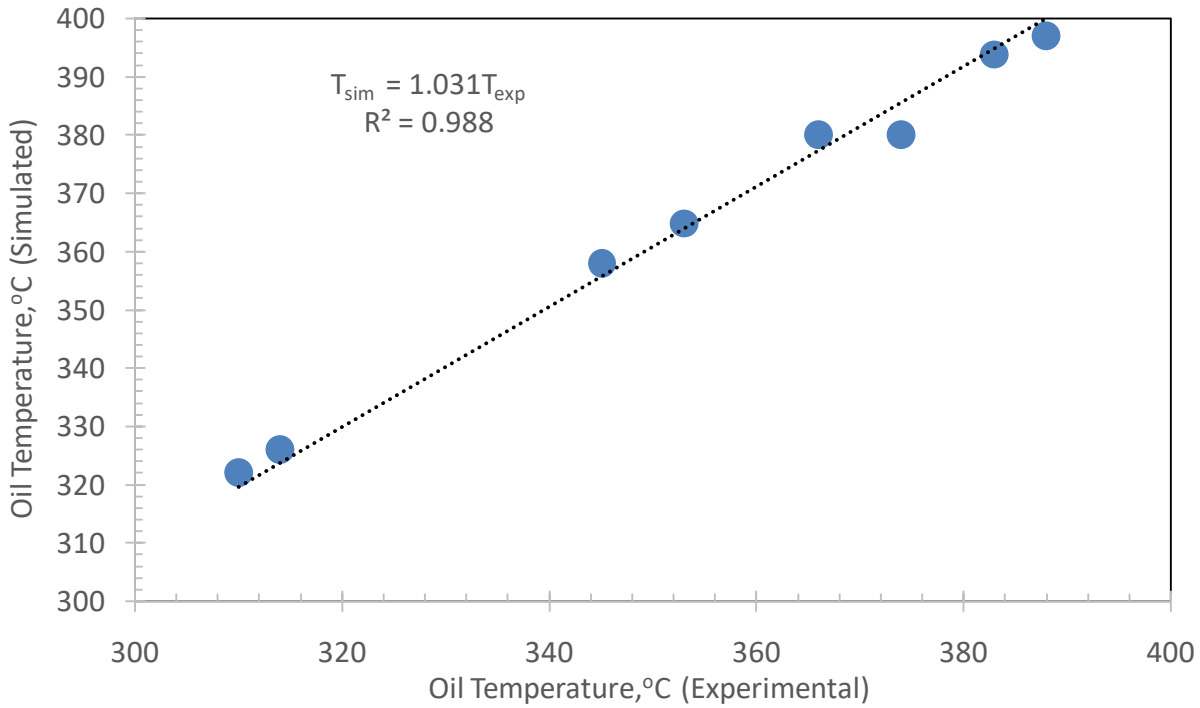


Figure 4.40: Oil Temperature Experimented Against Simulated

The results were all higher than the experimented with small margin. A linear relationship between simulated temperature (T_{sim}) and experimented temperature (T_{exp}) of $T_{sim} = 1{,}031T_{exp}$ was obtained with R^2 value of 0.988. A minimum difference of 6^{o}C (1.6%) between experimented and simulated results was observed for SAE 30 at 2200 rpm and a maximum of 14^{o}C also at 2200 rpm for EJBL05 (3.8%). The closeness of the results indicates that the simulation was valid.

4.11.2 Exhaust Valve Temperature

Figure 4.41 depicts the exhaust valve temperatures, experimented against simulated. There are no much differences between the experimented and the simulated results. The results show that experimented results are little bit higher than the simulated results. The relationship between simulated temperature (T_{sim}) and experimented temperature (T_{exp}) was determined to be $T_{sim} = 0.977T_{exp}$ with R^2 value of 0.977. The lowest margin of 12^{o}C (3.66%) was observed at a speed of 1118 rpm for EJBL05 and the highest of 71^{o}C (20 %) at a speed of 3450 rpm for SAE 30. The differences observed between the experimented and simulated results were as attributed to random and systematic errors during the experiments.

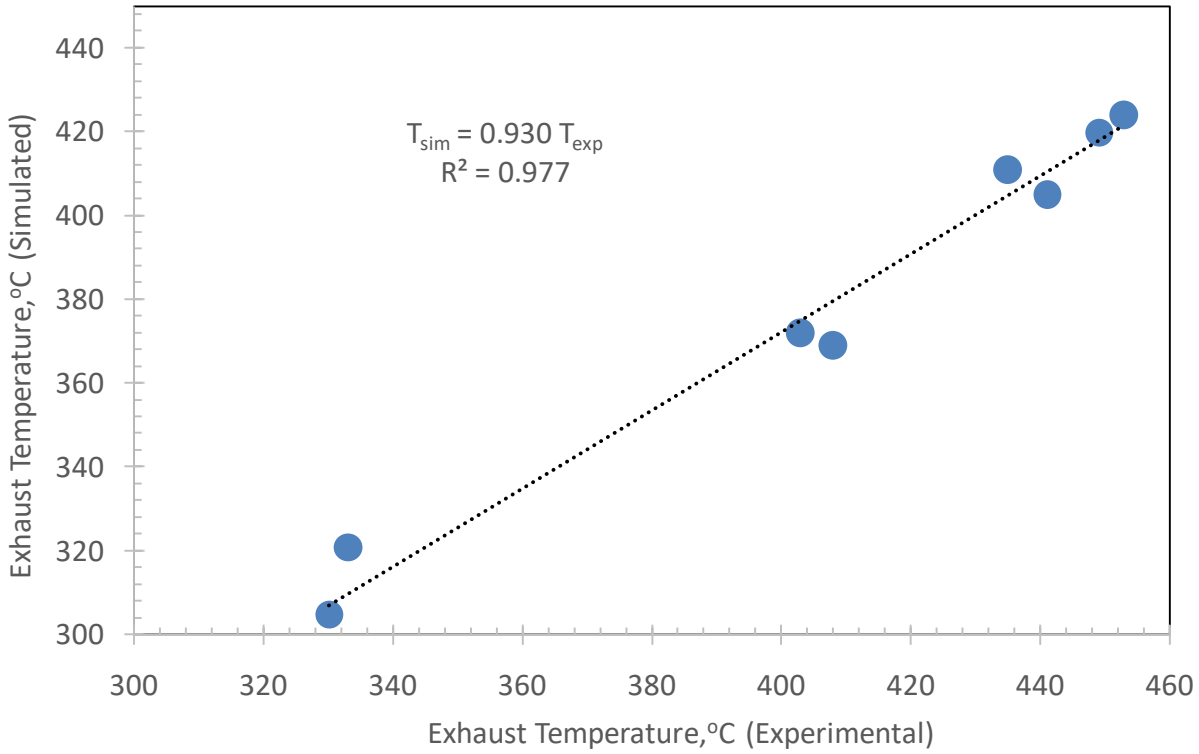


Figure 4.41: Exhaust Valve Temperatures Experimented Against Simulated

4.11.3 Engine Outer Surface Temperature

Figure 4.42 presents the engine outer surface temperatures, experimented against simulated. There are no much differences between the experimented and the simulated results. A linear relationship between simulated temperature (T_{sim}) and experimented temperature (T_{exp}) of T_{sim} = 1,043T_{exp} was obtained with R^2 value of 0.969. Minimum difference of 11°C (3.5 %) were recorded for EJBL05 at 1500 rpm. The maximum difference of 27°C (7.4%) was seen for EJBL05 at 3450 rpm.

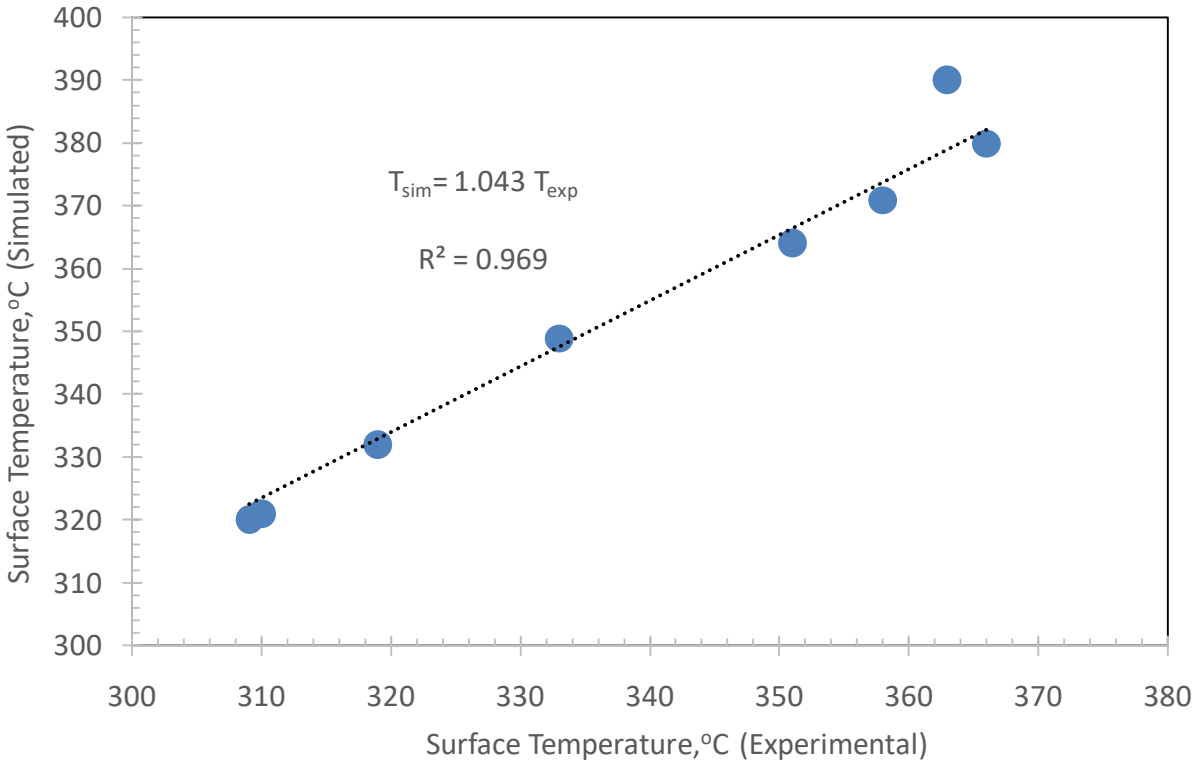


Figure 4.42: Engine Surface Temperature Experimented Against Simulated

CHAPTER FIVE

CONCLUSIONS, RECOMMENDATIONS AND CONTRIBUTIONS TO KNOWLEDGE

5.1 Conclusion

The following are the conclusions drawn for this research:

1. Epoxidation of crude jatropha oil, and confirmation of epoxides formation using Fourier Transform Infra Red Spectroscopy (FTIR) and Iodine Value have been successfully carried out. The thermal and oxidative stabilities of jatropha oil were greatly improved through epoxidation.
2. Physico-chemical properties of the epoxidized jatropha oil are comparable to that of mineral base oils (NS 100, NS 150, NS 500 and BS 150);
3. Epoxidized jatropha biolubricant was successfully formulated and blended with BO 23232/B23333 automotive additive package (1- 10 %) to form EJBL, EJBL01, EJBL02, EJBL03, EJBL04, EJBL05, EJBL06, EJBL07, EJBL08, EJBL09 and EJBL10.
4. Physico-chemical properties of the epoxidized jatropha biolubricant and its blends were comparable with those of spark ignition engine lubricating oils (SAE30, SAE40, SAE50 and 15W- 40). EJBL05, EJBL06, EJBL07 and EJBL08 (i.e. epoxidized jatropha bioluricant blended with 5 %, 6 %, 7 % and 8 % additive respectively) satisfied the minimum SAE and API/ILSAC requirements for spark ignition engine lubricants and can be safely used in spark ignition engines, depending on the engines' viscosity requirements. Only EJBL05 can be used on TecQuipment TD 201 test engine as per the manufacturer's recommendation.

5. The torques developed by the test engine (TecQuipment TD 201) for EJBL05 within the test range used (0- 3450 rev min^{-1}) were 0 – 9.9 Nm and for SAE30 (reference engine oil), 0 – 9.4 Nm; Similarly the engine Brake Powers for EJBL 05 were 0 – 3577 W and for SAE30, 0 – 3396 W; The Brake Mean Effective Pressures (BMEP) for EJBL05 were 0 – 6.22 bar and for SAE30, 0 - 5.90 bar. The Brake Specific Fuel Consumptions (BSFC) for EJBL05 were 0 – 0.3492 kg/kWh and for SAE 30, 0 – 0.3762 kg/kWh. The initial BSFC for EJBL05 was much higher than that for SAE30.

6. The temperatures for EJBL05 within the test range (0 – 3450 rev min^{-1}) were 36^{o}C – 110^{o}C; and for SAE 30, 41^{o}C – 115^{o}C. The exhaust valve temperatures for EJBL05 were 43^{0}C – 176^{0}C; and for SAE30, 45^{o}C – 180^{o}C. The engine surface temperatures recorded for EJBL05 were 30^{o}C – 90^{o}C; and for SAE 30, 33^{o}C – 93^{o}C. The simulated results obtained for oil temperatures, engine surface temperatures and exhaust valve temperatures were close to the experimented results with R^2 value of 0.988, 0.969 and 0.977 respectively; signifying that the simulation was valid.

   Thus all the six research objectives have been achieved.

5.2 Recommendations

1. Further studies may consider blending with bio-based additive and compare their physico-chemical properties and engine performance with those blended with chemical additives.

2. Where indicator or pressure transducer is fitted with the test engine, total engine friction can be determined for biobased lubricant and mineral base lubricant so that frictional power/frictional losses for both lubricants can be determined and compared.
3. The test engine used for this work uses splash lubrication system and does not have oil filter. Engine oil Filtration Test (EOFT) may be carried out to ascertain the filterability of the biolube.

5.3 Contribution to Knowledge

1. This work has established that EJBL05, EJBL06, EJBL07 and EJBL08 (i.e. epoxidized jatropha bioluricant blended with 5 %, 6 %, 7 % and 8 % BO 23233/23333 additive respectively) satisfied the minimum SAE and API/ILSAC requirements for SI engine lubricants and can be safely used in spark ignition engines, depending on the engines' viscosity requirements.
2. Parameters required for SI engine oil Such as Evaporation Loss, Foaming Tendency, Demulsibility, Seal Compatibility, etc for epoxidized jatropha biolube and its blends with additive have been investigated for the first time. Their applicability to spark ignition engine is now known.
3. Performance of epoxidized jatropha biolube in spark ignition engine has been determined and compared with that of mineral base engine oil. It has been determined that the power developed by SI engine lubricated with biolubricant,

EJBL05 is 5 % higher than that of similar engine operating under the same condition but lubricated with SAE 30 mineral base engine oil;

4. Addition of 1-10 % BO 23233/23333 by volume reduced the thermal conductivity of EJBL by 40 % from 0.25 to 0.15 kW/mk and increased specific heat capacity by 25 % from 2.0 to 2.5 kJ/kgk.

5. It has been established that chemical additive BO 23233/23333 can be blended with biolube and used in spark ignition engine. In the past such additives were only used with mineral base oils.

REFERENCES

ACEA (2016). Oil sequence, service fill oil for gasoline engines, light-duty diesel engines, engine with after treatment devices and heavy-duty diesel engine. Retrieved on September 23rd 2017 from www.acea.be/news/article/.

Agrira, A.I.A. (2012). *Internal combustion engine heat transfer-transient thermal analysis.* PhD Thesis, faculty of engineering & surveying, university of southern Queensland.

Aji, M. M., Kyari, S. A. and Zoaka, G. (2015). Comparative studies between bio lubricants from jatropha oil, neem oil and mineral lubricant, (Engen super 20W/50). *Applied Research Journal*, 1(4): 252-257.

Alejandro, S.R., Victor, H., Romos, S., and David, C.F. (2018)**.** Lipase catalyzed epoxidation of fatty acid methyl esters derived from unsaturated vegetable oils in absence of carboxylic acid. *Chem Cent Journal*, 1(2): 39, doi: 10.1186/s 13065-2.

Annand, W.J.D. (1963). Heat transfer in the cylinders of reciprocating internal combustion engines. *Proc. Institute of Mechanical Engineers*. 177(36): 973-996.

API/ILSAC Engine oil Classifications, (2015). Service fill oil for gasoline engines, light-duty diesel engines. Retrieved on September 23rd 2017 from www.infineum.com.

Arbain, N. and Salimon, J. (2009). Synthesis and characterization of ester trimethylolpropane based jatropha curcas oil as biolubricant base stock. J. Sci Technol, 47-58

Audibert, F. (2006). Waste engine oils re-refining and energy recovery. *Elsevier*. Amsterdan 10-11.

Bekal, S. and Bhat, N. R., (2012). Bio-lubricant as an alternative to mineral oil for a CI engine—an experimental investigation with pongamia oil as a lubricant. *Energy Sources*. 34(11): 1016–1026.

Bergstra, (2016). Advanced biolubricants and re-refining. -Biosynthetic.com– MTN Consulting Associates.

Bilal,S., Muhammad-Dabo, I. A., Nuhu, M., Kasim, S. A., Almustapha, I.H. and Yamusa, Y.A. (2013). Production of biolubricant from jatropha *curcas* seed oil. *Journal of Chemical Engineering and Materials Science*, 4(6):72-79.

Bongfa, B., Peter, A.A., Barnabas, A. and Adeoti, M. O. (2015). Comparison of lubricant properties of castor oil and commercial engine oil. *Jurnal Tribologi, Malaysian Tribology Society*, 5: 1-10.

Borman, G. and Nishiwaki, K. (1987). Internal combustion engine heat transfer. *Prog. Energy Combust Sci.*133:1-46.

Brilling, N.R. (1935). Investigating of working process and heat transfer in diesel engine. *Moscow*, 210-256.

Bugaje, I.M. and Muhammad, I. A. (2008). *Biofuels Production Technology*. Science and Technology Forum (STF), Zaria, Nigeria. 2-55.

Ĉernŷ, J. and Zelinka, M. (2004). Oxidation stability of lubricants measured by a PDSC technique. *Petroleum and Coal.* 46(3): 56-62.

Cheenkachorn, K. and Fungtammasan, B. (2010). Development of engine oil using palm oil as a base stock for four stroke engine. *Energy*, 35(6): 2552-2556.

Cheing, B.W., Ibrahim, N.A., Then, Y.Y. and Loo, Y.Y. (2017). Epoxidized jatropha oil as a sustainable plasticizer to polylactic acid), *Polyners*, 9 (204): 2-10.

Chen, J. Beaufort, M.L., Gyurik, L., Dorresteijn, J., Otta, M. and Gebbink, R.J.M. (2019). Highly efficient epoxidation of epoxidation oils catalyzed by a manganese complex with hydrogen

peroxide and acetic acid. *Royal Society of Chemistry*. Doi: 10.1039/C8GC03857K.21: 2436-2447.

Datta, J., and Singh, S.S. (2017). Thermal analysis on piston of various materials and comparison with each other by using finite element analysis technique. International Journal of Engineering Sciences and Research Technology. Code N: IJE SS7.

Dinda, S., Patwardhan, A.V., Goud, V.V. and Pradhan, N.C. (2008). Epoxidation of cotton seed oil by aqueous hydrogen peroxide catalysed by liquid inorganic acids. *Bioresources Technology*, 99: 3737-3744.

Dominic, W. and Gao, S. (2017). A computational study of the effect of intake design on volumetric efficiency for best performance in motor sport. *World academy of science engineering and technology international journal of mechanical engineering*, 2(5).

Durak, E. (2004). A study on friction behavior of rapeseed oil as an environmentally friendly additive in lubricating oil. *Industrial Lubrication and Tribology*, 56 (1): 23–37.

Eichelberg, G. (1939). Some New Investigations on Old Combustion Engine Problems. *Engineering* 148: 446-463.

Erhan, S.Z., Sharma, B.K., and Perez, J.M. (2006). Oxidation and low Temperature Stability of Vegetable oil-based lubricants. *ScienceDirect, Industrial Crops and Products* 24: 292-299.

Fan, W. T. (2010). *Regeneration of used petroleum-based lubricants and biolubricants by a novel green and sustainable technology*. A PhD dissertation presented to the faculty of the Usc Graduate School University of Southern California. pp. 20-89.

Garg, A. and Garg, K. (2017)**.** Optimization of Piston head of Single Cylinder Diesel Engine. *International Journal of Engineering Sciences and Research Technology*. ISSN 2277-9655. CODE N: IJESS7.

Ghobadian, B., Gholamhassan, N. and Masoud, D. S. (2015). TOPSIS Multi-Criteria Decision Modeling Approach for Biolubricant Selection for Two-Stroke Petrol Engines. *Energies*, 8: 13960–13970; doi: 10.3390/en81212408.

Gill, P.S. (2013). *Automobile Engineering- I.* S.K. Kataria & Sons. New Delhi-110002, pp. 3-285.

Graziano, E., Bruno, L., Corrado, P. and Pierson, S. (2019). Set-up and validation of an integrated engine thermal model in GT-Suite for heat rejection prediction. SAE Technical Paper, doi.org/10.4271/2019-24-0078.

Goud, V.V., Patwardhan, A.V. and Pradhan, N.C. (2006). Studies on the epoxidation of mahua oil (*madhumica indiaca*) by hydrogen peroxide. *Bioresources Technology*, 97:1365-1371.

Guibert, P. (2005). Engine Cycle Modeling-Spark Ignition Engines (in French). *Technique de I ingenieur. BM*, 1-28.

Han, Z. and Reitz, R.D. (1997). Temperature wall function formulation for variable-density turbulent flows with application to engine convective heat transfer modeling. *International Journal of Heat and Mass Transfer*, 40(3): 613-625.

Haqui, B.I. and Raddy, D.R. (2015)**.** Design and simulation of an inline 4- cylinder engine. *International Journal of Professional Engineering Studies* , 4(5): 231-238.

Hassan, A.B., Abolarin, M.S., Nasir, A. and Ratchel, U. (2006). Investigation on the use of palm olein as lubrication oil. Leonardo *Electronic Journal of Practices and Technologies*, 8:1–8.

Heywood, J.B. (1989). Internal combustion engine fundamentals. MicGraw-Hill, New York, 143-197.

Hohenberg, G.F. (1979). Advanced approaches for heat transfer calculations. *Society of Automotive Engineers.* Paper No. 790825, SAE Transactions, 88:61-79.

Hsien, W.L.Y. (2015). Towards green lubrication in machining. *Springer Briefs in Green Chemistry for Sustainability,* DOI 10,1007/978-981-287-266-1_2.

Hua, T., Gequn, S., Chen, H., , Xiaoya, L., Zhigang, Y. and Mingtao, W. (2019). Analysis and optimization of coupled thermal management systems used in vehicles. *Energies*, 1265; doi: 10.3390/en12071265.

Humphrey, B. (2016). Using engine oil to improve fuel economy. *OEM Technical Laison-HD Driveline, Petro-Canada Lubricants.* LUB 3431E, pp. 1-4.

Ja'afar, A., and Mohammed, I.L. (2018). *Introduction to energy conversion and heat transfer*. Mudraj Publication. pp 61-92.

Ja'afar, A., Garba, U.A. and Danjuma, M.N. (2018). Epoxidation: an important technique for enhancing thermal stability of biolubricants base stock. *Journal of Research in National Development,* 16(1): 1596-8308.

Joshua, F. (2013). Production of biodiesel (B100) from jatropha oil using hydroxide as catalyst. *Journal of Petroleum Engineering,* 20(13). Article ID 956479.

Krishna, T.K.S., Shouri, K., and Kumar, R.D. (2013). Design and analysis of electronic fuel injection of diesel engine. *International Journal of Scientific and Engineering Research*, 4(10): 2-8.

Kumar, A. and Sharma, S. (2011). Potential of non-edible oil resources as bio diesel feedstock: an indian perspective. *Renew Sustain Energy Rev*; 15: 1791–800.

LeFeuvre, T., Myers, P.S. and Uyehara, O.A. (1969). Experimental instantaneous heat fluxes in a diesel engine and their correlation. *Society of Automotive Engineers*, SAE.

Lounici, M.S., Loubar, K., Balistrou, M. and Tazerout, M. (2010). Investigation on heat transfer evaluation for a more efficient two-zone combustion model in the case of natural gas SI Engines. *Applied Thermal Engineering, Elsevier,* 31 (2-3):319.

Manji, A. J., Sarah, E.E., and Modibbo, U.U. (2013). Studies on the potential of balanites *aegytiaca* seed oil as raw material for the production of liquid cleansing agents. *International Journal of Physical Sciences,* 8(33):1655-1660.

Menacar, I., Soualmia, A., Belhout, C. and Bouchetara, M. (2017)**.** The convective heat transfer rate evaluation of a 6-cylinder in-line turbocharged direct injection diesel engine. *Mechanika,* 23(4): 528-536.

Meyer, W.J. (2004). *Concepts of mathematical modeling*. Dover Publications, Inc. Mineola New York, pp. 2-50.

Mobarak, H. M., Mohammed, N. E., Masjuki, H. H., Kalam, M. A. and Al Mahmud, K. A. H. (2014). The prospects of biolubricants as alternatives in automobile applications. *Journal of Renewable and Sustainable Energy Reviews*, 33:34-43.

Mofijur, M., Masjuki, H.H., Kalam, M.A., Hazrat, M.A. Liaquat, A.M. and Shahabuddin, M. (2012). Prospects of biodiesel from jatropha in Malaysia. *Renew Sustain Energy Rev*; 16: 5007–5020.

Mohammed, N. (2015). *Synthesis of Biolubricant from Vegetable oils*. Msc Thesis Department of Chemical Engineering, Ahmadu Bello University, Zaria, pp. 1-74.

Mohammed, N.A. (2016). *Production and performance evaluation of biodegradable grease (Biogrease) from Balanite aegyptiaca (Desert Date) seeds oil.* Unpublished Master's Thesis Submitted to Mechanical Engineering Department, ABU, Zaria, pp. 1-80.

Mohammed, A., Yaghoubi, M. and Rashidi, M. (2008). Analysis of Local Convective Heat Transfer in a Spark Ignition Engine. *International Communication in Heat and Mass Transfer*, 35:215-224.

Morel, T. and Keribar, R. (1985). A model for predicting spatially and time-resolved convective heat transfer in bowl-in-piston combustion chambers. *SAE paper* 850204.

Navindgi, M.C. (2012). Performance evaluation, emission characteristics and economic analysis of four non-edible straight vegetable oils on a single cylinder CI engine. *ARPN Journal of Engineering and Applied Sciences*, 7(2): 89-96.

Nigerian Industrial Standard (NIS) 370, (2017). Standard for Motor oil and Engine Lubricating oils. *Standard Organisation of Nigeria*.

Nitware, P.T. and Giri, P.S. (2015). Design optimization of an air cooled internal combustion engine fins using CFD. *Journal of multi-disciplinary engineering science and technology*, 2(11): 3129-3131.

Nusselt, W. (1928). Der Warmeubergang zwischen Arbeitmedium und Zylinderwand in Kolbenmaschinen. Forachungsarb. Geb. Ing.

Nykulshyn, I., Pikh Z., Shevchuk, L. and Meinyk, S. (2017)**.** Examining Epoxidation Process of Soybean oil by Peracetic Acid. *Eastern-European Journal of Enterprise Technologies.* ISSN 1729-3774.

Obasi, A.U., Udeagbara, S.G. and Anusiobi, O.J. (2014). Effects of additives on the performance of engine oil. *International Journal of Engineering and Technological Research*, 2(9): 1-11.

Ollivier, E. (2006). *Contribution to the characterization of heat transfer in spark ignition engines (in French).* Application to knock detection. PhD Thesis ENSTIM de Nantes, France.

Poulos, S.G. and Heywood, J.B. (1983). The effect of chamber geometry on spark ignition engine combustion. *SAE paper* 830334.

Pranita, A., Vinod, K., Sanjeev, B, and Ashwini, M. (2018). A simulation study of cooling system for heavy duty diesel engine. *MATEC Web of Conferences* 172, 02002 ICDAMS 201 https://doi.org/10.1051/matecconf/201817202002

Rajaendran, V., Salimon, J. and Yusop, R.M. (2016). Synthesis and characterization of epoxidized neopenthyl glycol diolete as an intermediate of biolubricant. *Malaysian Journal of Analytical Sciences*, 20 (6): 1329-1337

Rashedul H.K., Kalam, M.A., Masjuki, H.H., Ashraful, A.M., Imtenan, S., Sajjad, H. and Wee, L.K. (2015). Numerical study on convective heat transfer of a spark ignition engine fueled with bioethanol. *International Communications in Heat and Mass Transfer,* 58: 33-39.

Reddy, G.K. and Vadithe, B.N. (2017). Design and analysis of connecting rod. *Intrnational Journal of Research in Advanced Engineering Technology,* 6(1):

Sachdeva, R.C. (2008). *Fundamentals of Engineering Heat and Mass Transfer*. New Age International (P) Limeted, Publishers.3rd Edition. pp 94-109.

Salimon, J. and Abdullahi, R. (2008). Physico-chemical Properties of Malaysian Jatropha curcas Seed Oil. *Sians Malaysiana* 37(4): 379-382.

Salimon, J. and Fong, M. N. F. (2012). Epoxidation of Palm Kernel Oil Fatty Acids. *Journal of Science and Technology*, pp. 87-97.

Sammaiah, A., Korlipara, V. P. and Rachapudi B. N. P. (2014). Synthesis of Epoxy Jatropha Oil and its Evaluation for Lubricant Properties. *Journal of Oleo Science, Japan oil Chemist's Society*. J-STAGE Advance Publication, doi: 10.5650/jos.ess13172: 1-7.

Saremi, K., Tabarsa, T., Shakeri, A., and Babanalbandi, A. (2012). Epoxidation of Soybean Oil. *Annals of Biological Research*, 3(9): 4254-4258.

Saurabh, T., Patnaik, M., Bhagt, S.L. and Rang, V.C. (2011). Epoxidation of Vegetable Oils: a Review. *International Journal of Advanced Engineering Technology*, 2(4):491-501.

Scott, W., Paul, S., Herold, P. and Ernest, S.E. (2005). Heat Transfer Properties of Engine Oils. *Preceedings of World Tribology Congress III, Washington, D.C., U.S.A.* 64315, pp. 1-2.

Shaari, M.S., Rahman, M.M., Noor, M.M., Kadirgan, K. and Amiruddin, A.K. (2010) **.** Design of Connecting rod of Internal Combustion Engine. A topology Optimization Approach**.**

Shahabuddin, M., Masjuki, H. H., Kalam, M.A., Bhuiya, M. M. K. and Mehat, H. (2013). Experimental investigation into tribological characteristics of biolubricant formulated from jatropha oil. pp 597-606.

Sharma, B.K., Karmakar, G. and Ghosh, P. (2017). Chemically modifying vegetable oils to prepare green lubricants. *Lubricants*, 5(44): 5-17.

Shigley, J.E. and Mischke, C.R. (2001). *Mechanical Engineering Design*. McGraw-Hill Higher Education, pp. 78-235.

Singh, K. (2004). Automotive Engineering, Vol. II. Standard Publishers and Distributors. 1705-B, Nai Sarak, Delhi-110006, pp. 1-283.

Spitsov, O. (2013). *Heat Transfer inside Combustion Engine: Modelling and Comparison with experimental data*. Msc Thesis, Faculty of Technology, Lappeenranta University of Technology, pp. 20-50.

Srivastava, A. and Sahai, P. (2013). Vegetable Oils as Lube Base Stocks: A review. *African Journal of Biotechnology* 12(9): 880-891.

Stone, R. (1999). Introduction to Internal Combustion Engines. MacMillan Publishers.

Taylor, R.I. (1997). Engine friction: the influence of lubricant rheology. Proceedings of the institution of Mechanical Engineers, Part J. *Journal of Engineering Tribology*, 214: 1-15.

Tiwari, D. and Santosh, R.W. (2015). Simulation investigation of effect of bio-lubricant between tribological system of piston ring and cylinder liner. *International Journal of Innovative Research in Science, Engineering and Technology*, 8: 7999-8007.

Torregrosa, A.J., Olmeda, P.C. and Romero, C.A. (2008). Revising engine heat transfer. *Journal of Engineering, Annals of Faculty of Engineering,* Hunedoara, Tome VI, Fascicule 3.

Totten, G. E. (2006). Fuels and lubricants handbook: technology, properties, performance, and testing. *ASTM manual series*; MNL 37, pp. 169-1015.

Trophy, J.D. (1981). Heat transfer in internal combustion engines- measurement and modelling (in French), *Revue Generale de Thermique* 233: 385-390.

Vidovic, E. (2014). Development of lubricating oils and their influence on the seals. *Goriva i maziva*, 53(3): 220-235.

Vijayakumar,T., Krishna Reddy K. S. V., Naval, K. and Umesh, K. (2014). Experimental investigation on usage of palm oil as a lubricant to substitute mineral oil in CI engines.

Wang, C.S. and Berry G.F. (1985). Heat transfer in internal combustion engines. *The American Society of Mechanical Engineers,* 85-WA/HT-23: 1-7.

Wong, J.L., Aung, M.M., Lim, H.N., Jamil M. and Sitti, N. (2017), Spectroscopic analysis of epoxidized jatropha oil and acrylated epoxidized jatropha oil. *Journal of Tropical Agricultural Science*. 40(3): 435-448.

Woschni, G. (1967). A universally applicable equation for the instantaneous heat transfer coefficient in the internal combustion engines. *SAE transactions Paper*, no. 670931, 76:3065.

Yang, L., Takase, M., Zhang, M., Zhao, T. and Wu, X. (2014). Potential of non-edible oil feedstock for biodiesel production in Africa. *Renewable and Sustainable Energy Reviews.* 38: 461-477.

Zaku, S.G., Emmanuel, S. A., Isa, A. H., and Kabir, A. (2012). Comparative studies on the functional properties of neem, jatropha, castor, and moringa seeds as potential feed stocks for biodiesel production in nigeria. *Global Journal of Science Frontei Research Chemistry*. 12(7): 23-26.

Zulkifli, N.W. M., Masjuki, H. H., Kalam, M. A., Yunus, R. and Azman, S. S. N. (2014). Lubricity of bio-based lubricant derived from chemically modified jatropha methyl ester. *Journal Tribologi*, 1: 17-39.

APPENDICES

Chart 1: FTIR Interpretation

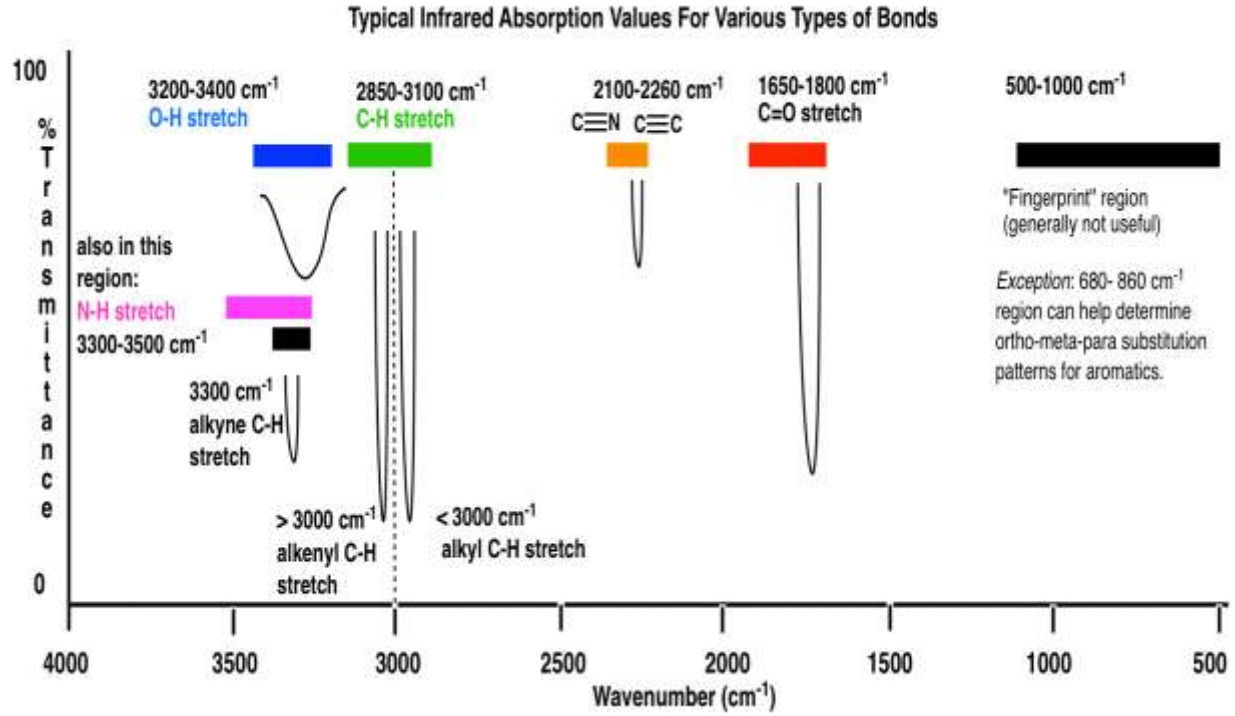


Table A. 1: Physico-chemical Properties of CJO and EJO with Standards

Lubricant Feed Stock and Standards	Water Content (%)	Refractive Index	Iodine Value (mg I_2 /g)	Saponification Value (mg/g)
CJO	0	1.4583	77	195.86
EJO	0	-	38	96.77
API	0.25	-	-	-
ISO	-	1.3000 - 1.7000	-	-
EN	-	-	120	-

Table A. 2: Physico-chemical Properties of CJO, EJO and Mineral Base Oils

Lubricant Feed Stock	Viscosity @ 40°C (cSt)	Viscosity @ 100°C (cSt)	Viscosity Index	Flash Point (°C)	Pour Point (°C)
CJO	34.06	7.5	197	192	-2
EJO	170.63	17.6	112	249	-5
SN 100	-	-	100	182	-18
SN 150	-	-	101	200	-12
SN 500	-	-	97	210	-6
BS 150	-	-	95	232	-6

APPENDIX B

Table B. 1: Physico-chemical Properties of EJBL, EJBL Blends and NIS Standards

Lubricants and Standards	Density (kg/m^3)	Viscosity Index	Flash Point (°C)	Pour Point (°C)	Evaporation Loss (%)	High Temperature High Shear (HTHS) Viscosity @ 150°C (cSt)
EJBL	924		209	-3	20	2.0
EJBL01	925		209	-4	20	2.2
EJBL02	925		213	-4	21	2.5
EJBL03	927		215	-7.5	19	2.6
EJBL04	928		216	-11	18	3.0
EJBL05	929		218	-14	18	3.0
EJBL06	930		222	-15	18	3.3
EJBL07	931		223	-16	17	3.3

EJBL08	932		226	-18	16	3.5
EJBL09	932		230	-18	16	3.8
EJBL10	933		232	-20	16	3.9
NIS SAE30 min	870	95	204	-18	-	-
NIS SAE30 max	-		-	-	22	2.9
NIS SAE40 min	880	95	220	-9	-	-
NIS SAE40 max	-		-	-	22	3.5
NIS SAE50 min	890	95	220	-9	-	-
NIS SAE50 max	-		-	-	22	3.7
NIS 15W-40 min	880	120	220	-21	-	-
NIS 15W-40 max	-		-	-	22	3.7

Table B. 2a: Physico-Chemical Properties of EJBL, EJBL Bblends and Various Engine Oil Grades

Lubricants	Demulsibility (min)	Specific Heat Capacity (kJ/kgK)	Coefficient of Thermal Conductivity (kW/mK)
EJBL	18	2.02	0.25
EJBL01	20	2.01	0.23
EJBL02	19	2.02	0.22
EJBL03	20	2.09	0.20
EJBL04	22	2.2	0.18
EJBL05	22	2.33	0.18
EJBL06	21	2.37	0.17
EJBL07	23	2.4	0.15
EJBL08	24	2.39	0.14
EJBL09	24	2.46	0.14
EJBL10	23	2.5	0.14
SAE30	25	2.025	0.16
SAE40	26	2.13	0.17
SAE50	25	2.18	0.18
15W-40	26	2.20	0.16

Table B. 2b: Physico-chemical Properties of EJBL, EJBL Blends and Various Engine Oil Grades

Lubricants and Standards	Sulfur Content (mg/kg)	Phosphorus Contents (mg/kg)	Total Base Number (mg KOH/g)	Acid Number (mgKOH/g)	Copper Strip Corrosion	Colour
EJBL	0.074	0.023	4.0	0.33	1a	No Match
EJBL01	0.08	0.025	4.9	0.34	1a	No Match
EJBL02	0.0816	0.027	5.7	0.36	1a	1.5
EJBL03	0.0833	0.027	6.5	0.36	1a	2.0
EJBL04	0.085	0.028	7.6	0.37	1a	2.0
EJBL05	0.085	0.029	8.9	0.38	1a	2.0
EJBL06	0.0899	0.029	9.2	0.39	1a	2.5
EJBL07	0.09	0.031	8.4	0.39	1a	2.5
EJBL08	0.126	0.032	8.3	0.39	1a	2.5
EJBL09	0.1457	0.032	7.6	0.42	1a	2.5
EJBL10	0.163	0.033	7.4	0.41	1a	2.5
SAE30	0.254	0.037	8.3	0.46	1a	2.0
SAE40	0.328	0.047	8.6	0.71	1a	3.0
SAE50	0.1835	0.032	9.0	0.76	1a	2.5
15W-40	0.334	0.047	8.6	0.69	1a	3.0
API/ILSAC min	-	0.06	-	-	-	-
API/ILSAC max	0.5	0.08	-	-	-	-
ASTM	-	-	8.0	-	1a/3b	-

Table B. 3: ILSAC Passenger Car Engine Oil Laboratory Tests Standard for GF-1 Class

Requirements	Test Method	Unit	Limits GF-1
Viscosity Grades	SAE J300		Manufacturer sets targets within SAE J300 specification
Foam Tests	ASTM D892	mL mL mL	10/0 max 50/0 max 10/0 max
Homogeneity and Miscibility	Federal Test Method 791B, Method 3470	None	Pass
Volatility	ASTM D2887	%	17 max
Flash Point	ASTM D93 ASTM D92	^{o}C ^{o}C	185 200
HTHS Viscosity @ 150^{o}C and 10^{6} s^{-1}	ASTM D4683, ASTM D4741	cSt	2.9 (min)
Phosphorus	ASTM D4951	%	0.12 max
Sulfur	ASTM D4951	%	NR

Table B. 4: API/ILSAC Passenger Car Engine Oil Laboratory Tests Standard for SJ/GF-2 Class

Requirements	Test Method	Properties	Unit	Limits SJ/ EC GF-2
Viscosity Grades	SAE J300	All those apply, typically SAE 0W-20, 0W-30, 5W-20,5W-30 and 10W-30		Manufacturer sets targets within SAE J300 specification
Foam Tests	ASTM D892	Sequence I, tendency/stability Sequence II, tendency/stability Sequence III, tendency/stability	mL mL mL	10/0 max 50/0 max 10/0 max
Homogeneity and Miscibility	ASTM D6922	Oil Compatibility	None	Pass
Volatility	ASTM D5800	Evaporation Loss	% off @250^{o}C	22 max
Flash Point*	ASTM D93 ASTM D92	Flash Point	185 ^{o}C 200 ^{o}C	
Phosphorus	ASTM D4951	Phosphorus content	%	0.10 max
Sulfur	ASTM D4951	Sulfur content of SAE 0W and 5W multi-grades	%	NR

- This is for GF-2 Class only

Table B. 5: API/ILSAC Passenger Car Engine Oil Laboratory Tests Standard for SL/GF-3 Class

Requirements	**Test Method**	**Properties**	**Unit**	**Limits SL/ EC GF-3**
Viscosity Grades	SAE J300	All those apply, typically SAE 0W-20, 0W-30, 5W-20,5W-30 and 10W-30		Manufacturer sets targets within SAE J300 specification
Foam Tests	ASTM D892	Sequence I, tendency/stability Sequence II, tendency/stability Sequence III, tendency/stability	mL mL mL	10/0 max 50/0 max 10/0 max
Homogeneity and Miscibility	ASTM D6922	Oil Compatibility	None	Pass
Volatility	ASTM D5800	Evaporation Loss	% off @250^{o}C	15 max
Phosphorus	ASTM D4951	Phosphorus content	%	0.10 max
Sulfur	ASTM D4951	Sulfur content of SAE 0W and 5W multi-grades	%	NR (Not required)

Table B. 6: API/ILSAC Passenger Car Engine Oil Laboratory Test Standard for SM/GF-4 Class

Requirements	**Test Method**	**Properties**	**Unit**	**Limits SM/GF-4**
Viscosity Grades	SAE J300	All those apply, typically SAE 0W-20, 0W-30, 5W-20,5W-30 and 10W-30		Manufacturer sets targets within SAE J300 specification
Foam Tests	ASTM D892	Sequence I, tendency/stability Sequence II, tendency/stability Sequence III, tendency/stability	mL mL mL	10/0 max 50/0 max 10/0 max
Homogeneity and Miscibility	ASTM D6922	Oil Compatibility	None	Pass
Volatility	ASTM D5800	Evaporation Loss	% off @ 250°C	15 max
Phosphorus	ASTM D4951	Phosphorus content	%	0.06-0.08
Sulfur	ASTM D4951	Sulfur content of SAE 0W and 5W multi-grades	%	0.5 max

Table B.7: API/ILSAC Passenger Car Engine Oil Laboratory Tests Standard for SN/GF-5 Class

Requirements	Test Method	Properties	Unit	Limits SN-RC/GF-5
Viscosity Grades	SAE J300	All those apply, typically SAE 0W-20, 0W-30, 5W-20,5W-30 and 10W-30		Manufacturer sets targets within SAE J300 specification
Foam Tests	ASTM D892	Sequence I, tendency/stability Sequence II, tendency/stability Sequence III, tendency/stability	mL mL mL	10/0 max 50/0 max 10/0 max
Homogeneity and Miscibility	ASTM D6922	Oil Compatibility	None	Pass
Volatility	ASTM D5800	Evaporation Loss	% off @250 ^{o}C	15 max
Phosphorus	ASTM D4951	Phosphorus content	%	0.06-0.08
Sulfur	ASTM D4951	Sulfur content of SAE 0W and 5W multi-grades	%	0.5 max
Elastomer Compatibility				
Polyacrylate Rubber (ACM-1)	ASTM D471	Volume Hardness	% change pts	-5,9 -10,10
Hydrogenated Nitrile (HNBR-1)	ASTM D471	Volume Hardness	% change pts	-5,10 -10,5
Silicone Rubber (VMQ-1)	ASTM D471	Volume Hardness	% change pts	-5,40 -10,10
Fluorocarbon Rubber(FKM-1)	ASTM D471	Volume Hardness	% change pts	-2,3 -6,6
Ethylene Acrylic Rubber (AEM-1)	ASTM D471	Volume Hardness	% change pts	-5,30 -20,10

Appendix C: Engine Performance Results

Table C. 1: Engine Torque and Power

Engine Speed (RPM)	Torque (Nm) (SAE 30)	Torque (Nm) (EJBL05)	Power (W) (SAE30)	Power (W) (EJBL05)
0	0	0	0	0
1118	6	5.5	702.5512	644.0053
1220	6	5.6	766.648	715.5381
1330	6.3	5.9	877.5606	821.8425
1450	6.2	6	941.5527	911.18
1500	7	6.3	1099.7	989.73
1745	7.2	6.5	1315.87	1187.938
1890	7.2	6.9	1425.211	1365.827
1950	7.7	7.8	1572.571	1592.994
2030	8.5	8.7	1807.174	1849.695
2200	8.8	9	2027.637	2073.72
2425	9.3	9.5	2361.999	2412.794
2575	10	10.2	2696.883	2750.821
2850	10.9	11.5	3253.541	3432.635
3100	10.3	10.7	3344.135	3474.005
3450	9.4	9.9	3396.502	3577.167

Table C. 2: Brake Specific Fuel Consumption

Engine Speed (RPM)	Fuel Consumption (kg/s) (SAE30)	Fuel Consumption (kg/s) (EJBL05)	Brake Specific Fuel Consumption [kg $(kWh)^{-1}$] (SAE30)	Brake Specific Fuel Consumption [kg $(kWh)^{-1}$] (EJBL05)
0	0	0	0	0
1118	0.000131	0.000162	0.671268	0.905583
1220	0.000132	0.000178	0.619841	0.89555
1330	0.000145	0.000189	0.594831	0.827896
1450	0.000165	0.000175	0.630873	0.691411
1500	0.000179	0.00018	0.585978	0.654724
1745	0.000192	0.000188	0.52528	0.569727
1890	0.000232	0.000197	0.586018	0.519246
1950	0.000265	0.00025	0.60665	0.564974
2030	0.000282	0.000266	0.561761	0.517707
2200	0.000298	0.000285	0.529089	0.494763
2425	0.000314	0.000296	0.478578	0.441646
2575	0.000328	0.000301	0.437839	0.393919
2850	0.000336	0.000319	0.37178	0.334553
3100	0.000341	0.000324	0.36709	0.335751
3450	0.000355	0.000347	0.376269	0.349215

Table C. 3: Brake Mean Effective Pressure and Thermal Efficiency

Engine Speed (RPM)	BMEP (bar) SAE30	BMEP (bar) EJBL05	Thermal Efficiency (SAE 30)	Thermal Efficiency (EJBL05)
0	0	0	0	0
1118	3.7704	3.4562	0.122443	0.099012
1220	3.7704	3.51904	0.132601	0.098334
1330	3.95892	3.70756	0.138177	0.106009
1450	3.89608	3.7704	0.130283	0.122838
1500	4.3988	3.95892	0.140264	0.139485
1745	4.52448	4.0846	0.156472	0.159802
1890	4.52448	4.33596	0.140255	0.165173
1950	4.83868	4.90152	0.135485	0.143614
2030	5.3414	5.46708	0.146311	0.155112
2200	5.52992	5.6556	0.155346	0.162432
2425	5.84412	5.9698	0.171742	0.182185
2575	6.284	6.40968	0.187722	0.20456
2850	6.84956	7.2266	0.243387	0.256358
3100	6.47252	6.72388	0.239117	0.251663
3450	5.90696	6.22116	0.232382	0.237739

Table C.4: Engine Temperature Profile

Speed (RPM)	Oil Temperature (^{o}C) SAE 30	Oil Temperature (^{o}C) EJBL05	Exhaust Valve Temperature (^{o}C) (SAE 30)	Exhaust Valve Temperature (^{o}C) (EJBL05)	Surface Temperature (^{o}C) SAE 30	Surface Temperature (^{o}C) EJBL05
0	41	36	45	43	33	30
1118	41	37	57	60	46	36
1220	54	48	110	108	48	49
1330	60	55	114	117	52	55
1450	72	65	119	122	56	57
1500	80	72	134	130	60	62
1745	89	80	140	135	65	64
1890	92	84	148	140	68	67
1950	95	89	153	147	71	69
2030	97	90	165	160	75	73
2200	101	93	168	162	85	78
2425	105	97	172	163	88	82
2575	108	99	175	169	91	87
2850	110	103	177	172	91	88
3100	112	106	179	174	92	88
3450	115	110	180	176	93	90

Appendix D: Simulation Parameters

Table D. 1: Heat Transfer Parameters

Heat transfer mode	Medium	Values Used for Simulation
Conduction	Engine Cylinder/Block	k = 15 W/mK
	Cylinder head	k = 15 W/mK
	Piston	k = 52 W/mK
	Rings	k = 15 W/mK
	Boundary layer oil	k = 0.18 W/mK (EJBL05) k = 0.16 W/mK (SAE 30)
Convection	Combustion gases	T = Imposed by GT h_g = Calculated by GT
	Splashed oil	T = 36 ^oC to 115 ^oC h_{eo} = 32,890 W/m^2K (EJBL05) h_{eo} = 31,020 W/m^2K (SAE 30)
	air	T = 32 ^oC h_a = 0.654 W/mK h_a = 0.664 W/mK

Table D.2: Air Properties at Mean Bulk Temperature

Air Properties @	SAE 30 @ 52^{o}C	EJBL05 @ 51^{o}C
Density (kg/m^{3})	1.086	1.092
Specific heat capacity (kJ/kgK)	1.008	1.008
Kinematic Viscosity (kg/ms)	19.52 x 10^{-6}	19.52 x 10^{-6}
Coefficient of thermal Conductivity (W/mK)	28.15 x 10^{-3}	27.99 x 10^{-3}
Prandtl's number	0.702	0.702
Grashoff's number	5.17 X 10^{4}	5.0 x 10^{4}
Reynold's number	5.311 x 10^{4}	5.37 x 10^{4}

Table D.3: Simulation results I

Speed (rpm)	Oil Temperature (^{o}C)			
	EJBL05		SAE 30	
	Experimented	Simulated	Experimented	Simulated
1118	310	322	314	326
1500	345	358	353	365
2200	366	380	374	380
3450	383	394	388	397

Table D.4: Simulation results II

Speed (rpm)	Engine Outer Surface Temperature (^{o}C)			
	EJBL05		SAE 30	
	Experimented	Simulated	Experimented	Simulated
1118	309	320	319	332
1500	310	321	333	349
2200	351	364	358	371
3450	363	390	366	380

Table D.5: Simulation results III

Speed (rpm)	Engine Outer Surface Temperature (^{o}C)			
	EJBL05		SAE 30	
	Experimented	Simulated	Experimented	Simulated
1118	333	321	330	305
1500	403	372	408	369
2200	435	411	441	405
3450	449	420	353	424